Mechanical Behavior of Reinforced Concrete Beams with Locally Corroded Shear Reinforcement

局所的に腐食したせん断補強鉄筋を有する
鉄筋コンクリートはりの力学特性

By

Rahmat Ullah

A dissertation submitted to Hokkaido University in partial fulfillment
of the requirements for the Doctoral Degree of Engineering

Examination Committee: Prof. Hiroshi Yokota (Supervisor)
Prof. Tamon Ueda
Dr. Koshiro Nishimura

Division of Engineering and Policy for Sustainable Environment
Graduate School of Engineering, Hokkaido University
September 2017

Acknowledgements

Up and above anything else, praises are due to Almighty Allah alone, the omnipotent, and the omnipresent.

It is a matter of great pleasure and honor for me to express my heartiest gratitude and appreciation to respected and learned research supervisor Prof. HiroshiYokota, under whose kind supervision and sympathetic attitude, the present research was completed. His guidance enabled me to treat this work objectively and comprehensively.

Sincere appreciation goes to MEXT (Ministry of Education, Culture, Sports, Science and Technology, Japan) for awarding highly prestigious "Monbukagakusho Scholarship" to support this study in Hokkaido University.

Honest appreciation must be extended to Ex-Assistant Prof. Katsufumi Hashimoto. To all students and staff of the Lifetime Engineering Laboratory, the author wishes to express his sincere appreciation for the friendly and supportive atmosphere that certainly helped him to carry out this research in a pleasant working environment.

Earnest appreciation must go to the author's colleagues, especially Mr. Kento Shinya and Mr. Koji Shinagawa. Their support contributed in many ways for the completion of this study. This appreciation must also be extended to our laboratory technicians Mr. Tsutomu Kimura (Late) and Mr. Tomohiro Yamagami. They were readily available for any trouble shooting and guidance during all the experiments. Lastly, sincere thanks to my friends all over the world for their continuous prayers and best wishes, especially Ms. Zulayat Kuerban who was always there through thick and thin. Her support and advice always helped me and constant motivation kept my morale very high. This dissertation holds as a testament of her support and encouragement.

No acknowledgement would ever adequately express my obligation to my parents and siblings who have always wished to see me flying high up at the skies of success. The present work could not have been accomplished without their prayers, motivation and encouragements all the time.

Rahmat Ullah

September, 2017

Abstract

Corrosion of steel reinforcement is one of the major causes of damage of reinforced concrete structures. Corrosion products formed have a volume six times more than the steel, which exerts pressures on the surrounding concrete. The pressure leads to cracking and spalling of cover concrete, deteriorates the bond between the steel reinforcement and concrete, and finally reduces the ultimate strength which sometimes result in brittle failure. A lot of research have been carried out to understand the detrimental effects of corrosion of flexural reinforcement in reinforced concrete beams. A large number of experimental studies have shown that the corrosion of flexural reinforcement considerably reduces load-carrying capacity and ductility. However, shear reinforcement (stirrup) has not been given much consideration and there is not much literature available on the effects of corrosion of stirrup. Therefore, in this study, a detailed experimental research has been conducted to observe the behavior of reinforced concrete beams with locally corroded stirrup.

Thirty-nine beams of 1800 mm long, 100 mm wide and 150 mm high were casted, and corrosion of stirrup was electro-chemically accelerated. The beams before suffering from stirrup corrosion were designed to show the flexural failure mode or the shear failure mode. For this purpose, three kinds of flexural reinforcement were used; two D10, two D13 and two D16, all of which were epoxy coated to avoid corrosion. The stirrup was a deformed bar of 6 mm in diameter with the spacing of 80 mm, 120 mm and 160 mm. The location of stirrup corrosion is also a significant factor in this research; accordingly, stirrup was locally corroded in the shear span, in the middle span, or the full span while using 120 mm stirrup spacing. Mild and severe corrosion levels were prepared, mass loss of which were approximately 10% and 20%, respectively. After the corrosion accelerating treatment, corrosion cracks were marked and their widths were measured to observe their distributions and influences on flexural cracking in the bending test. Four-points bending test was applied to observe the ultimate strength of the corroded beams. Finally, the stirrup was taken out to check the degree of corrosion.

It was found that the most of the corrosion cracks lie in the crack width range of 0.03-0.05 mm, which is the narrowest crack width range. The corrosion cracks in the severely corroded beams were more, and wider cracks were observed as compared with the mildly corroded beams. At the critical locations, the corrosion cracks acted as the pre-defined failure paths and the flexural or shear cracks followed the corrosion cracks during the bending test. The flexural or shear cracks were wider in the corroded beams than those generated in the control beams. Although stirrup is not responsible for flexural capacity but the results showed reduction in the flexural capacity after corrosion of stirrup. In all cases, the beams with stirrup corrosion had less flexural capacity than the control beams. The reduction in the capacity was more in the beams where the stirrup was corroded in the full span and the shear span for mild and severe corrosion and shear failure occurred in the severely corroded beams. The stirrup in the middle span did not contribute to the flexural capacity of the beam, as there is zero shear force and maximum bending moment in the middle span. However, the stirrup corrosion induced the corrosion cracks in the middle span. The flexural cracks followed the corrosion cracks during the bending test, and were mainly responsible for reducing the flexural capacity of the corroded beams. The corrosion cracks occurring due to stirrup corrosion were vertical cracks along the length of the stirrup with some horizontal or connecting cracks which passed through the vertical cracks. These horizontal cracks and the vertical cracks tended to widen during the bending test. At higher values of applied load, the horizontal and vertical cracks presented in the middle span at the top of the beam in the compression zone, also tended to widen, separating the concrete cover in the compression zone resulting in spalling of the concrete cover. This reduced the cross-sectional area of the beam as the top concrete cover was spalled out, reducing the width of the compression zone and hence lowering the flexural capacity of the corroded beam. This phenomenon was more obvious and clear for full span or middle span corrosion as all stirrups in the middle span were corroded and had corrosion cracks. In case of shear span corrosion, the corrosion cracks were critical at the junction of shear and middle span, just under the applied point load. Because of these reasons, the failure mode of a few beams with full span or middle span corrosion were changed from flexural tension failure to flexural compression failure, after stirrup corrosion. The severely corroded beams had higher strength loss and all D13 and D16 severely corroded beams with shear span or full span stirrup corrosion failed in shear. D10 beams had the flexural reinforcement ratio well below the ratio at balanced failure and the shear reinforcement ratio is high enough and the probability of shear failure is minimal after stirrup corrosion. This is the reason, only one D10 severely corroded beam failed in shear and all other failed in flexure.

The ultimate capacity loss of corroded beams was more for higher transverse (shear) reinforcement ratio, which was the case of closely spaced stirrup. When the stirrups were closely spaced, the strength contribution of the stirrup was more, and once the stirrup was corroded, the strength loss observed was also more. The failure modes of the corroded beams were also changed particularly when the stirrup was severely corroded. Depending on the location of corrosion, most of the severely corroded beams failed in shear despite having yielding of flexural reinforcement for the control beams. The beams failed in shear had higher capacity loss than those failed in flexure. Hence, the stirrup corrosion strongly influenced the capacity of the beam, which further depended on the location and the amount of corrosion. The stirrup corrosion had a strong tendency to change the failure mode and even to reduce the flexural capacity of reinforced concrete beams.

The deflection ductility was also significantly reduced after the stirrup corrosion. For lower flexural reinforcement ratio, the deflection ductility was reduced considerably as the deflection ductility of the control beams was much higher for the lower flexural reinforcement ratio which was governed by the flexural design of the beams. The residual shear capacity of the stirrup corroded beams was predicted using some empirical models including the width of corrosion crack. The predicted values did not give enough accurate results as these empirical models were developed considering one or two straight corroded rebars which were larger in diameter and mostly used as longitudinal reinforcement. However, the stirrups are rectangular in shape and the diameter of stirrup is usually smaller than the longitudinal reinforcement. Moreover, there is an interaction of the tensile stress induced due to the corrosion of the adjacent stirrups which results in more cracking which are vertical and horizontal cracks. When the stirrup is closely spaced and the shear reinforcement ratio is higher, more horizontal corrosion cracks are observed which pass through the vertical cracks. These corrosion cracks are the indication of confinement loss provided by stirrup which also results in the loss of compressive strength of concrete, and are absent in case of longitudinal reinforcement corrosion. This makes the behavior of stirrup corrosion a bit different from the straight rebars which are widely used as longitudinal reinforcement. Therefore, more research should be carried out to study the effect of stirrup corrosion by varying the design parameters and new empirical models should be established considering the stirrup shape, interaction of the tensile stresses due to the stirrup corrosion while using smaller diameters.

Dedication

To

Prof. Hiroshi YOKOTA, My havened Parents

&

All my teachers

Table of Contents

CHAPTER 1

INTRODUCTION

Chapter 1

INTRODUCTION

1.1 GENRAL BACKGROUND

Numerous studies in the past showed that corrosion of reinforcing steel has adversely affected the mechanical behavior of RC structures [1-10]. According to these studies, the structural performance of RC beam reduces with the increase in corrosion level. Corrosion of reinforcing steel is one of the most common and hazardous problems of RC structures. It can cause premature deterioration and failure of a member which can endanger the serviceability and safety of the structures. Aggressive external agents such as chloride ion ingress and carbonation facilitate corrosion process and the corrosion becomes much faster in their presence. Reinforced concrete structures which are exposed to severe environment conditions, where de-icing salts are sprayed during winters often encounter chloride ion penetration. Marine or coastal structures are always in contact with sea water and are more prone to chloride ion attack resulting in faster corrosion.

Corrosion products formed have a volume six times more than the steel, which exerts pressures on the surrounding concrete and cracks start occurring on the surfaces of concrete [22]. This cracking results in delamination and subsequent spalling of concrete cover. This phenomenon keeps on increasing with the higher levels of corrosion. The study of these cracks is very important to assess durability and service life of RC structures [13, 14, and 19]. As the corrosion process continues the steel cross-sectional area starts reducing resulting in loss of nominal strength and elongation. The bond strength between concrete and steel also reduces because of corrosion and this loss has a considerable contribution in the reduction of ultimate strength and maximum deflection [18-20].

Many previous research showed the behavior of RC beams in which the main longitudinal reinforcement and transverse (shear) reinforcement (stirrup) are corroded simultaneously. There is a considerable loss of ultimate load-carrying capacity and maximum deflection when both the reinforcement is corroded. The failure mode may also change because of corrosion and ductility loss [14, 19]. However, there are not much literature available when only the transverse (shear) reinforcement is corroded. When the shear reinforcement (stirrup) is corroded, there will be reduction in cross section with some volumetric changes and spalling of concrete cover. These losses in RC beam can lead to diagonal tension failure or shear failure which will cause brittleness and sudden failure in the beam [20]. The ductility of RC beam relies on longitudinal reinforcement elongation and good flexure control design but with the corrosion of stirrup it can result in diagonal tension and sudden failure which is not at all desired. The corrosion of stirrup aggravates localized failure which is more vulnerable as it is difficult to predict and control. Field investigations and tests on beams showed that cover cracking and spalling is more prominent in areas with stirrups [13]. If the stirrups are closely spaced the effect is more adverse.

The diameter of stirrups is generally small compared to that of longitudinal reinforcement, so relative loss of the cross-sectional area due to corrosion in the stirrups is expected to be much more significant than that of longitudinal reinforcement [21]. Also since stirrup is generally located more close to the surface of RC member than longitudinal reinforcement, it is much easier to corrode due to chloride ion ingress from the environment. Therefore, the effect of stirrups corrosion on crack initiation, crack propagation and cover spalling needs to be investigated in more detail. Influence of corrosion of stirrup on the structural performance is a new field of study and got attention just recently, since 2006. Before 2006, the data on the detrimental effect of stirrup corrosion was not available in many of the esteemed international journals.

A detailed research program is carried out to investigate the effect of corrosion of stirrup in this study. The main longitudinal bars were factory epoxy coated to avoid corrosion. Thirty-nine beams of 1800 mm long, 100 mm wide and 150 mm high were casted, and corrosion of stirrup was electro-chemically accelerated. The beams before suffering from stirrup corrosion were designed to show the flexural failure mode or the shear failure mode. For this purpose, three kinds of longitudinal reinforcement were used: two D10, two D13 and two D16 mm, all of which were epoxy coated to avoid corrosion. The stirrup was 6 mm in diameter with the spacing of 80 mm, 120 mm and 160 mm. The location of stirrup corrosion is also a significant feature in this research; accordingly, stirrup was locally corroded in the shear span, the middle span, or the full span while using 120 mm stirrup spacing. Mild and severe corrosion levels were prepared, the target mass losses of which were 10% and 20%, respectively. After the corrosion accelerating treatment, corrosion cracks were marked and their widths were measured to observe their distributions and influence on flexural cracking in the bending test. Four-points bending test was applied to observe the mechanical behavior of the corroded beams. Finally, the stirrup was taken out to check the degree of corrosion. Although the stirrups do not have much contribution towards flexural strength in the middle span but results show reduction in flexural strength because of stirrup corrosion. The results of stirrup corrosion only in the shear span are also important to understand the effect. Other results showed that the corrosion of stirrup has an effect on the structural performance of beams but this effect is varied for every case. The ultimate capacity was decreased in all the cases and the design failure mode was also changed for the beams with severely corroded stirrup.

1.2 RESEARCH SIGNIFICANCE

Higgins and Farrow [13] showed that the reinforced concrete bridges are at risk for build-up of chlorides (used in deicing salts) which can lead to corrosion as illustrated in Figure 1.1. Higher risk areas for chloride contamination are the deck surface (deicing salts) and the interior of bridge girders and the underside of the deck (wind-born ocean salt). The fascia girder is typically at a lesser risk due to washing from rainfall.

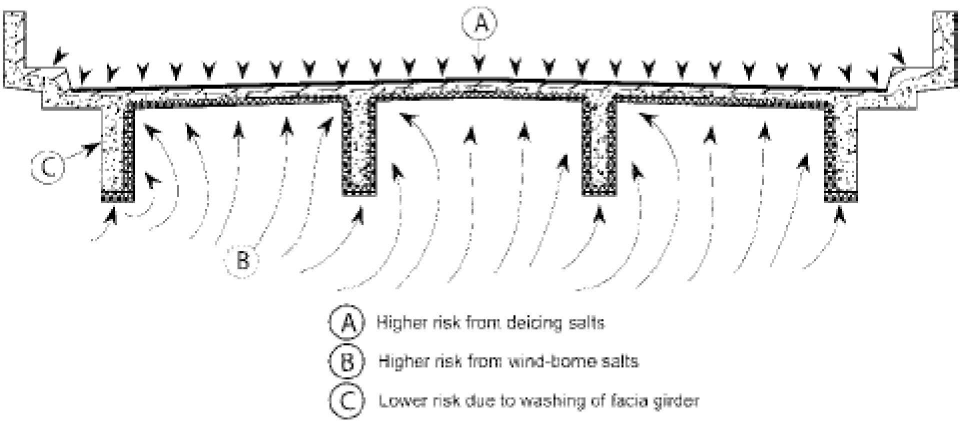

Figure 1.1 Reinforced concrete bridge cross section showing areas at risk from deposition and retention of chloride ions on structural elements [13]

Examination of a concrete bridge girder built in 1954 removed from service showed the corrosion induced distress including concrete cracking, rust staining, delamination, and spalling of concrete cover [13]. After removing the delaminated concrete from the bridge for further examination, it was noted that two stirrups were discontinuous and part of them completely gone due to corrosion at locations A and B as shown in Figure 1.2.

The impact of stirrup corrosion on the shear capacity of reinforced concrete beams has not been widely studied. Existing rating and evaluation guidelines, based on overall visual distress of stirrup corrosion, have not been correlated with actual structural performance for corrosion damaged members [13]. The concrete cover to the stirrup is less than that of longitudinal reinforcement, and the amount or ratio of stirrup is also more than the longitudinal reinforcement. Results on corroded longitudinal reinforcement showed that it is high probability that the beam will still fail in flexure with reduced ultimate capacity and deflection. However, the stirrup corrosion might change the failure mode and the beam might fail in shear after stirrup corrosion. These concerns make the study of stirrup corrosion very important.

Many research are carried out to investigate the structural performance of the rehabilitated beams which suffer corrosion of longitudinal reinforcement. The flexural capacity of such corroded beams is rehabilitated in the experimental studies but if the mechanical behavior of stirrup corrosion is not well-known then the rehabilitated beam might fail in shear instead of flexure which is more catastrophic. Therefore, a thorough investigation is required to understand the effect of stirrup corrosion. Also, the stirrup diameter is much lesser than the longitudinal reinforcement and hence more cross-sectional area loss will occur in stirrup as compared with the longitudinal reinforcement.

This research contributes to the understanding of the effect of stirrup corrosion on the structural performance of the stirrup corroded RC beams. The results of the stirrup corroded damaged beams can help in estimating the residual capacity of the stirrup corroded beams and also validation of the previous models can be done which are available to predict the residual capacity of beams after corrosion. Different flexural designs were used to investigate the mechanical behavior of beams with corroded stirrups.

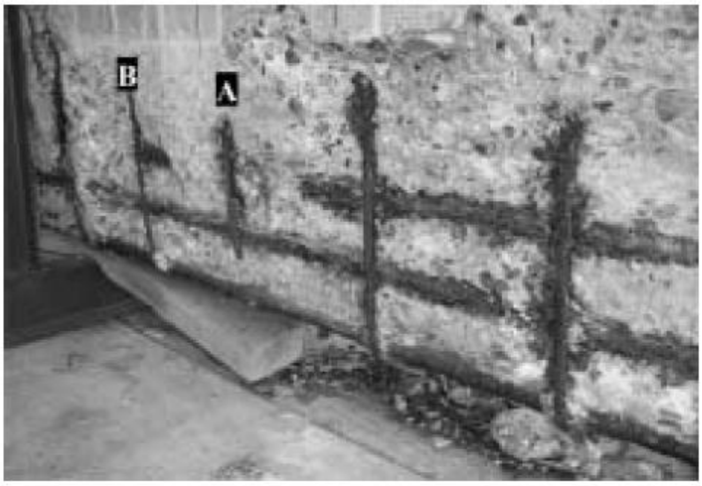

Figure 1.2 Chloride-induced corrosion damage to reinforced concrete deck girder removed from Brush Creek Bridge in 1998 [13]

1.3 LITERATURE REVIEW

1.3.1 Corrosion of Steel in Concrete

Steel is found in nature in the form of oxides and with some percentages of carbon. In the extraction or manufacturing of steel, the oxides are removed in order to obtain pure iron with less percentages of carbon. The ductility and strength of steel also depends on the carbon content in the steel.

Iron and plain carbon steel are thermodynamically unstable materials. Nature will try to bring these materials back to their naturally stable forms, namely oxides, i.e. rust-like materials. When iron or steel has a contact with oxygen and water simultaneously, the corrosion process of steel will start. Oxygen and water are the essential components to start corrosion and in the absence of any of this component corrosion will not start. There are many other factors which accelerate or decelerate the corrosion process. The process of corrosion is provided by electrochemical reactions, i.e. chemical reactions involving transfer of electrons and electric charges at the interface between the metal and the water. Different types of iron oxides (which are termed as rust or corrosion products) may be formed depending on exposure conditions:

Iron / Steel + Water + Oxygen → Iron oxides/rust . . . . .… (1.1)
(Fe) (H_2O) (O_2) $Fe(OH)_2$ / Fe_3O_4 / Fe_2O_3

Figure 1.3 shows the schematic illustration of corrosion of reinforcing steel in concrete. Corrosion process is a formation of a microcell within the steel. A part of steel will act as anode and another part will act as cathode. The formation of anode and cathode within the steel body and the distances between them depend on the exposure conditions. The distance between anode and cathode can be very close to each other (microscopic distances), or separated by macroscopic distances. The distance between them and the exposure conditions determine the rate and amount of corrosion of steel. At the anode the oxidation of iron occurs and it loses electrons and becomes in unstable state, producing ferrous ions. These ferrous ions are unstable and they want to get in stabilize state by chemical reaction:

Anodic reaction – oxidation of iron

$$Fe \longrightarrow Fe^{+2} + 2e^{-} \quad \text{………} \ (1.2)$$

The liberated electrons from the oxidation of iron will travel to cathode and are consumed by oxygen in the presence of water to form hydroxyl ions (OH^-):

Cathodic reaction – Formation of hydroxyl ions

$$1/2O_2 + H_2O + 2e^{-} \longrightarrow 2OH^{-} \quad \text{………..} \ (1.3)$$

If there is no external electric source of electrons, the anodic reaction must generate electrons at exactly the same rate as the cathodic reaction consumes them. The algebraic sum of these two reactions makes the total reaction, called the corrosion cell reaction:

$$Fe^{+2} + 2OH^{-} \longrightarrow Fe(OH)_2 \quad \text{…………} \ (1.4)$$

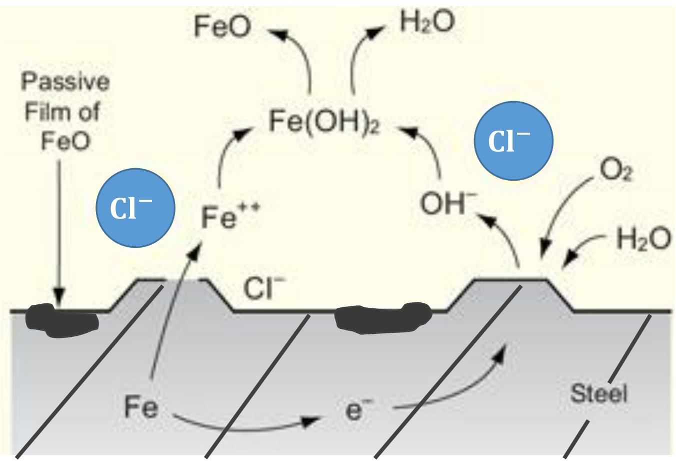

Figure 1.3 Schematic illustration of a steel corrosion in concrete

If the distance between the electrodes within the steel is widely separated (macroscopic distance), it is termed as the macrocell corrosion and when it is sufficiently close, or essentially at the same location (microscopic distances), it is defined as the microcell corrosion. It is well known that the macro cell corrosion is dominant when steel is embedded in concrete. It should be noted that other forms of anodic and cathodic reactions may occur in specific cases depending on the availability of oxygen and the pH of the cement paste pore solution in the vicinity of the steel.

For sound concrete, the pH of the pore solution ranges from 13.0 to 13.5. This shows the extreme alkaline nature of concrete. A protective passive layer is formed on the steel concrete interface in the form of the iron oxides, Fe_3O_4 and Fe_2O_3 or hydroxides of these compounds. This passive layer prevents somehow the corrosion of steel in the concrete. If the protective layer is sufficiently thick it can inhabit corrosion by providing a diffusion barrier in between the reacting species (e.g. Fe, H_2O and O_2). In case of concrete, however, this protective passive layer formed is very thin and can be affected by other aggressive chemical agents. The pH around the steel and concrete can also be reduced due to carbonation or pozzolanic reaction, which can be adverse to this protective passive layer. The presence of chloride ion directly affects this protective layer and destroys the performance of this layer. Once this protective layer is damaged, the steel in concrete is more susceptible to corrosion. Nevertheless, whatever the thickness of passive layer it cannot stop the corrosion process rather than reducing the intensity. Studies found that in the passive state generally the corrosion rate is 0.1 µm/yr which could be at least three orders in magnitude is case of existence of no passive film [23].

1.3.2 Corrosion of Reinforcing Steel in Reinforced Concrete Beams

A lot of research has been carried out to study the effect of corrosion on the structural performance of concrete beams. The reinforcing steel, including tension and compression longitudinal reinforcement and stirrups are allowed to corrode in these research. Some of the research focused on the actual components of marine structures and after years of exposure to severe chloride environments, these beams are tested to check the strength losses and weight loss of steel due to corrosion. In some other research, the corrosion of reinforcing steel is allowed in the laboratory by applying salt sprays on the beams at regular intervals. The duration to apply the salt sprays varies in different research depending on the corrosion level to be obtained and perception of the researchers to simulate to the real environment. One such research was presented by *Vu Hiep Dang et al* [19]. In this research the structural performance of 27 years old corroded beams were investigated. The cross-sectional area loss, load-carrying capacity, mid-span deflection and force‑elongation of some of the corroded reinforcing steel bars were measured. A batch of 36 RC beams of common dimensions (15 x 28 x 300 cm) as shown in Figure 1.6 were casted with two different section types, A and B, were stored in a chloride environment under sustained loading. At the same time, another batch of 36 RC beams of the same composition, serving as control beams, were cast but stored under laboratory conditions (non-aggressive environment) in order to provide a comparison at each term of the design process. The beams were loaded in three-point bending by coupling a type A beam with a type B beam (see Figure 1.5). The beams were kept in a salt fog (35 g/L of NaCl corresponding to the salt concentration of sea water) generated by four sprays located in each upper corner of a confined room. After 6 years of storage, the beams were subjected to wetting‑drying cycles in order to accelerate the corrosion process.

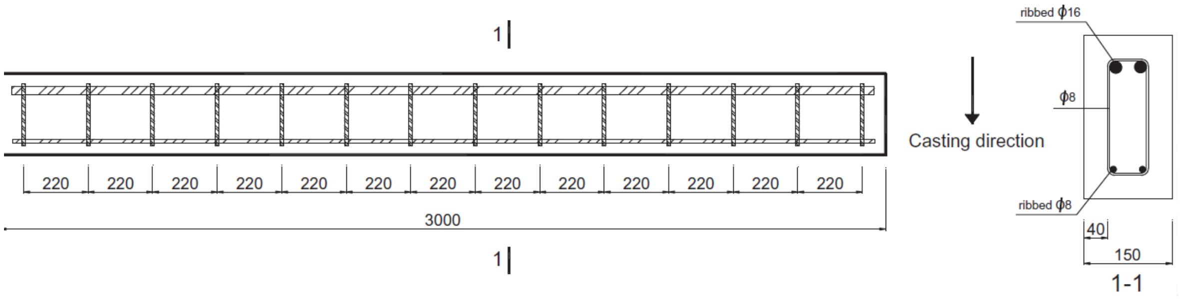

Figure 1.4 Layout of reinforced concrete beam type A (dimensions in mm) [19]

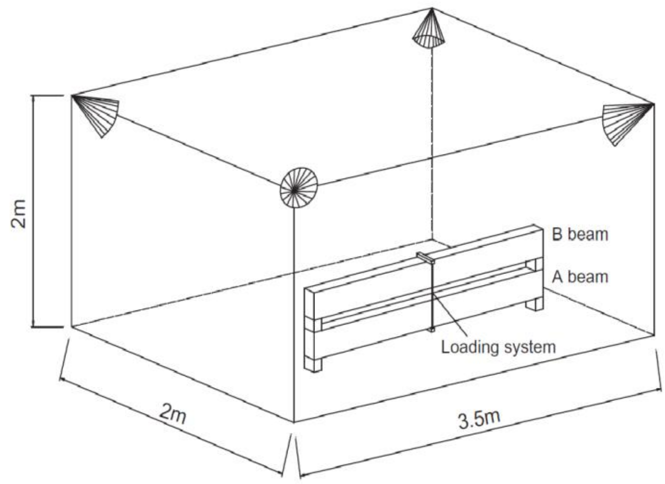

Figure 1.5 Loading system and conditional exposure of beams in the saline room [19]

After 27 years of corrosion, the corrosion cracks were marked and measured. The cracks distribution and width show the typical behavior of corrosion cracks when flexure and shear reinforcements, both are allowed to corrode. The corrosion crack widths depend on many factors which can change the mechanical behavior of the beam also. The corrosion cracks were present on all four sides of the beam. At different locations, the crack widths are dissimilar because the amount of corrosion is not the same throughout the reinforcement. This also reflects to real time structures as the corrosion process starts from one point and it continues randomly in the member of structure depending on the exposure conditions. Figure 1.6 shows the corrosion cracks width and distribution on the front and back sides of a 27-year old corroded beam.

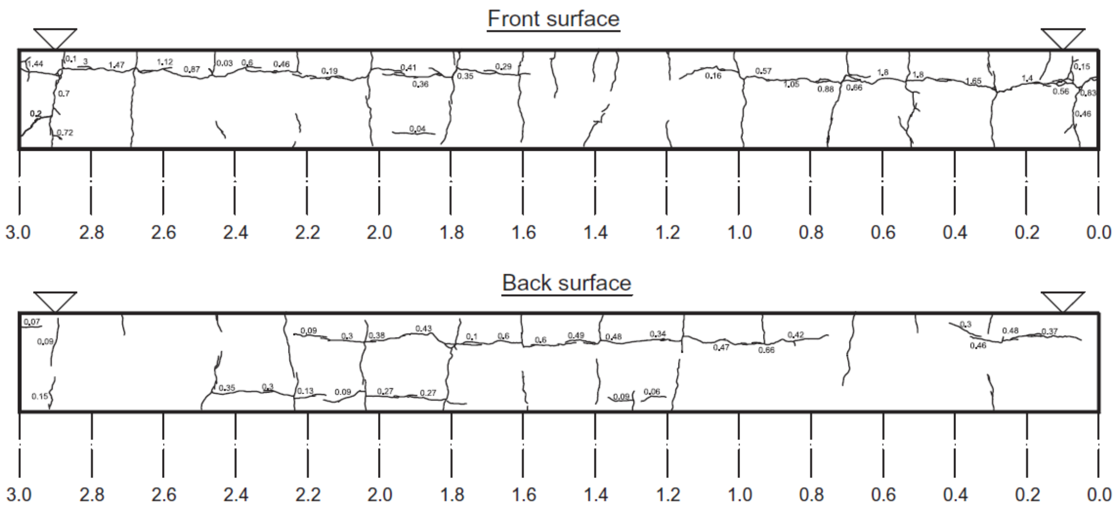

Figure 1.6 Corrosion cracking map of a 27-year corroded beam [19]

For the bending test, three point loading test was applied. The beam was simply supported and a symmetrical load was applied at a distance of 1400 mm from the supports. The results obtained by testing the control beam A2T and the corroded beam A2CL1 (beam corroded for 27 years) are plotted in figure 1.7. The yield loading values of A2T and A2CL1 were roughly 66 and 48 kN respectively. The peak loading values were 73 kN for A2T and 54 kN for A2CL1. The reduction in both the yielding and ultimate load in A2CL1 was about 26% in comparison with A2T. However, the ductility of the two beams was quite distinct, with a sharp reduction (47%) for A2CL1.

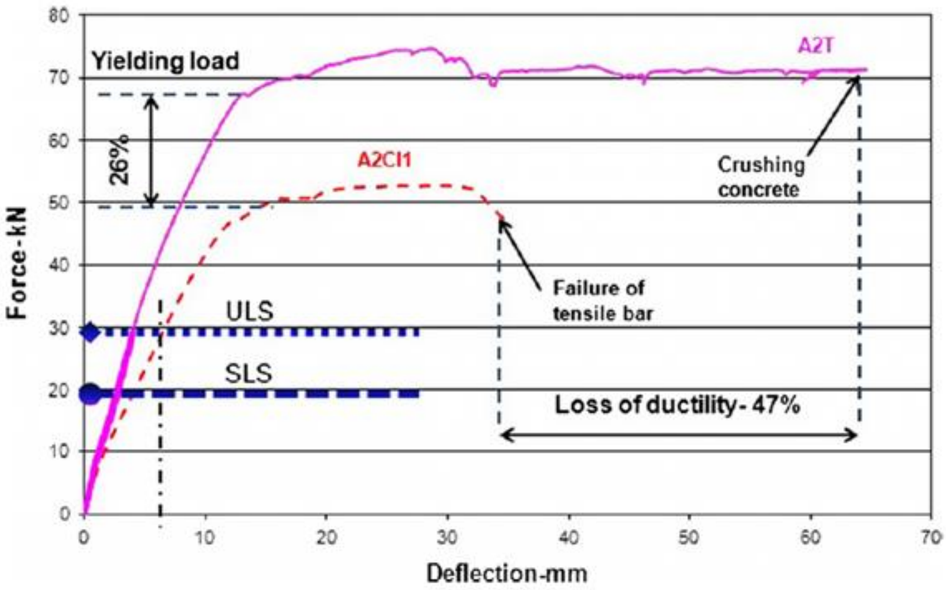

Figure 1.7 Comparison of load-deflection curves for control beam A2T and 27-year corroded beam A2CL1 [19]

The failure mode of control beam A2T was crushing of concrete but after 27 years of corrosion, the failure mode of corroded beam A2CL1 changed from crushing of concrete to yielding of tensile reinforcement which is more ductile than the control beam. Hence, after corrosion there is a strong tendency that the design failure mode of RC beam can change depending on the amount of corrosion and flexural design.

Figure 1.8 shows the force-elongation curve of the tensile and compression bars after 27 years of corrosion. It is clear that the typical force-elongation curves of all steel bars did not comprise a yield plateau like that recorded with the sound steel bar. The brittle fracture with no indication of necking occurred just when the stress reached its maximum value. The experiment showed that all corroded steel bars had smaller ultimate elongation. The reason for this was stress concentration at the tips of the corrosion pits, which led to premature yielding of the steel cross-section during loading and thus reduced the plasticity reserve of the steel at pit locations. Moreover, this phenomenon must depend on the shape and depth of pit corrosion that leads to more brittle behavior.

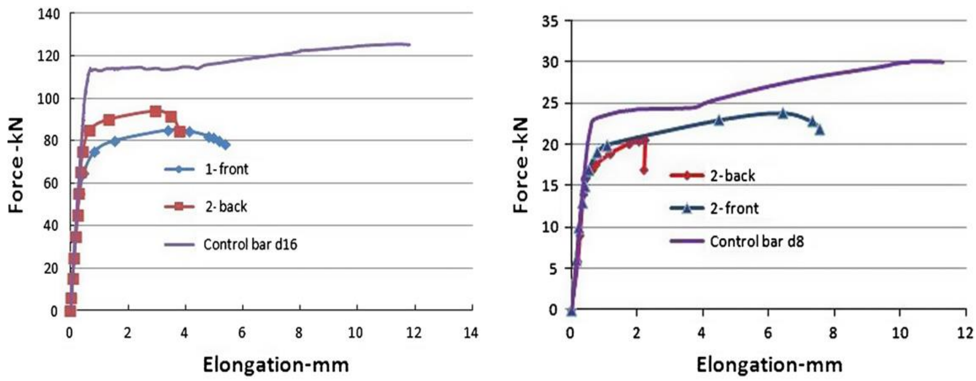

(a) tensile bars (b) compressive bars

Figure 1.8 Force-elongation curves of corroded bars [19]

The key findings of this research are:

- Long term corrosion appeared to be independent of the initial cracking pattern.
- The corrosion led to a change in the failure mode from concrete crushing to tensile bar failure.

- Ultimate deflection of the corroded beam was 47% reduced. This is because of the reduction of ultimate elongation of steel bars.
- For tensile bars, average cross-sectional area loss of front bar was 14.2% and back bar was 8.2% in spite of similar conditions.
- The total percentage of steel loss for compression bars is 31% and for tension bars 22.5%. Because of smaller initial cross-sectional area 8 mm for compression bars.

1.3.3 Corrosion of only Stirrups in Reinforced Concrete Beams

As mentioned earlier, a lot of research have been carried out to study the effect of corrosion of either longitudinal reinforcement or both shear and longitudinal reinforcement of the beam. However, the effect of corrosion of shear reinforcement only is not considered much and there is no significant literature available on its effect. Though, shear reinforcement is more prone to corrosion than the longitudinal reinforcement as the concrete cover to shear reinforcement is less than the longitudinal reinforcement. Hence the chances of shear reinforcement to get corroded are much higher which can lead to abrupt shear failure in beams. Moreover, the behavior and the structural performance of the beam will also change including the ductility and load carrying capacity of the beam. To investigate the effect of stirrup corrosion, a small study was conducted by *O'Flaherty et. al* [11].

The term under-reinforced concrete beams is used for such beams that are designed to have less tensile moment of resistance (M_t) than the moment of resistance of the compressive zone (M_c); resulting in a ductile failure. Beams are usually designed considering failure by yielding of tensile reinforcement. This means that the top reinforcement in compression part is greater than the bottom reinforcement in tension provided in beams. The shear reinforcement in beams was sufficiently provided to ensure that the shear capacity of the specimens is greater than its flexure capacity. The aim of this study was to explore the influence of corroded shear reinforcement on the strength of RC beams.

Beams with 100 mm x150 mm x 910 mm (width x depth x length) dimensions were casted in the laboratory. The research plan consists of two types of variation, i.e. variation in under-reinforcement ratios (M_t/M_c ratio) and variation in the corrosion level for each under-reinforced beam. The diameter of tensile flexure reinforcement was changed in order to change the under-reinforcement ratio. Two under-reinforcement ratios (M_t/M_c ratio) were used in this research. Type A beams which have two bars of 8mm diameter as flexure reinforcement whereas type B have two bars of 12 mm diameter as flexure reinforcement with the nominal characteristic strength of 460 N/mm^2. By only varying the tensile longitudinal reinforcement, M_t/M_c ratio changes and in both cases M_c will remain the same. The main steel remained un-corroded during the entire set of experiments. The stirrups used for both types comprise of 6 mm plain round mild steel bars of nominal characteristic strength 250N/mm^2 at a spacing of 65 mm. Concrete cover was 50 mm to the shear reinforcement for all the beams. The target corrosion of 0-15% along the cross sectional area of stirrups with 5% increment was induced in the specimens. These specimens were corroded using accelerated corrosion process.

The samples were casted using ordinary Portland cement and a mix proportion of 1:1.5:2.9 adding anhydrous calcium chloride $CaCl_2$ (1% by weight of cement) to promote corrosion process. These specimens were casted in steel moulds and then cured in a curing room at 20°C and 95% relative humidity. After demoulding, they were cured in water for 28 days. When the specimens have gained sufficient strength at 28 days they were moved to a saline solution (3.5% $CaCl_2$ solution) tank for accelerated corrosion. Galvanostatic corrosion process in an electrolytic cell by means of direct current multi-channel power supply was used. In order to avoid corrosion in main steel bars, wrap tubing was provided at the points of contact with the shear reinforcement to break the circuit. A constant current density of 1mA/cm^2 was passed through the reinforcement. Each corrosion level was selected to provide a predefined percentage reduction in bar diameter.

Testing of the control and test specimen in flexure was carried out. Control specimens giving 0% corrosion were tested after 28 days while others specimens were tested at 42, 45 and 48 days age for the target corrosion level of 5, 10 and 15% respectively.

The corroded bars were removed from each specimen, weighed and percentage reduction in weight was calculated. The corrosion was generally spread along the length of the reinforcement. Serious cross sectional area loss of rebar occurs at higher percentages of corrosion. Actual reinforcement corrosion varies from the target corrosion level due to difficulties in using the accelerated current technique. The main bars were not corroded at confirming the response of the beams is due to corrosion of stirrups only. The tensile moment of resistance and compressive moment of resistance was calculated for control specimens and test specimens. This was done to obtain the under-reinforcement ratio (M_t/M_c) in each specimen. By relating M_t/M_c ratio and percentage shear reinforcement weight loss a linear equation for each series of beams was tabulated along with the co-efficient of correlation R^2. After testing it was observed that though all of them had corroded shear reinforcement, majority fail in flexure in a ductile manner. Shear failure was observed in type A beam with 15% corrosion level (but actually it was 18.7%).

Flexural strength loss was detected in both A and B types of beams showing that corrosion of stirrups have an adverse influence on flexure strength. Flexural strength loss of B type (higher M_t/M_c ratio than A type) was more than the A type which showed that flexure strength loss due to shear reinforcement is more rapid in beams with higher M_t/M_c ratio. It can be said that due to shear reinforcement corrosion, the beams with higher flexural capacity will have more flexural strength loss than those with less flexural capacity if the dimensions of the beam is constant. Shear failure only occurred for higher percentage corrosion level (>18.7%) which displays that the shear reinforcement corrosion can also change the failure mode of the beams after attainting to a certain corrosion level. In this case the failure will be abrupt without any ample warning indicated by deflections or cracking before failure.

1.4 OBJECTIVES AND LAYOUT OF THIS STUDY

The corrosion of either shear or flexural reinforcement, localized or general has ability to change the failure type which can be abrupt failure also. The use of overly conservative or inappropriate methods of analysis was reported to be responsible for the majority of the failures. Design engineers believe that by over designing they are increasing the service life of the structure but actually, the failure mode can change due to corrosion or it can adversely affect the service life. It is very difficult to predict the location from which corrosion can start. Efforts can be made to minimize the chances to start corrosion but when the corrosion initiates it can occur from anywhere, flexural or shear reinforcement. The chances of shear reinforcement to get corroded are more as the concrete cover to shear reinforcement is less than the flexural reinforcement. Therefore research in this area is very important to fully understand the behavior of RC members when stirrup is corroded in order to make safe and economic design. The effects of stirrup corrosion will be different for different kinds of beams e.g. stirrup spacing, stirrup diameter, depth of the beam, a/d ratio, flexure-reinforcement ratio, design failure mode etc.

The primary objective of this study is to investigate structural behavior of RC beams when only stirrups are corroded. For structural behavior of corroded beams, the ultimate strength loss and the ductility are the important parameters to study. To achieve the primary objectives following sub-objectives are also discussed in this study.

a) To examine the mass loss of stirrups after corrosion.

b) To mark and measure the corrosion crack widths and distribution after stirrup corrosion.

c) To mark and measure the flexural or shear cracks widths and distribution after four point bending test of corroded beams.

d) To observe the loss in ultimate capacity, failure mode and ductility of the corroded beams.

e) To estimate the residual shear capacity of the beams failed in shear after corrosion using the existing models for corroded rebars.

f) To compare structural behavior of stirrup corrosion by varying different parameters. This will help in understanding better the behavior of stirrup corrosion. For this study, following parameters were varied :

i. The stirrup spacing was varied and 80 mm, 120mm and 160mm stirrup spacing were used in this study.

ii. Design failure mode without corrosion was altered. The design failure mode selected for this study was flexure tension failure occurring by yielding of flexural reinforcement, yielding of flexural reinforcement with shear cracks and flexural compression failure due to crushing of concrete in respective beams.

iii. The flexural reinforcement ratio was changed. Two D10, two D13 and two D16 mm diameter deformed bars as longitudinal reinforcement were used.

iv. Two levels of corrosion were selected, mild and sever corrosion. Mild corrosion referred as 10% average mass loss and severe corrosion as 20% average mass loss of stirrups after corrosion.

v. The location of corrosion was varied using 120 mm stirrup spacing. Stirrups were corroded in shear span, middle span or full span with mild and severe corrosion levels.

***CHAPTER* 2**

EXPERIMENTAL METHODOLOGY

Chapter 2

EXPERIMENTAL METHODOLGY

2.1 BACKGROUND

In almost all concrete structures, beams are the essential part of the structure. There are different shapes of beams but rectangular beams are widely used. In beams there are two kinds of reinforcement present, longitudinal and transverse reinforcement. Longitudinal reinforcement resists the bending moment load and the transverse reinforcement (stirrup) resists shear force. There are many ways which cause damage to these beams and the service life and safety of the structure is endangered. One such deterioration is corrosion of reinforcement in concrete and mostly this process is accelerated by the penetration of chloride ions. The corrosion of steel reduces the cross-sectional area of steel and elongation resulting in the reduction of ultimate strength and ductility. Many researches show the results of corrosion of longitudinal and transverse reinforcement. However, in this study, the effect of corrosion of shear (transverse) reinforcement such as stirrup is only studied.

2.2 RESEARCH CONCEPT

A detailed research plan was prepared to observe the effect of corrosion when only stirrups are corroded. The structural behavior of the RC beam depends on the good flexural design with enough shear capacity to resist the applied shear forces. To understand the behavior of stirrup corroded beam, the design and failure mode of the control beams without stirrup corrosion are very important. Different researcher used different beam designs to understand the behavior of corroded beams. To study the effect of stirrup corrosion which may result in reduction of shear capacity, the design failure mode chosen was shear failure. The shear failure mode will give direct reduction in the shear capacity of the beam as comparison will be very easy for beams with and without stirrup corrosion. The comparison can easily be made with the experimental shear capacity of stirrup without and with corrosion.

In this study, the two different design failure modes were considered with three different designs. Flexural tension failure which was designed by under reinforced sections and flexural compression failure (crushing of concrete) by over reinforced sections. Most of the real time structures have good flexural design and the expected failure mode is flexure in real structures. Also, one of the aspect of this study is to investigate if there is any reduction in the ultimate capacity with stirrup corrosion, and if stirrup corrosion can change failure mode. The flexural compression failure (crushing of concrete) failure was selected to make the beams strong enough to avoid flexural failure and the shear capacity of the section can be studied after stirrup corrosion. It was expected that these beams will fail in shear after corrosion as being adequately designed for flexure. For under reinforced beams, there were two design beams; (i) 2-D10 longitudinal rebars which had the longitudinal reinforcement ratio well below the balanced failure showing very good ductile and long plastic region after yielding in the load-deflection curves, and (ii) 2-D13 longitudinal rebars which also had longitudinal reinforcement ratio below the balanced failure ratio but higher than D10 beams resulting in relatively shorter plastic region after yielding in the load-deflection curve. For over reinforced beams, 2-D16 longitudinal rebars were used and the longitudinal reinforcement ratio was a little higher than the balanced failure ratio illustrating flexural compression failure near the yield load. Details of these beams are provided in the subsequent sections.

Another important aspect in beam designs was consideration of the stirrup spacing. As discussed in the introduction, stirrup spacing is critical when the stirrups are corroded. When the stirrups are closely spaced, there is an interaction of the forces exerted on the surrounding concrete by the adjacent corroding stirrups. For this reason, the stirrup spacing was varied in this study and 80 mm, 120 mm and 160 mm stirrup spacing was used.

In the four-point bending test of a beam, two types of loads will be acting on the beam, bending moment and shear force. There will be two shear span zones at the sides and a maximum bending moment zone in the middle. Figure 2.1 shows the forces on the beam, shear force and bending moment diagram. The stirrups are equally spaced and provided throughout the beam. This means that stirrups are in both the shear spans and in the maximum moment span. In this research, the stirrups are corroded in shear span (only one span); the middle span (zone where maximum bending moment occur) or the full span.

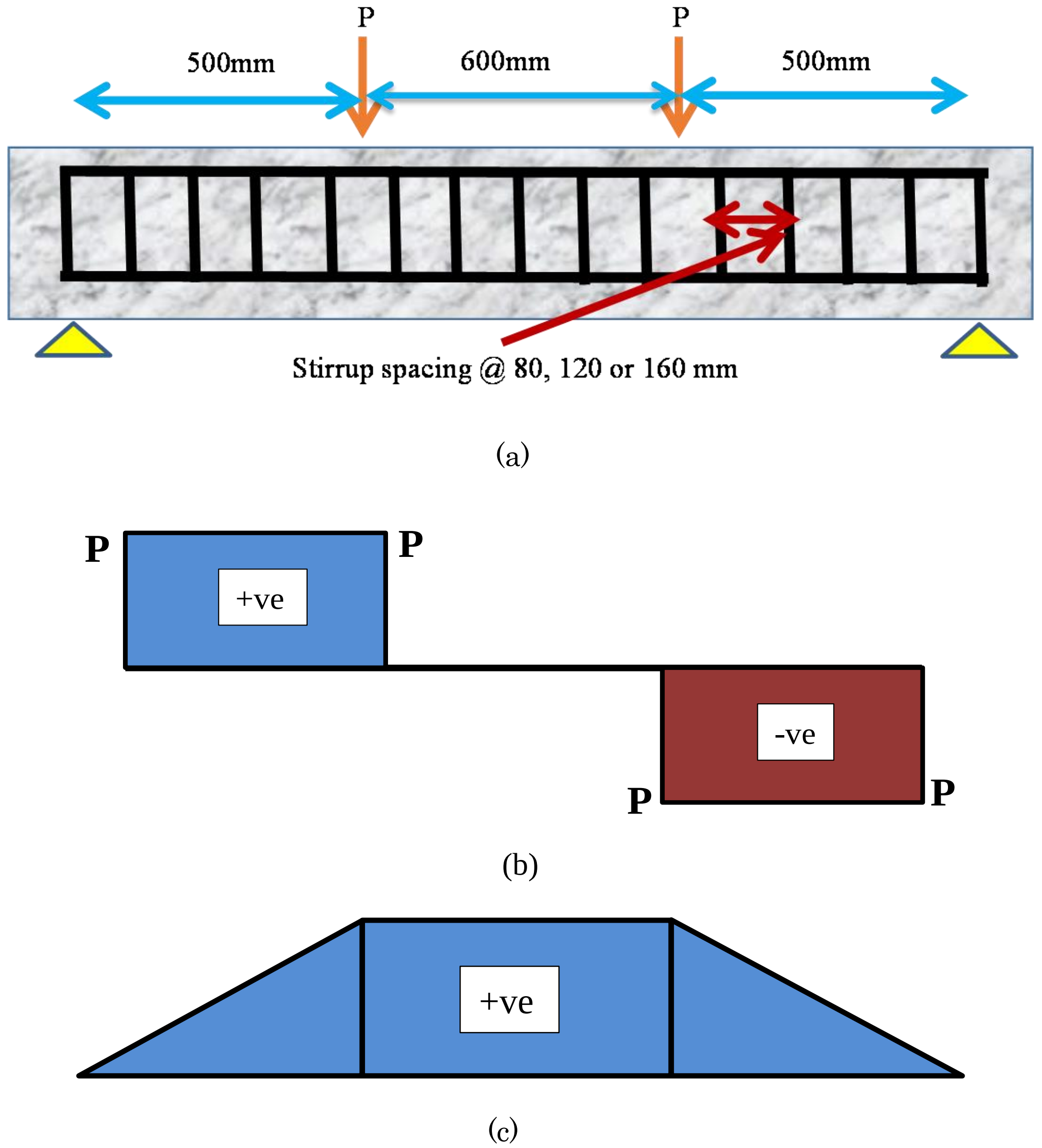

Figure 2.1 (a) Four-point bending test, (b) Shear force diagram, (c) Bending moment diagram

In the middle span, there is no shear force acting but stirrups are still provided. When the stirrups in the middle span will be corroded, there will be reduction in the cross-sectional area of the stirrup, reduction in the strength of steel along with loss in ductility. This reduction will have no effect on the structural performance of the beams which have good flexural designed and failure mode is also flexure. However, corrosion of stirrups will deteriorate the surrounding concrete, initiating and propagating corrosion cracks; and because of these deterioration, structural performance of the beam will be effected.

During the corrosion process the stirrup will be expanded and the corrosion products formed have a volume six times more than the steel, which exerts pressures on the surrounding concrete. This pressure increases with the increase in corrosion level and will exert tensile stresses in the concrete. Concrete is weak in tensile strength and by the exertion of tensile stresses by the corroding steel, it will cause cracking in the concrete. Moreover, the bond between stirrups and concrete will also be adversely affected. The flexural strength of beam comes from the contribution of longitudinal reinforcement and concrete. As the longitudinal reinforcement will not be corroded, there should not be any reduction in strength from this component. For the concrete, there should be some reductions in strength as the concrete will be deteriorated due to corrosion of stirrup. This reduction in strength of concrete is important to observe and for this reason, stirrups in the middle span is also corroded.

Previous research showed that the shear strength loss is also depended on the level of corrosion. With the increase in corrosion there will be increase in the average mass loss or area loss of stirrup and vice versa. For this reason, two levels or degree of corrosion was selected; mild and severe corrosion referring to 10% and 20% average mass loss respectively.

In brief, the factors which were varied in this study are (i) design failure mode which was governed by varying longitudinal reinforcement ratio, 2-D10; 2-D13 and 2-D16 mm longitudinal reinforcement were used, (ii) stirrup spacing, 80 mm; 120 mm and 160 mm spacing was used, (iii) location of corrosion, shear span; middle span or full span stirrup corrosion was allowed using 120 mm spacing, (iv) level of corrosion, mild corrosion (10% average mass loss) and severe corrosion (20% average mass loss) were used.

Accelerated corrosion technique was applied to corrode the stirrup using the direct current method. After corrosion, the distribution and width of corrosion cracks were marked and measured. Four-point loading test was carried out after marking and measuring the corrosion cracks. The distribution and width of flexural cracks were also measured and marked. At last the stirrups were taken out of the beams to quantify the mass loss in stirrups.

2.3 SPECIMEN PREPARATION

2.3.1 Beam Specifications

All the beams were casted with the same dimensions measuring 1800 mm long, 100 mm wide and 150 mm high with 30 mm concrete cover as shown in Figure 2.2. 100 mm from each side of the beam was left for the supports and loading span was 1600 mm. The beams were designed as doubly reinforced beams. Four-point bending test was applied to test the ultimate capacity of the beams with shear span of 500 mm on both sides and 600 mm the middle span as shown in Figure 2.2.

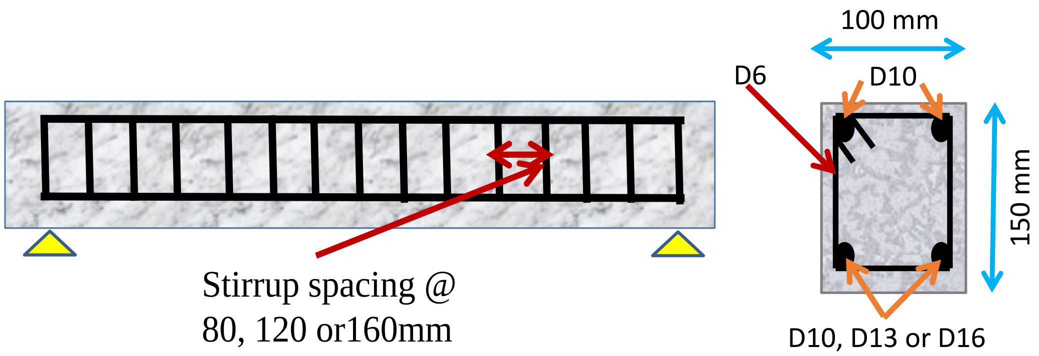

Figure 2.2 Beam layout and specifications

2.3.2 Concrete

All the beams were casted using high early strength Portland cement while coarse and fine aggregates were obtained from Shizunai River, Japan. The specific gravities of cement, coarse and fine aggregate are 3.16 g/cm^3, 2.77 g/cm^3 and 2.64 g/cm^3 respectively. The mix proportion for one cubic meter of concrete is shown in Table 2.1

Table 2.1 Mix proportion of concrete

	W/C (%)	s/a (%)	Water (kg)	Cement (kg)	Sand (kg)	Gravel (kg)
1 m^3 concrete	55	44.5	185	333	802	969

The water-to-cement ratio of 0.55 was used and f'c = 32 MPa was obtained. The results of stress-strain of concrete during cylinder tests is shown in Figure 2.3.

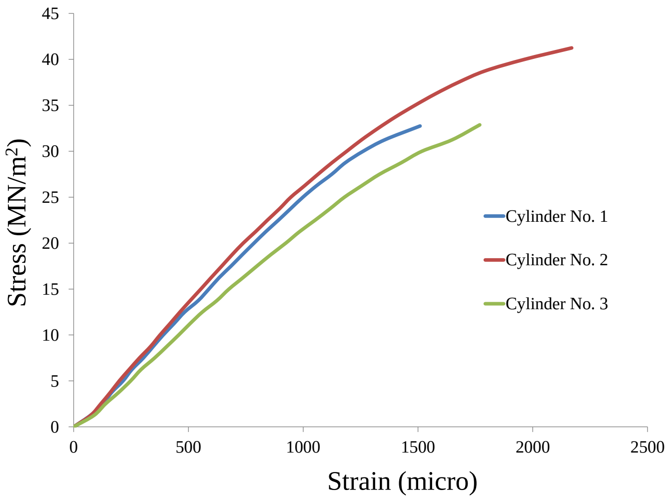

Figure 2.3 Stress-strain curves of concrete

2.3.3 Steel Rebars

Deformed steel bars of diameter 10 mm, 13 mm and 16 mm, where D10 bars are SD295A while D13 and D16 bars are SD345. The actual yield strength of longitudinal reinforcement was f_y = 387 MPa and were factory epoxy coated to avoid corrosion.

For stirrup, deformed steel bar of 6 mm in diameter with nominal yield strength f_y = 395MPa was used for all beams. Figure 2.2 illustrates the size and location of the reinforcing steel.

2.3.4 Experiment Design

The research plan consists of designing of three types of beams, (i) Beams with 2-D10 longitudinal reinforcement (ii) Beams with 2-D13 longitudinal reinforcement and (iii) Beams with 2-D16 longitudinal reinforcement. The failure mode of D10 and D13 beams is yielding of longitudinal reinforcement and ultimately fail in flexure while D16 beams will fail in flexural compression failure (crushing of concrete) somewhere near the yield strength of the longitudinal reinforcement. The stirrup spacing of all these beams are either 80 mm, 120 mm or 160 mm and each type of design will have two beams of similar spacing. One of the beam will have mild stirrup corrosion (10% average mass loss) while the other will have severe corrosion (20% average mass loss). In total, 39 beams were casted and each type of design contains 13 beams. Out of these 13 beams, three beams are the control beams with stirrup spacing 80 mm, 120 mm or 160 mm without stirrup corrosion. Each case has only one beam to represent to limit the quantum of work. Using 80 mm and 160 mm stirrup spacing, the stirrups were corroded in full span with both levels of corrosion, mild and severe corrosion.

To study the effect of stirrup corrosion at different locations, the stirrups are corroded in the shear span, the middle span or the full span using 120 mm stirrup spacing only. All the three types of beams (D10, D13 and D16) has stirrup corrosion in shear span, the middle span or the full span using 120 mm stirrup spacing. The corrosion of stirrups was produced using accelerated electrochemical method by using direct electric current. Two levels of corrosion were considered for this case also, mild and severe corrosion; and the expected mass loss for corroded stirrups was 10% and 20% respectively. Figure 2.4 shows the corrosion of stirrups at different locations in the beam with 120 mm stirrup spacing.

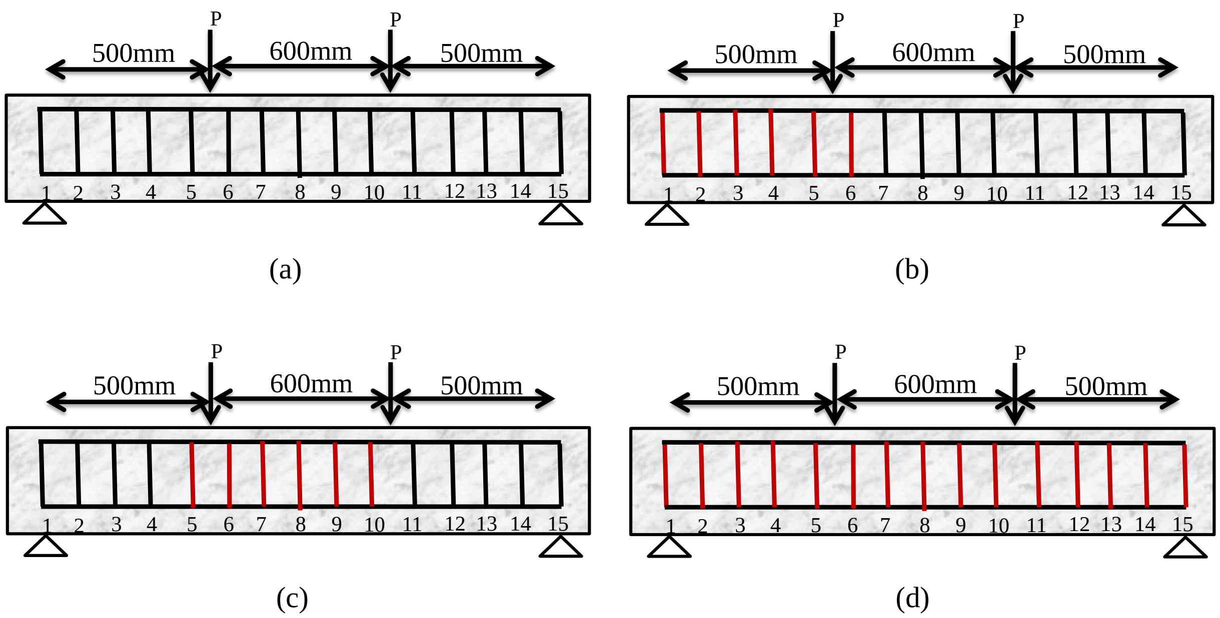

Figure 2.4 Corrosion of stirrups at different locations, (a) Control beams with no corrosion, (b) Corrosion of stirrups in the shear span, (c) Corrosion of stirrups in the middle span, and (d) Corrosion of stirrups in the full span

The stirrup in shear or full span is corroded to investigate the shear capacity of the corroded beam whereas in the middle span is corroded to study the effect of stirrup corrosion on the flexural behavior of stirrup corroded beams. Different behavior was observed for all the beams and with different levels of corrosion. Results of these beams are discussed in the subsequent sections. Figure 2.5 shows the pictorial experimental deign while table 2.2, 2.3 and 2.4 shows the beam test variables of D10, D13 and D16 beams respectively, in tabular form with the beam names. The nomenclature of the beams is also defined in the tables. Simply the beams are named as “B” beam no. mildly, severely corroded or control beam (M/S/C) “-” location of corrosion (FS/MS/SS) “-” diameter of longitudinal reinforcement/spacing of stirrups. For example, B22S-SS-13/120 is beam no. 22, corroded in the shear span, longitudinal reinforcement as 13 mm in diameter and stirrup spacing of 120 mm.

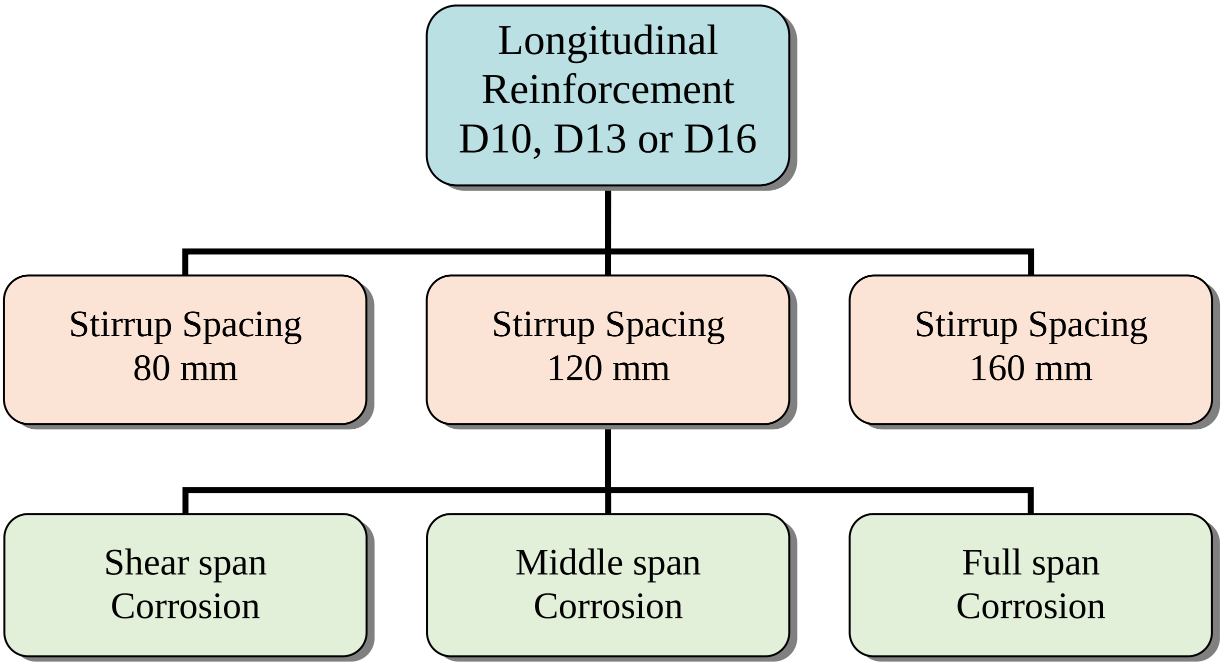

Figure 2.5 Experimental design of corroded and control beams

Table 2.2 Beams Test Variables of D10 beams

Beam No.	Call No.	Beam Description
1	B1C-10/80	Control beam with Bar No. 10 flexure reinforcement and 80mm stirrup spacing
2	B2C-10/120	Control beam with Bar No. 10 flexure reinforcement and 120mm stirrup spacing
3	B3C-10/160	Control beam with Bar No. 10 flexure reinforcement and 160mm stirrup spacing
4	B4M-FS-10/80	Beam Mildly corroded Full span with Bar No. 10 reinforcement and 80mm stirrup spacing
5	B5S-FS-10/80	Beam Severely corroded Full span with Bar No. 10 reinforcement and 80mm stirrup spacing
6	B6M-SS-10/120	Beam Mildly corroded Shear span with Bar No. 10 reinforcement and 120mm stirrup spacing
7	B7M-MS-10/120	Beam Mildly corroded Middle span with Bar No. 10 reinforcement and 120mm stirrup spacing
8	B8M-FS-10/120	Beam Mildly corroded Full span with Bar No. 10 reinforcement and 120mm stirrup spacing
9	B9S-SS-10/120	Beam Severely corroded Shear span with Bar No. 10 reinforcement and 120mm stirrup spacing
10	B10S-MS-10/120	Beam Severely corroded Middle span with Bar No. 10 reinforcement and 120mm stirrup spacing
11	B11S-FS-10/120	Beam Severely corroded Full span with Bar No. 10 reinforcement and 120mm stirrup spacing
12	B12M-FS-10/160	Beam Mildly corroded Full span with Bar No. 10 reinforcement and 160mm stirrup spacing
13	B13S-FS-10/160	Beam Severely corroded Full span with Bar No. 10 reinforcement and 160mm stirrup spacing

Table 2.3 Beams Test Variables of D13 beams

Beam No.	Call No.	Beam Description
14	B14C-13/80	Control beam with Bar No. 13 flexure reinforcement and 80mm stirrup spacing
15	B15C-13/120	Control beam with Bar No. 13 flexure reinforcement and 120mm stirrup spacing
16	B16C-13/160	Control beam with Bar No. 13 flexure reinforcement and 160mm stirrup spacing
17	B17M-FS-13/80	Beam Mildly corroded Full span with Bar No. 13 reinforcement and 80mm stirrup spacing
18	B18S-FS-13/80	Beam Severely corroded Full span with Bar No. 13 reinforcement and 80mm stirrup spacing
19	B19M-SS-13/120	Beam Mildly corroded Shear span with Bar No. 13 reinforcement and 120mm stirrup spacing
20	B20M-MS-13/120	Beam Mildly corroded Middle span with Bar No. 13 reinforcement and 120mm stirrup spacing
21	B21M-FS-13/120	Beam Mildly corroded Full span with Bar No. 13 reinforcement and 120mm stirrup spacing
22	B22S-SS-13/120	Beam Severely corroded Shear span with Bar No. 13 reinforcement and 120mm stirrup spacing
23	B23S-MS-13/120	Beam Severely corroded Middle span with Bar No. 13 reinforcement and 120mm stirrup spacing
24	B24S-FS-13/120	Beam Severely corroded Full span with Bar No. 13 reinforcement and 120mm stirrup spacing
25	B25M-FS-13/160	Beam Mildly corroded Full span with Bar No. 13 reinforcement and 160mm stirrup spacing
26	B26S-FS-13/160	Beam Mildly corroded Full span with Bar No. 13 reinforcement and 160mm stirrup spacing

Table 2.4 Beams Test Variables of D16 beams

Beam No.	Call No.	Beam Description
27	B27C-16/80	Control beam with Bar No. 16 flexure reinforcement and 80mm stirrup spacing
28	B28C-16/120	Control beam with Bar No. 16 flexure reinforcement and 120mm stirrup spacing
29	B29C-16/160	Control beam with Bar No. 16 flexure reinforcement and 160mm stirrup spacing
30	B30M-FS-16/80	Beam Mildly corroded Full span with Bar No. 16 reinforcement and 80mm stirrup spacing
31	B31S-FS-16/80	Beam Severely corroded Full span with Bar No. 16 reinforcement and 80mm stirrup spacing
32	B32M-SS-16/120	Beam Mildly corroded Shear span with Bar No. 16 reinforcement and 120mm stirrup spacing
33	B33M-MS-16/120	Beam Mildly corroded Middle span with Bar No. 16 reinforcement and 120mm stirrup spacing
34	B34M-FS-16/120	Beam Mildly corroded Full span with Bar No. 16 reinforcement and 120mm stirrup spacing
35	B35S-SS-16/120	Beam Severely corroded Shear span with Bar No. 16 reinforcement and 120mm stirrup spacing
36	B36S-MS-16/120	Beam Severely corroded Middle span with Bar No. 16 reinforcement and 120mm stirrup spacing
37	B37S-FS-16/120	Beam Severely corroded Full span with Bar No. 16 reinforcement and 120mm stirrup spacing
38	B38M-FS-16/160	Beam Mildly corroded Full span with Bar No. 16 reinforcement and 160mm stirrup spacing
39	B39S-FS-16/160	Beam Severely corroded Full span with Bar No. 16 reinforcement and 160mm stirrup spacing

2.3.4 Structural Design of Beams

2.3.4.1 Flexural Design of Beams

Under reinforced beams

All the beams were designed as doubly reinforced beams using beam theories proposed by Nilson et al. [26] and using ACI 318-11 code provisions. The failure mode of these beams was designed as flexural failure and the longitudinal reinforcement ratio is below the balanced condition. At first the beams will face yielding of the longitudinal reinforcement at a strain value of 0.004. After yielding, the beam will show plastic behavior as indicated in the load-deflection curves with an increase in the load carrying capacity and the deflections. In the plastic region, higher than the yield load and less than the peak load, the longitudinal reinforcement has already been yielded and more flexural cracks will occur. At the peak load the strain in the concrete will reach to 0.003. This type of design is mostly followed for real structures as it gives ample warning time before failure. Excessive cracking in concrete in the tension region occurs, when the tensile stresses in longitudinal reinforcement reach yield load. These excessive cracks and deflections in the concrete beam during loading are the indications of failure of the beam. The ACI building code also limits the strain in steel as 0.004 to ensure the balanced failure condition. Balanced failure condition means that tensile steel starts yielding at failure and the strain in concrete is about 0.003. The longitudinal reinforcement ratio at balanced failure condition is 0.024 for all of the beams.

Following are the design parameters and nominal load of beams according to ACI code [25]:

D10 Beams

The longitudinal reinforcement ratio of D10 beams is well below the ratio at balanced failure which shows that the beam follows a perfectly typical ductile behavior. The longitudinal reinforcement ratio of D10 beams is 0.0095 whereas the ratio at balanced failure is 0.024. Basic information relating to the beam design is as follows:

Area of steel of 10 mm diameter = 71 mm^2

Area of steel provided for compression reinforcement (10 mm dia) = A_s' = 71 x 2 = 142 mm^2

Area of steel provided for tensile reinforcement = A_s = 71 x 2 = 142 mm^2

Compressive strength of concrete = f'_c = 32 MPa

Maximum tensile reinforcement ratio for balance failure = ρ_b = 0.0241

Maximum area of steel provided = A_s = 142 mm^2
(which is **less than $A_{s,max}$=361.5 mm^2**, so yielding of longitudinal reinforcement will occur)

Nominal yield load capacity of all D10 beams = P = 14.44 kN
It is the single load P of four-point bending test. For ultimate nominal load multiply P with 2.

Ultimate nominal yield capacity of D10 beams = 2P = 28.88 kN

D13 Beams

The longitudinal reinforcement ratio of D13 beams is also below than the ratio at balanced failure which illustrates that the beam will also fail in flexure. However, the longitudinal reinforcement ratio of D13 beams are higher than D10 beams showing that D13 beams will have lesser plastic region than

D10 beams. In other words, the deflection or cracking from the yield load to the ultimate load will be lesser than the D10 beams and shorter plastic behavior will be reflected in the load-deflection curve. The longitudinal reinforcement ratio of D13 beams is 0.0172 as compared to 0.0241 which is the ratio at balanced failure. Basic information relating to the beam design is as follows:

Area of steel of 13 mm diameter = 129 mm^2

Area of steel provided for compression reinforcement (10 mm dia) = A_s' = 71 x 2 = 142 mm^2

Area of steel provided for tensile reinforcement = A_s = 129 x 2 = 258 mm^2

Compressive strength of concrete = f'_c = 32 MPa

Maximum tensile reinforcement ratio for balance failure = ρ_b = 0.0241

Maximum area of steel provided = A_s = 258 mm^2
(which is **less than $A_{s,max}$=361.5 mm^2**, so yielding of longitudinal reinforcement will occur)

Nominal yield load capacity of all D13 beams = P = 20.6 kN
It is the single load P of two point loading test. For ultimate nominal load multiply P with 2.

Ultimate nominal yield capacity of D13 beams = 2P = 41.2 kN

Over reinforced beams

Over reinforced beams are the beams which have longitudinal reinforcement ratio higher than the ratio at the balanced failure. These beams were designed so that the flexural capacity should not be exhausted much earlier than the shear capacity and can provide much higher loads. The behavior of stirrup corrosion can be investigated easily and a good connection in the results can be established between under and over reinforced beams. D16 beams design is the over reinforced beam design and is explained as follows.

D16 Beams

The longitudinal reinforcement ratio of D16 beams is 0.0265 which is slightly higher than the ratio at balanced failure conditions which is 0.0241. The difference between the two ratios is not very high which means that D16 beams will fail at a load somewhere near the yield load. The plastic region in the load-deflection curve will be the smallest compared to D10 and D13 beams and will not be fully developed. Instead flexural compression failure due to crushing of concrete will occur and beams will fail near the nominal yield load. Basic information relating to the beam design is as follows:

Area of steel of 16 mm diameter = 199 mm^2

Area of steel provided for compression reinforcement (10 mm dia) = A_s' = 71 x 2 = 142 mm^2

Area of steel provided for tensile reinforcement = A_s = 199 x 2 = 398 mm^2

Compressive strength of concrete = f'c = 32 MPa

Maximum tensile reinforcement ratio for balance failure = ρ_b = 0.0241

Maximum area of steel provided = A_s = 398 mm^2
(which is ***greater than As_{max}=361.5 mm^2,*** theoretically failure will be crushing of concrete)

Nominal load capacity of all D16 beams = P = 30.65 kN
It is the single load P of two point loading test. For ultimate nominal load multiply P with 2.

Ultimate nominal yield capacity of D16 beams = 2P = 61.3 kN

2.3.4.2 Shear Design of Beams

The shear capacity of beams were designed using the shear design equations defined in chapter 11 of ACI 318-11. To make the design equations simple, shear strength of concrete was calculated using the concrete compressive strength f'c, effective width and depth of the beam. The shear strength of stirrup was calculated using effective area of the stirrup in the section, yield strength of stirrup, effective depth of the beam and stirrup spacing. In these calculations, the longitudinal reinforcement effect is not taken but research shows that the longitudinal reinforcement provides dowel action which increases shear strength a little. However, ACI does not account considerably this effect as the amount of longitudinal reinforcement is at the bottom and once the shear crack is formed in the concrete above the longitudinal reinforcement, the shear crack will propagate and shear failure may occur. To make a conservative design, as the shear failure is brittle, the influence of longitudinal reinforcement is not considered in ACI design equations and as well as in this study. The basic information of the shear design of the beams are as follows. With the change in the stirrup spacing, the shear capacity of the stirrup will change and the shear strength of concrete will be constant.

<u>For 80 mm stirrup spacing</u>

Shear strength of concrete = V_c = 23.08 kN

Shear strength provided by steel = V_s = 66.98 kN

Total nominal shear capacity of beams = 90.06 kN

<u>For 120 mm stirrup spacing</u>

Shear strength of concrete = V_c = 23.08 kN

Shear strength provided by steel = V_s = 44.66 kN

Total nominal shear capacity of beams = 67.74 kN

<u>For 160 mm shear stirrup spacing</u>

Shear strength of concrete = V_c = 23.08 kN

Shear strength provided by steel = V_s = 33.48 kN

Total nominal shear capacity of beams = 56.56 kN

If the flexural capacity and shear capacity of D10 beams are compared, it can be seen that the difference between the two capacities is very large and the beams will fail in flexure. After the stirrup corrosion it was also expected that the beam will still fail in flexure because it was assumed that the stirrup corrosion cannot reduced the capacity to that extend. The flexural capacity of D13 beams are higher than D10 beams but still considerably less than the shear capacity. It was expected that the severely corroded beams might fail in shear after stirrup corrosion. The flexural capacity of D16 beams is very large and in the comparable range of shear strength. The nominal shear capacity of D16 with 160 mm stirrup spacing is less than the flexural strength and for 120 mm stirrup spacing the difference is not so high. The shear strength of 80 mm spacing is quite large compared to the flexural strength. Therefore, it was expected that 160 mm and 120 mm stirrup spacing beams with D16 longitudinal reinforcement will fail in shear, for both mild and severe corrosion, but except for the middle span corrosion. It was also anticipated that severely corroded 80 mm spacing beam might also fail in shear but the mildly corroded beam will not fail. The test results including the type of failures are discussed in detail in chapter 3.

2.4 CORROSION TECHNIQUE AND ARRANAGEMENTS

The corrosion of stirrups was induced by accelerated electrochemical method and using direct electric current. A wire was connected at the top of stirrups using soldering to facilitate the passage of electric current for corrosion. The joint of wire with stirrup was epoxy coated to avoid corrosion at this place. If this joint is broken current will not pass through the stirrup and hence there will be no corrosion. Figure 2.6 shows the preparation of stirrups and soldering process to attach the wire on the top of stirrups.

(a)

(b)

Figure 2.6 (a) Preparation of stirrups and (b) soldering process

The longitudinal reinforcement, both compression and tension rebars were insulated at the stirrup location by using the insulation plastic tape to prevent any transmission of electrical current and to avoid corrosion of the longitudinal reinforcement. After attaching the wire at the top of each stirrup, the steel cage of the reinforcement was fixed and formwork was prepared. Figure 2.7 shows formwork arrangement and preparations for casting of the beams.

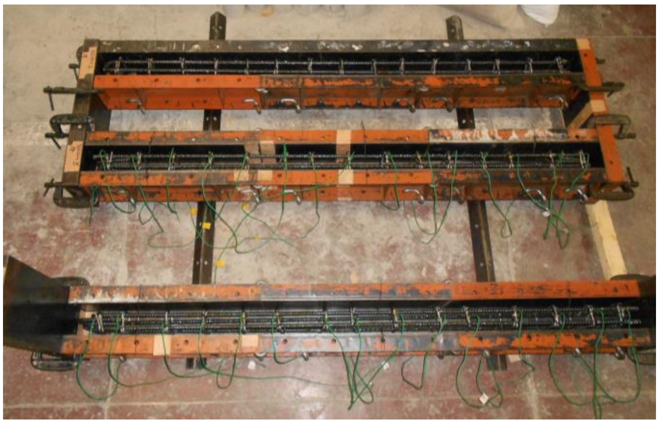

Figure 2.7 Formwork and other preparations for casting of concrete beams

After 14 days of curing, the beams were prepared for the accelerated corrosion exposure to corrode the stirrup. A sponge was placed on both sides of the beam and wrapped with towels all around. The sponge will facilitate the chloride ion penetration in the concrete from side surfaces which is the intended location of corrosion and towels will provide moist conditions. Major contribution of shear strength of stirrup is provided by the vertical sides of the stirrup in a cross-section, which is the reason why the sponges were attached on the sides of the beam. Figure 2.8 shows the prepared beams which are ready for the application of electric current for stirrup corrosion.

Figure 2.8 Beams attached with sponge and prepared for corrosion exposure

The beams were placed in a pool with 3% NaCl solution on one of its side. The height of solution was upto the mid of sponge level so that chloride ion can pass through the sponge and reach to the side of the concrete surface. The wires of the stirrups were connected to three sources of power supply called Supply A, B and C which was further connected to main DC controller power supply. This DC controller was the main control of the electric current and the amount of current can be adjusted through this device. Figure 2.9 shows the arrangement for electric current and beams in pool with 3% NaCl solution.

(a) **(b)**

Figure 2.9 (a) Current supply arrangement and (b) Beams in pool for accelerated corrosion

Corrosion was carried out in two series referring to mild and severe corrosion. A current density of 0.94 mA/cm^2 was passed for 13 days and 26 days for mild and severe corrosion respectively [24]. The sides of the beam was changed every two days so that the chloride penetration can be allowed on both sides and both sides should have identical exposure conditions. Moreover, this can also ensure the wet and dry cycles exposure which also accelerates corrosion process.

Current was measured once a day at 10:00 hours using clamp on the DC current meter. Different amounts of current passed through all the stirrups as the resistance changes for each of them. The resistance depends on the distance between the electrodes and the electrolyte present between them. In this case, the resistance depends on the pore size distribution and non-homogeneity of concrete. Different amounts of current resulted in different percentages of mass loss which also resembles natural conditions because corrosion is not uniform throughout the member.

The stirrups were connected to the positive terminal and acted as anode. A stainless steel plate was placed at the bottom of pool which acted as cathode. Figure 2.10 shows the schematic diagram for the corrosion exposure arrangement.

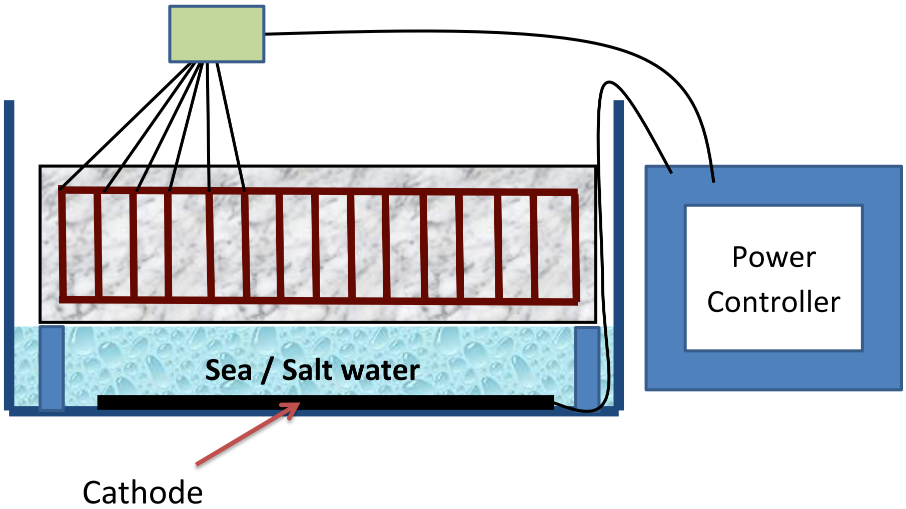

Figure 2.10 Schematic diagram for the accelerated corrosion exposure

2.5 EXPERIMENTAL TESTS AND PROCEDURES

After casting the beams and curing was allowed for 14 days, the beams were subjected to the accelerated electrochemical treatment to corrode the stirrup. The exposure duration was 13 days and 26 days for mild and severe corrosion respectively. Corrosion cracks distribution and width were marked after corrosion exposure and four-point bending test was conducted to observe the ultimate load carrying capacity of the corroded beams. After the beams were failed, the cracks produced during the loading, flexural or shear cracks, their distribution and widths were also marked and compared with each other. Finally the concrete was crushed and stirrups were taken out to measure mass loss.

2.5.1 Mass Loss

Mass loss is the parameter which can determine the amount of corrosion quantitatively. Roughly, 10% mass loss is referred to mild corrosion and 20% to severe corrosion. Before casting, each stirrup was weighed after attaching the wire and epoxy coating the electric joint, and a number was assigned to the stirrup. At the end of bending tests and marking the flexural cracks, the stirrups are taken out to by crushing the concrete. The stirrups are placed in 10% diammonium hydrogen citrate solution for 24 hours at 60^0C to remove the corrosion products. When the corrosion products are removed, the stirrups are weighed again to check the mass loss.

2.5.2 Marking Corrosion and Flexural Cracks

The corrosion and flexural cracks are measured using the manual crack meter scale. After measuring the cracks, corrosion cracks were marked with black marker and flexural or shear cracks with the red marker. A grid of 50 mm x 50 mm on the surfaces of the beam was made to estimate the crack width distribution and lengths of the corrosion, flexural or shear cracks. Figure 2.11 shows the crack meter scale used to measure cracks.

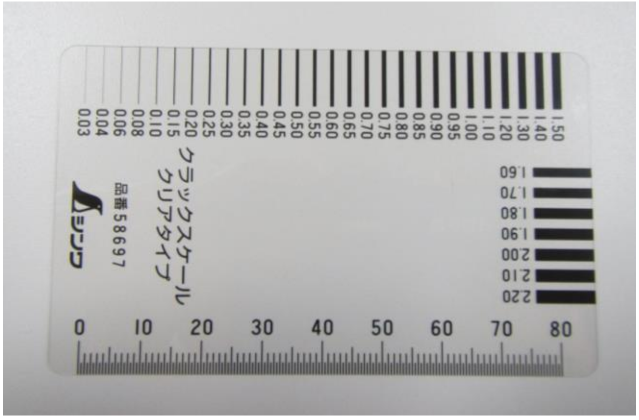

Figure 2.11 Crack meter scale for marking cracks

2.5.3 Four-Point Bending Test

After marking the corrosion cracks, the beams are subjected to four-point bending test. In four-point bending test, the central middle zone has zero shear force and maximum bending moment. The stirrups are provided in the middle zone also, but these stirrups have no contribution to the flexural strength. The deterioration of concrete can be observed as the cracks due to corrosion will damage and crack the concrete and it is assumed that the flexural load carrying capacity will be reduced. If one point load was selected, this phenomenon will be difficult to observe.

The beam was 1800 mm in length, and 100 mm from each side was excluded for the roller support. The two points load was applied at a distance of 600 mm from the ends of the beam. This makes the shear span from support as 500 mm and the middle span which is the maximum moment span as 600 mm. Two linear variable differential transformers (LVDT) were used to measure displacement / deflection at the mid-span of the beam. Eleven strain gauges, six at the center throughout the depth of the beam, three in a rosette near support, and two at an angle of 45° to each other in the center of the shear span, were used to measure the strains for future finite element analysis. The strain gauges and LVDTs were connected to the data logger which was attached to a computer to observe the strains and deflections. Figure 2.12 shows the schematic loading arrangement while Figure 2.13 shows the actual four-point bending arrangement.

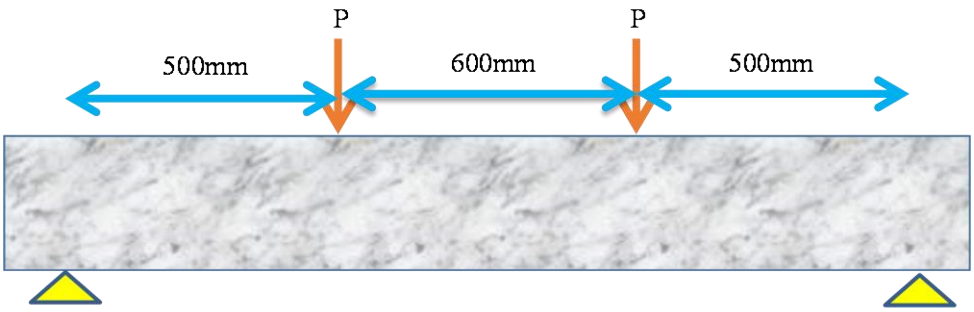

Figure 2.12 Four-point bending test schematic diagram

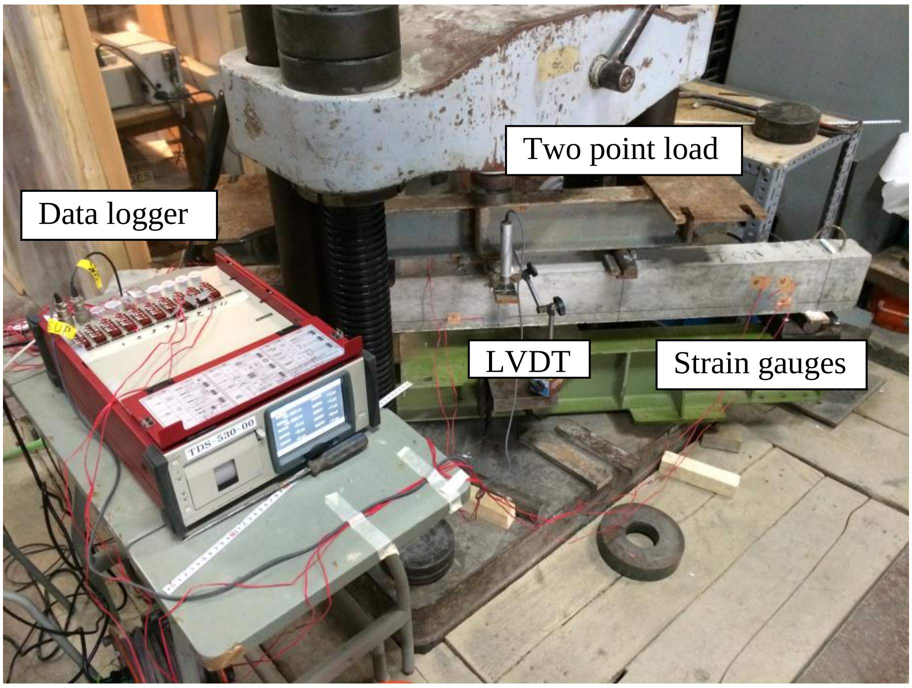

Figure 2.13 Four-point bending test arrangement

CHAPTER **3**

TEST RESULTS AND DISCUSSIONS

Chapter 3

TEST RESULTS AND DISCUSSIONS

In this chapter, test results of all the corroded beams and the control beams are discussed. The results of the mass loss of stirrup, frequency of corrosion cracks, location, crack widths and their distribution are summarized. After the four-point bending test, the flexural or shear cracks formation, their location and crack widths are documented. Finally the ultimate load carrying capacity of the corroded beams are compared with the control beams, the reduction in the load carrying capacity is evaluated and the residual shear capacity of the corroded beams is predicted.

The results of all the beams are divided in two groups based on the design of the un-corroded control beams. These groups are (i) under reinforced section (ii) over reinforced section. In both the groups, the beams are sub-grouped in 3 categories. Category (1) comprises of corroded beams with 80 mm stirrup spacing with mild and severe corrosion level. Category (2) includes the stirrup corrosion in shear span, middle span or the full span with mild and severe corrosion level. Category (3) consists of corroded beams with 1600 mm stirrup spacing with mild and severe corrosion level.

3.1 MASS LOSS OF STIRRUPS

The mass loss of each stirrup depended on the amount of electric current passed through them. Different amounts of current passed from all stirrups as the resistance changes for each of them. The resistance depends on the distance between the electrodes and the electrolyte present between them. In this case, the resistance depends on the pore size distribution and non-homogeneity of concrete. Different amounts of current resulted in different percentages of mass loss which also resembles real time conditions because corrosion is not uniform throughout the member.

Three kinds of corrosion were observed in the corroded stirrups. (i) Generalized corrosion, where the length of the stirrup has uniform corrosion (ii) Localized corrosion, formation of uneven and non-homogenous corrosion pattern was observed, concentration of corrosion at a specific along with some pitting corrosion. (iii) Vanished portion of stirrup, the corrosion at a specific location was too severe that part of the stirrup was completely gone because of corrosion, found in some severely corroded stirrup and very rare in the mildly corroded stirrup. The longitudinal reinforcement was checked for any signs of corrosion by removing the epoxy coating and was observed that the longitudinal reinforcement was not corroded. Few longitudinal reinforcement had corrosion stains which were due to the stirrup corrosion, while many of the longitudinal reinforcement did not have even corrosion stains.

Figure 3.1 shows the location of each stirrup in the beam for 120 mm stirrup spacing beam. The number of stirrups were 23, 15 and 11 for stirrup spacing 80 mm, 120 mm and 160 mm respectively. In all the graphs of mass loss, the stirrup number on horizontal axis represents the location of the stirrup in the beam whereas vertical axis displays the percentage average mass loss of each stirrup. This can give a good idea about the variations in the mass loss of stirrups in the corroded beams. The mass loss of few mildly and severely corroded stirrups area presented in the following section.

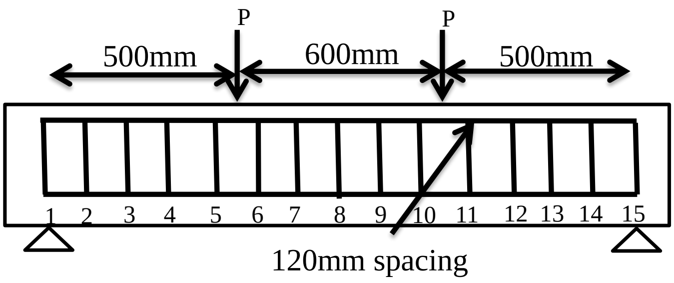

Figure 3.1 Stirrup location of beams with 120 mm spacing

3.1.1 Mildly Corroded Beams

Figure 3.2 represents the mass loss in percentage of all the stirrups of five mildly corroded beams. The mass loss of all the stirrup varied as the electrical current changes through each stirrup depending on the resistance provided by the concrete. This different amounts of current resulted in variation of the mass loss of each stirrup. The targeted mass loss for mild corrosion was 10% mass loss and the average of all the stirrups of one beam is almost 10% mass loss with a wide variation in the mass loss. B25M-FS-13/160 has an average mass loss of 11.41% and standard deviation of 3.99; while B38M-FS-16/160 had 11.04% and 2.67 respectively. These two beams had a little higher average mass loss. B30M-FS-16/80 and B33M-MS-16/120 had average mass loss approximately 10% and standard deviation of 3.79 and 3.31 respectively. B34M-FS-16/120 had mass loss a little lesser than 10%; which was 9.66% with the standard deviation of 5.04.

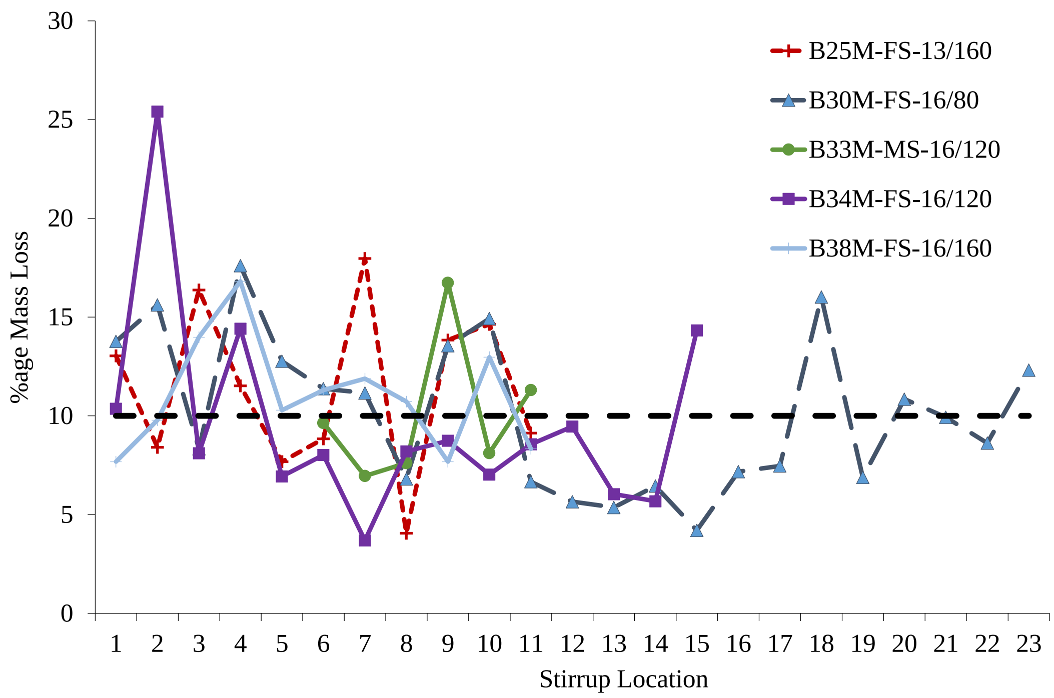

Figure 3.2 %age mass loss of mildly corroded beams

3.1.2 Severely Corroded Beams

Figure 3.3 illustrates the mass loss in percentage of all the stirrups of four severely corroded beams. As observed in mild corrosion, the variations in the mass loss was also observed in the severely corroded beams with a variation in the average mass loss too. B18S-FS-13/80 and B5S-FS-10/80 had average mass loss approximately 20% with the standard deviation of 5.98 and 7.15 respectively. B36S-MS-16/120 and B37S-FS-16/120 had average mass loss a little less than the targeted value; 19.11% and 16.54% respectively with the standard deviation of 5.06 and 6.57 respectively. The high values of the standard deviation shows that the mass loss variations of severely corroded beams is much higher than the mildly corroded beams.

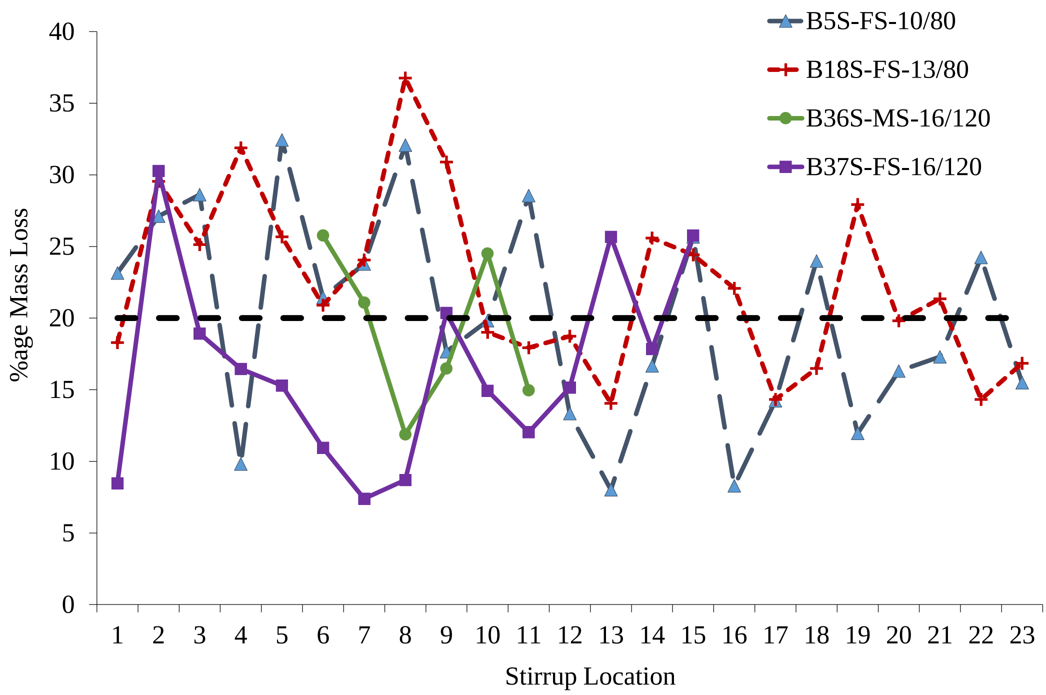

Figure 3.3 %age mass loss of severely corroded beams

3.2 CORROSION CRACKS OF CORRODED BEAMS

Corrosion of steel rebars in reinforced concrete structures produces cracking which causes strength reduction in both, reinforcing steel and concrete. The crack widths due to corrosion depends on the tensile stress induced to concrete by corroding steel rebar. The intensity of tensile stress due to stirrup corrosion depends on the stirrup diameter, bond conditions between concrete and steel, quality of concrete, concrete cover, transverse (stirrup) reinforcement ratio and the distance between two adjacent corroding rebars. The adjacent stirrups in a corroded beam will undergo the process of corrosion resulting the generation of tensile stresses in the surrounding concrete. The interaction and intensity of the tensile stresses produced will also depend on the stirrup spacing. If the stirrups are closely spaced, the surrounding concrete between the two adjacent stirrups will be less. This tensile stress is also a function of the amount of corrosion received by the stirrups. Hence, all of these factors, including the stirrup spacing and the amount of corrosion are important factors to determine the deterioration and cracking due to corrosion of stirrups.

The corrosion cracks in the corroded beams were present on all the four sides of the beam at the places where stirrup corrosion was accelerated. The corrosion cracks formed were of different lengths, widths and orientation. Each corrosion crack was marked one crack with similar crack width but irrespective of its length and orientation. Most of the cracks were along the length of the stirrups (vertical cracks along the depth of the beam) but few diagonal and horizontal cracks (along the length of the beam) were also observed. The corrosion cracks widths and their distribution formed on front and back sides of the corroded beams are also shown in the relevant sections. A gird of 5 x 5 mm was drawn on the beams to understand the corrosion cracks length and orientation. Detailed analysis of the corrosion cracks is discussed in the subsequent sections.

3.2.1 Under Reinforced Section

(1) Mildly corroded beams with 120 mm stirrup spacing

Figure 3.4 shows the corrosion crack widths frequency of beams with D10 as flexural reinforcement, 120 mm stirrup spacing and mildly corroded in shear span, middle span or full span. B6M-SS-10/120 has 34 total number of corrosion cracks. 15 cracks were found in the crack width range of 0.03-0.05 mm and about 44% corrosion cracks lie in this crack width range. 12 cracks lie in the crack with range of 0.06-0.09 mm which is 35% of the corrosion cracks. 20% corrosion cracks (7 cracks) were greater than 0.1 mm crack width. In this beam the number of corrosion cracks in the narrowest crack width range was the least. B7M-MS-10/120 beam had stirrup corrosion in the middle span. As the corrosion was in the middle span with mild level, most of the corrosion cracks were in the narrow crack width range. A total of 35 corrosion cracks were observed with 26 cracks in the range of 0.03-0.05 mm while 8 cracks in the crack width range of 0.06-0.09 mm was observed. 1 crack was present in the crack width range of 0.1-0.15 mm. The total number of corrosion cracks are almost same for shear span and middle span cases, as the number of stirrups allowed to b corroded was same (6 stirrups). B8M-FS-10/120 has 100 corrosion cracks with 69 cracks in the narrower crack width range 0.03-0.05 mm. Almost 70 % of the corrosion cracks lie in this crack width range. 3 cracks lie in the crack width range of 0.2-0.25 mm. The total corrosion cracks observed in the full span beam was more as the corroded number of stirrups. Figure 3.5 shows the corrosion crack widths and distribution of D10, 120 mm mildly corroded beams in shear span, middle or full span.

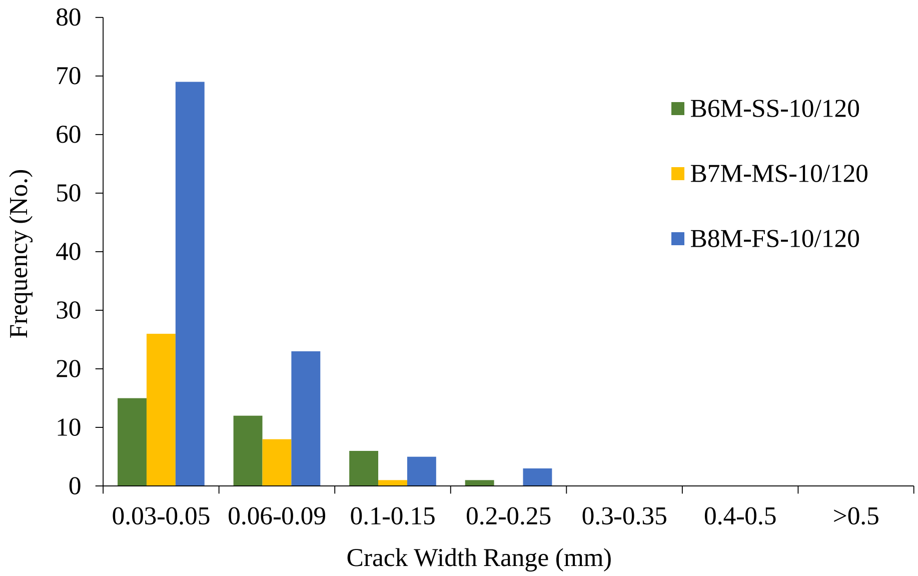

Figure 3.4 Corrosion cracks frequency of D10, 120 mm beams mildly corroded

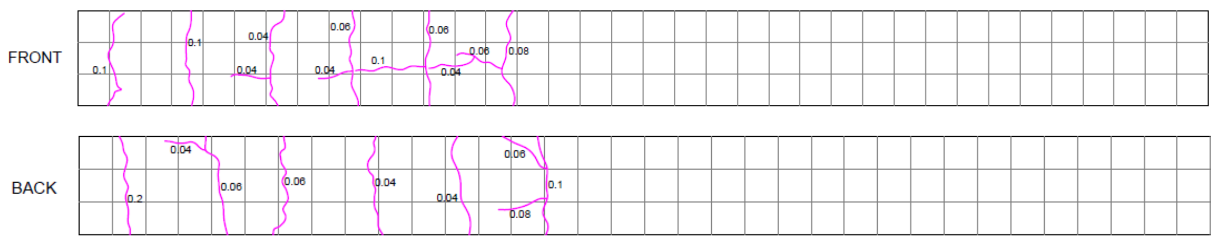

B6M-SS-10/120

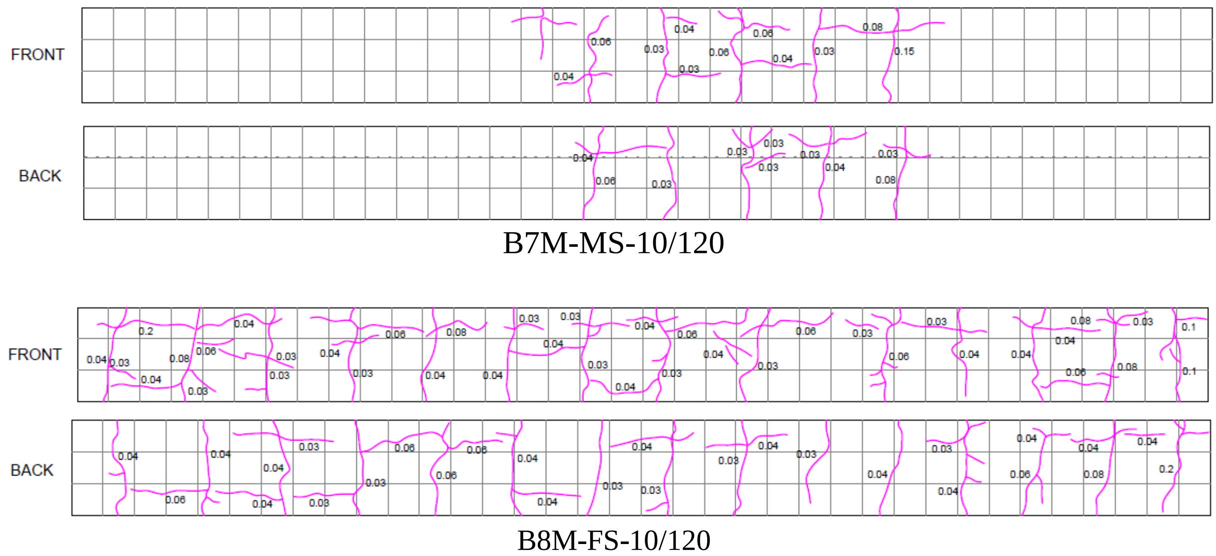

Figure 3.5 Corrosion cracks distribution of D10, 120 mm beams mildly corroded

(2) Severely corroded beams with 120 mm stirrup spacing

Figure 3.6 shows the corrosion crack widths frequency of beams with D10 as flexural reinforcement, 120 mm stirrup spacing and severely corroded in shear span, middle span or full span. B9S-SS-10/120 has a total number of 74 corrosion cracks compared to 34 which were present in the identical beam with mild corrosion level. It shows that with the increase in the degree of corrosion, the corrosion cracks increased. The maximum corrosion cracks lied in the crack width range of 0.03-0.05 mm with 47%. This means that still with the increase in the corrosion level, the maximum corrosion cracks were observed in the narrower crack width range. However, wider cracks in severely corroded beams were also observed, unlike the mildly corroded beams. 14 cracks were present in the crack width range of 0.1-0.15 mm while 6 cracks were present in the range of 0.2-0.25 mm. 32% corrosion cracks were wider than 0.1 mm while in the same identical beam with mild corrosion, B6M-SS-10/120 had 20%. B10S-MS-10/120 had a total of 109 corrosion cracks. In this beam 38 corrosion cracks, 35% were in the narrower crack width range of 0.03-0.05 mm. 35 cracks lie in the range of 0.06-0.09 mm making 32% of corrosion cracks. The percentage of wider cracks were more in this beam. B11S-FS-10/120 had total of 150 corrosion cracks with the maximum cracks in the narrower crack width range 0.03-0.05 mm, 43% of the total corrosion cracks. 48 corrosion cracks are in the range of 0.06-0.09 mm with 32%, while 21 cracks were in the range of 0.1-0.15 mm, 14%. Wider corrosion cracks in this beam was also observed compared with the identical mildly corroded beam. Figure 3.7 shows the corrosion crack widths and distribution of D10, 120 mm mildly corroded beams in shear span, middle or full span.

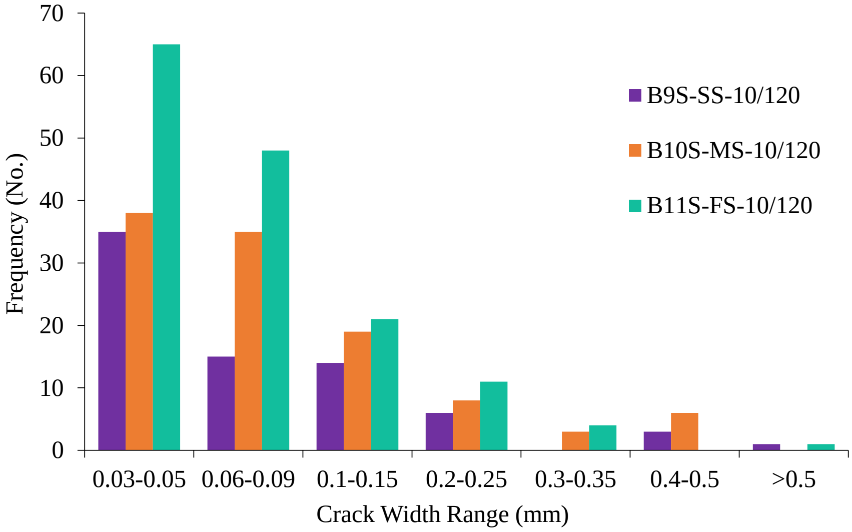

Figure 3.6 Corrosion cracks frequency of D10, 120 mm beams severely corroded

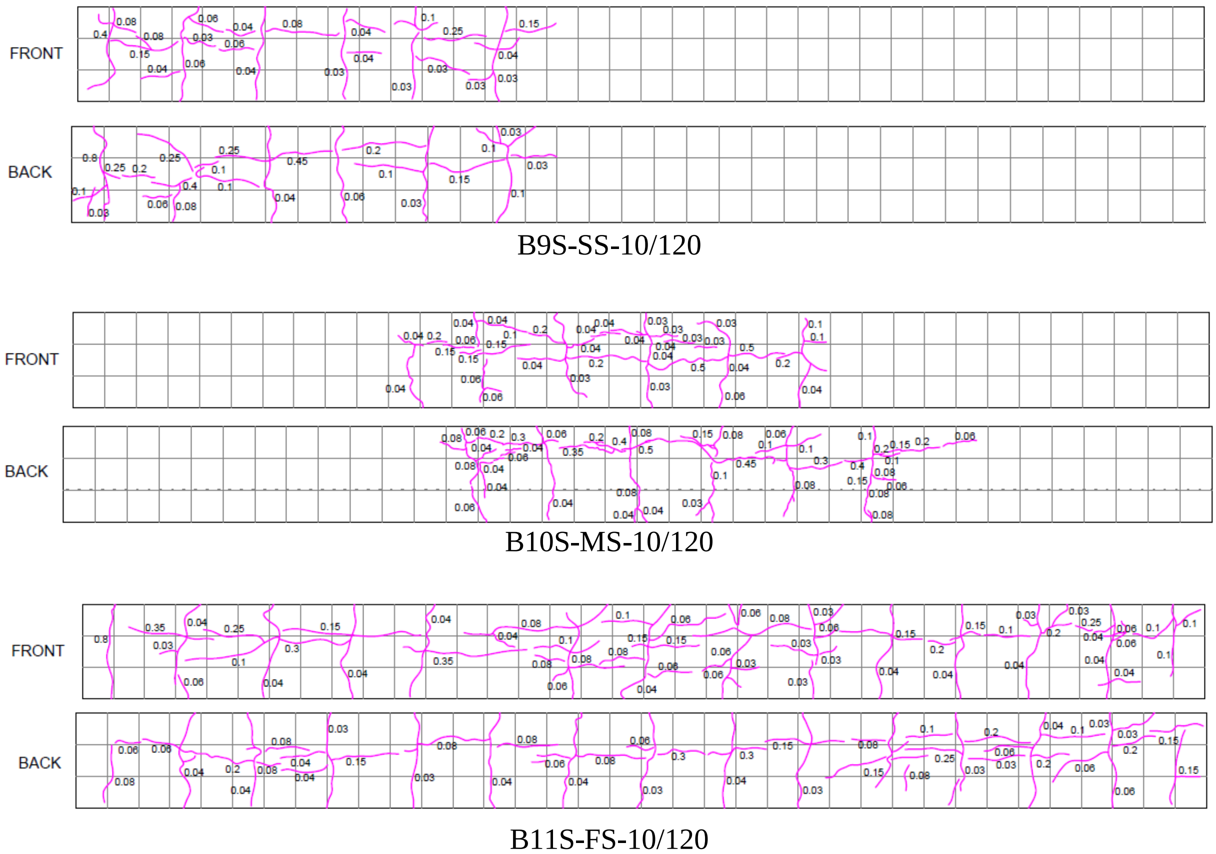

Figure 3.7 Corrosion cracks distribution of D10, 120 mm beams severely corroded

(3) Mildly and severely corroded beams with 80 and 160 mm stirrup spacing

Figure 3.8 shows the corrosion crack widths frequency of beams with D10 as flexural reinforcement, with stirrup spacing 80 mm and 160 mm, mildly and severely corroded in full span. It can be seen that as the corrosion level increases, the maximum number of corrosion cracks also increased. B4M-FS-

80/120 had 109 total corrosion cracks and 71 cracks lie in the narrower crack width range 0.03-0.05 mm which are 65% of the corrosion cracks. Narrower corrosion cracks were observed in this beam and only 3% corrosion cracks were wider than 0.2 mm, 3 cracks. B5S-FS-10/80 is the same identical beam as B4M-FS-10/80 except that the former is the mild level. B5S-FS-10/80 had 115 total corrosion cracks and 72 cracks were in the narrower crack width range of 0.03-0.05 mm, 63%. Though this beam was severely corroded, but the corrosion cracks of this beam are more towards narrower crack width range. This can be assumed that the stirrup did not undergo severe corrosion and the result of mass loss is important in this case. 25% corrosion cracks lied in the range of 0.06-0.09 mm, and 88% corrosion cracks were narrower than 0.1 mm which is unlike the other severely corroded beams. B12M-FS-10/160 had 67 total corrosion cracks and the beam with 80 mm stirrup spacing, B4M-FS-10/80 had 109 corrosion cracks. It can be said that as the stirrup spacing decreases, the total number of corrosion cracks increases which also depicts more deterioration. B12M-FS-10/160 had the maximum cracks in the narrower crack width range 0.03-0.05 mm which is 48% of the total corrosion cracks. The percentage of the corrosion cracks in the narrowest crack width range is a little less than the other mildly corroded beams which shows that the stirrup might receive a little higher corrosion than the other mildly corroded beams. The mass loss of stirrup in this case is also important and should be seen in line with the corrosion cracks data. However, wider corrosion cracks were not observed in this case and only 2 corrosion cracks were wider than 0.2 mm. B13S-FS-10/160 had 116 corrosion cracks with 55 cracks in the crack width range of 0.03-0.05 mm, 47% of corrosion cracks. 37 cracks lied in the range of 0.06-0.09 mm while 21% corrosion cracks were wider than 0.1 mm. Figure 3.9 shows the corrosion crack widths and distribution of D10, 80 mm and 160 mm stirrup spacing with mild and severe corrosion in the full span.

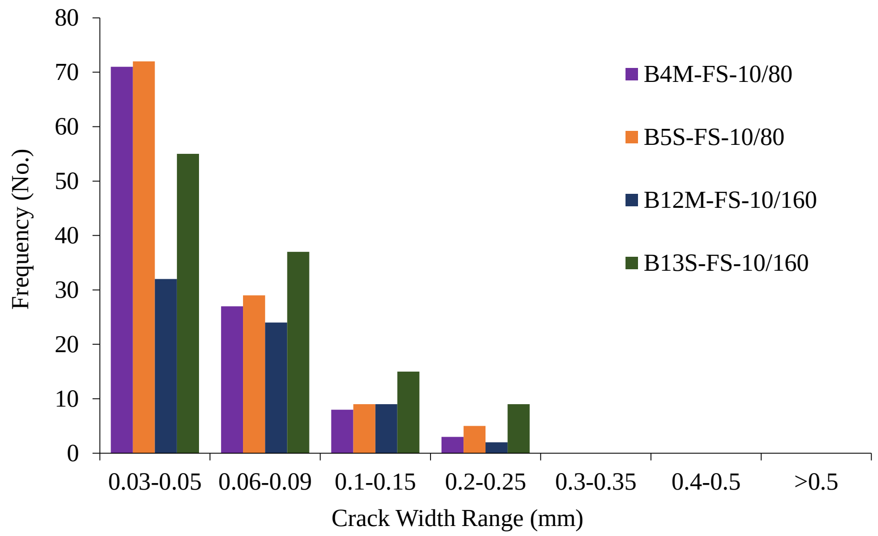

Figure 3.8 Corrosion cracks frequency of D10, 80 mm and 160 mm beams

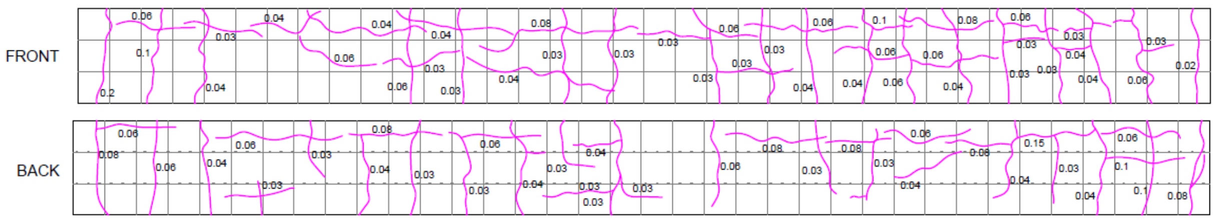

B4M-FS-10/80

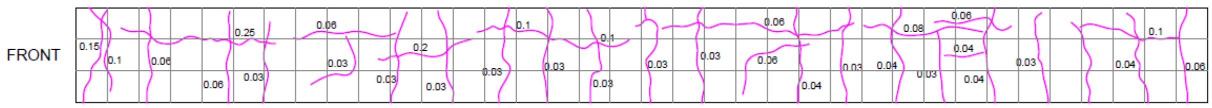

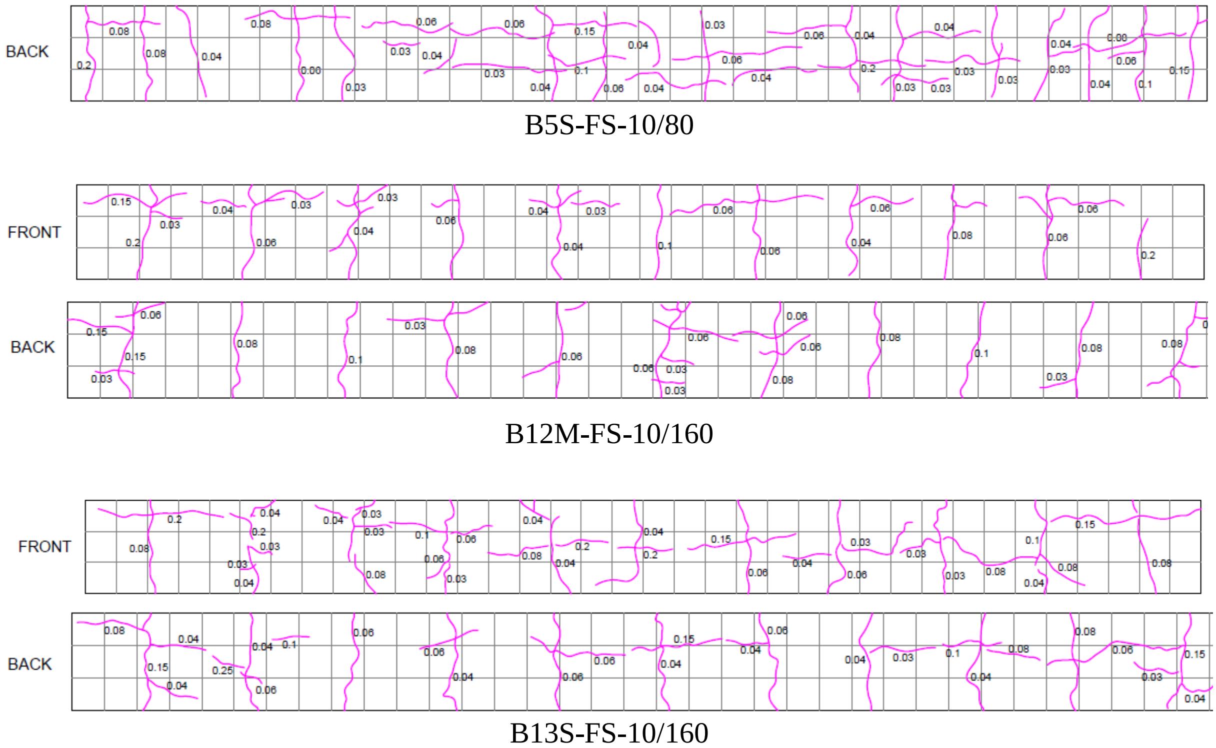

Figure 3.9 Corrosion cracks distribution of D10, 80 mm and 160 mm beams

3.2.2 Balanced Reinforced Section

(1) Mildly corroded beams with 120 mm stirrup spacing

Figure 3.10 shows the corrosion crack widths frequency of beams with D13 as flexural reinforcement, 120 mm stirrup spacing and mildly corroded in shear span, middle span or full span. B19M-SS-13/120 has a total number of 52 corrosion cracks with the maximum cracks in the narrower crack width range 0.03-0.05 mm, 32 cracks which comprises 61% of the corrosion cracks. 9 cracks lie in the range of 0.06-0.09 mm, 17% while 3 cracks were wider than 0.2 mm which is 6%. B20M-MS-13/120 had 53 corrosion cracks which is almost same as B19M-SS-13/120 because both beams at same degree of corrosion and same length of span. 40 corrosion cracks lie in the narrower crack width range of 0.03-0.05 mm which is 75% of corrosion cracks while 9 cracks lie in the range of 0.06-0.09 mm, 17%. Narrow corrosion cracks were observed in this beam and only 4 cracks were in the range of 0.1-0.15 mm. B21M-FS-13/120 had 85 corrosion cracks with maximum cracks in the narrower crack width of 0.03-0.05 mm with 57 cracks, 67% of corrosion cracks. 21 cracks lied in the range of 0.06-0.09 mm, 25% cracks. In this case also, narrower corrosion cracks were observed and 7 cracks lie in the range of 0.1-0.15 mm with no corrosion crack wider than 0.2 mm. Figure 3.11 shows the corrosion crack widths and distribution of D13, 120 mm mildly corroded beams in shear span, middle or full span.

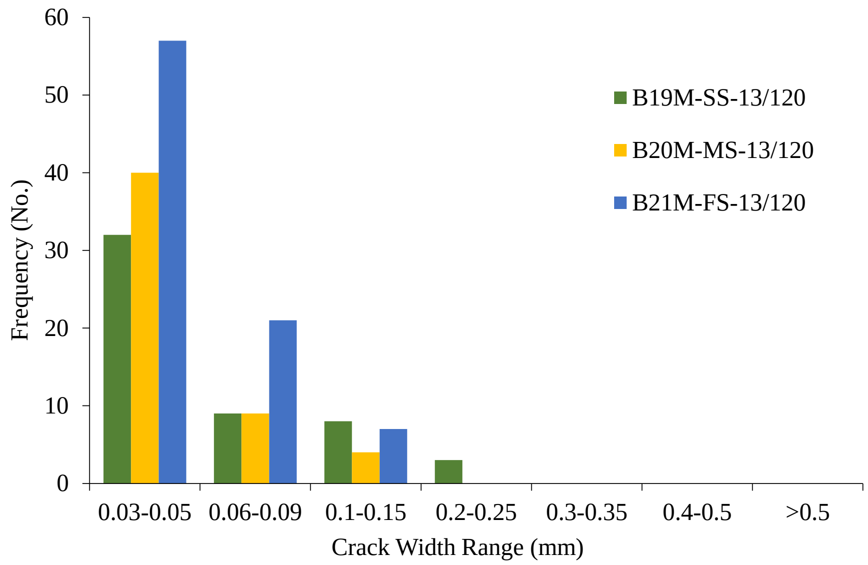

Figure 3.10 Corrosion cracks frequency of D13, 120 mm beams mildly corroded

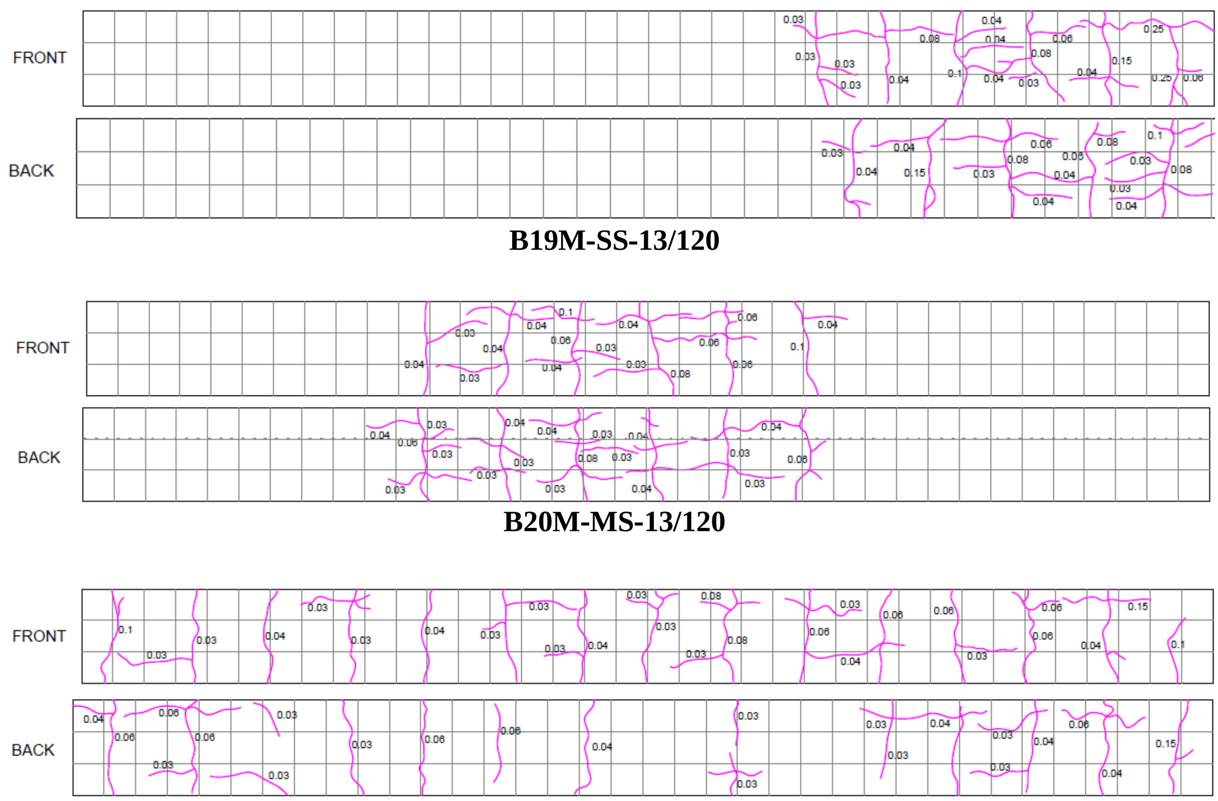

Figure 3.11 Corrosion cracks distribution of D13, 120 mm beams mildly corroded

(2) Severely corroded beams with 120 mm stirrup spacing

Figure 3.12 shows the corrosion crack widths frequency of beams with D13 as flexural reinforcement, 120 mm stirrup spacing and severely corroded in shear span, middle span or full span. B22S-SS-13/120 had 55 corrosion cracks with maximum cracks in the crack width range of 0.03-0.05 mm and 22 cracks were observed in this crack width range which constitutes 40 % of the corrosion cracks. Though the number of corrosion cracks are not much and maximum cracks lied in the narrower crack width range, but still relatively wider corrosion cracks were observed compared to identical mildly corroded beam B19M-SS-13/120 as this beam severely corroded. 16 cracks lied in the range of 0.06-0.09 mm while 12 cracks in 0.1-0.15 mm with 29% and 13% respectively. 10% corrosion cracks were wider than 0.2 mm. B23S-MS-13/120 had 47 corrosion cracks with 12 cracks in the narrower crack width range of 0.03-0.05 mm, 26%. In this beam wider corrosion cracks were observed and maximum cracks lied in the range of 0.06-0.09 mm with 18 cracks forming 38% of the total corrosion cracks. 9 corrosion cracks lied in the range of 0.1-0.15 mm, 19 % of the corrosion cracks while 8 cracks were wider than 0.2 mm which is 17% of the total corrosion cracks. B24S-FS-13/120 had 105 total corrosion cracks with maximum corrosion cracks in the narrower crack width range 0.03-0.05 mm, 58 cracks which is 55% of the total corrosion cracks. 15 cracks were in the range of 0.06 -0.09 mm while 14 cracks in the range of 0.2-0.25 mm comprising 14% and 13% of the corrosion cracks. As this beam is also severely corroded, wider corrosion cracks were observed in this beam too. Figure 3.13 shows the corrosion crack widths and distribution of D13, 120 mm severely corroded beams in shear span, middle or full span.

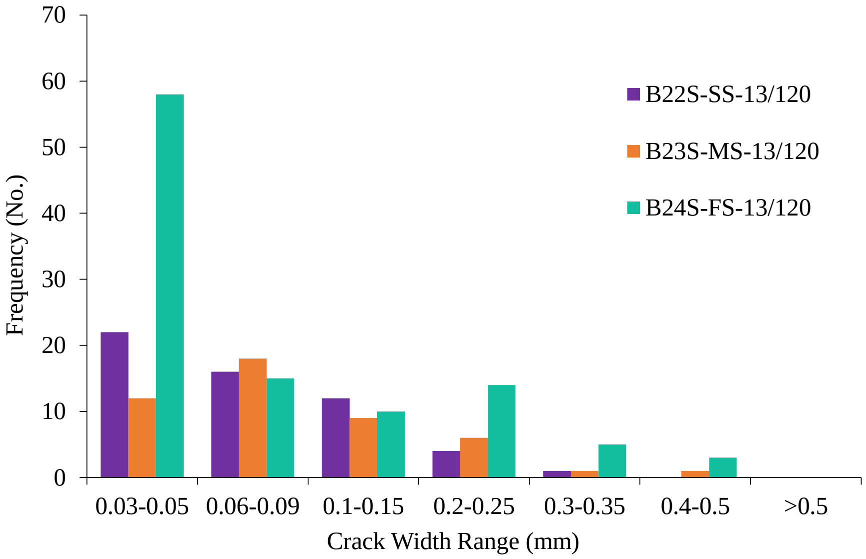

Figure 3.12 Corrosion cracks frequency of D13, 120 mm beams severely corroded

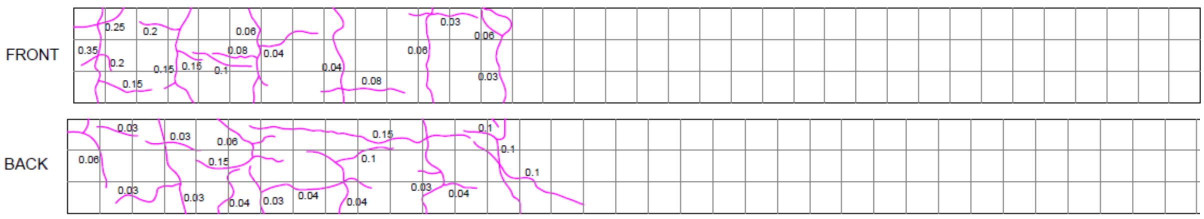

B22S-SS-13/120

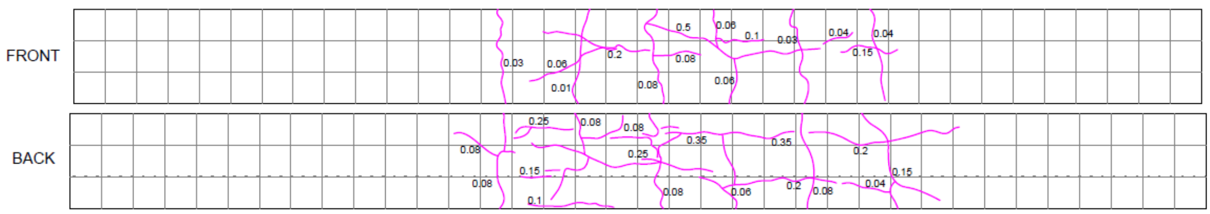

B23S-MS-13/120

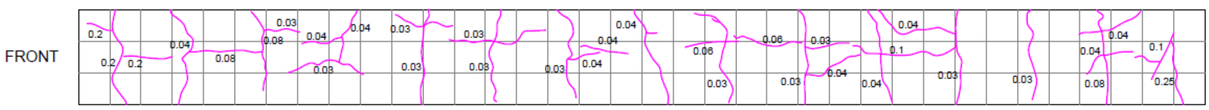

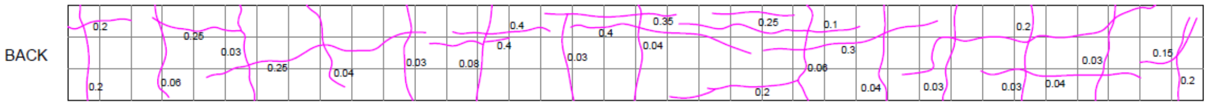

B24S-FS-13/120

Figure 3.13 Corrosion cracks distribution of D13, 120 mm beams severely corroded

(3) Mildly and severely corroded beams with 80 and 160 mm stirrup spacing

Figure 3.14 shows the corrosion crack widths frequency of beams with D13 as flexural reinforcement, with stirrup spacing 80 mm and 160 mm, mildly and severely corroded in full span. It can be seen clearly again that as the corrosion level increases, the maximum number of corrosion cracks also increased. B17M-FS-13/80 had a total of 110 corrosion cracks with maximum corrosion cracks in the crack width range of 0.03-0.05 mm and 79 cracks were observed with 72% of corrosion cracks. Narrower corrosion cracks were observed in this beam as it was mildly corroded and no crack was wider than 0.2 mm. 215 corrosion cracks lied in the range of 0.06-0.09 mm while 7% were 0.1-0.15 mm. B18S-FS-13/80 had 138 corrosion cracks and maximum corrosion cracks lied in the range of 0.03-0.05 mm forming 60% of the corrosion cracks. However, relatively wider corrosion cracks were observed in this beam compared to the same identical beam with mild corrosion B17M-FS-13/80 and 40% of the corrosion cracks were wider than 0.06 mm. B25M-FS-13/160 had 58 corrosion cracks which is far less than 80 mm mildly corroded beam B17M-FS-13/80. This implies that as the stirrup spacing is increased the number of corrosion cracks decreased because the number of stirrups which will be corroded also decrease. Maximum corrosion cracks lied in the crack width range of 0.03-0.05 mm and 67% of the corrosion cracks were present in this crack width range. 11 cracks were in the range of 0.06-0.09 mm while 7 cracks in the range of 0.1-0.15 mm. Relatively less corrosion cracks were observed in this beam compared to 80 mm mildly corroded beam and narrower corrosion cracks were observed compared to severely corroded 160 mm stirrup spacing beam. B26S-FS-13/160 had 115 total corrosion cracks and maximum corrosion cracks lied in the range of narrower crack width range 0.03-0.05 mm with 62 cracks making 54% of corrosion cracks. 31 cracks lied in the range of 0.06-0.09 mm while 13 lied in 0.1-0.15 mm with 27% and 11% respectively, whereas 9 cracks were wider than 0.2 mm. Figure 3.15 shows the corrosion crack widths and distribution of D13, 80 mm and 160 mm stirrup spacing with mild and severe corrosion in the full span.

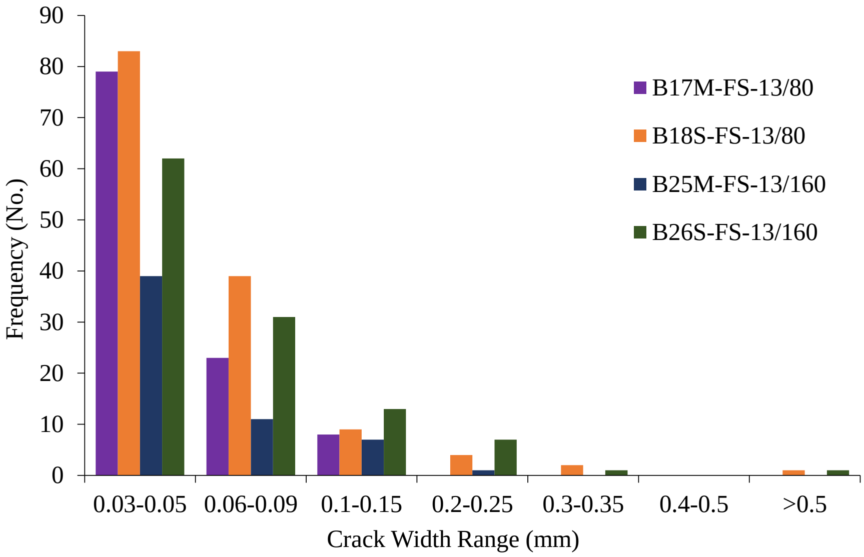

Figure 3.14 Corrosion cracks frequency of D13, 80 mm and 160 mm beams

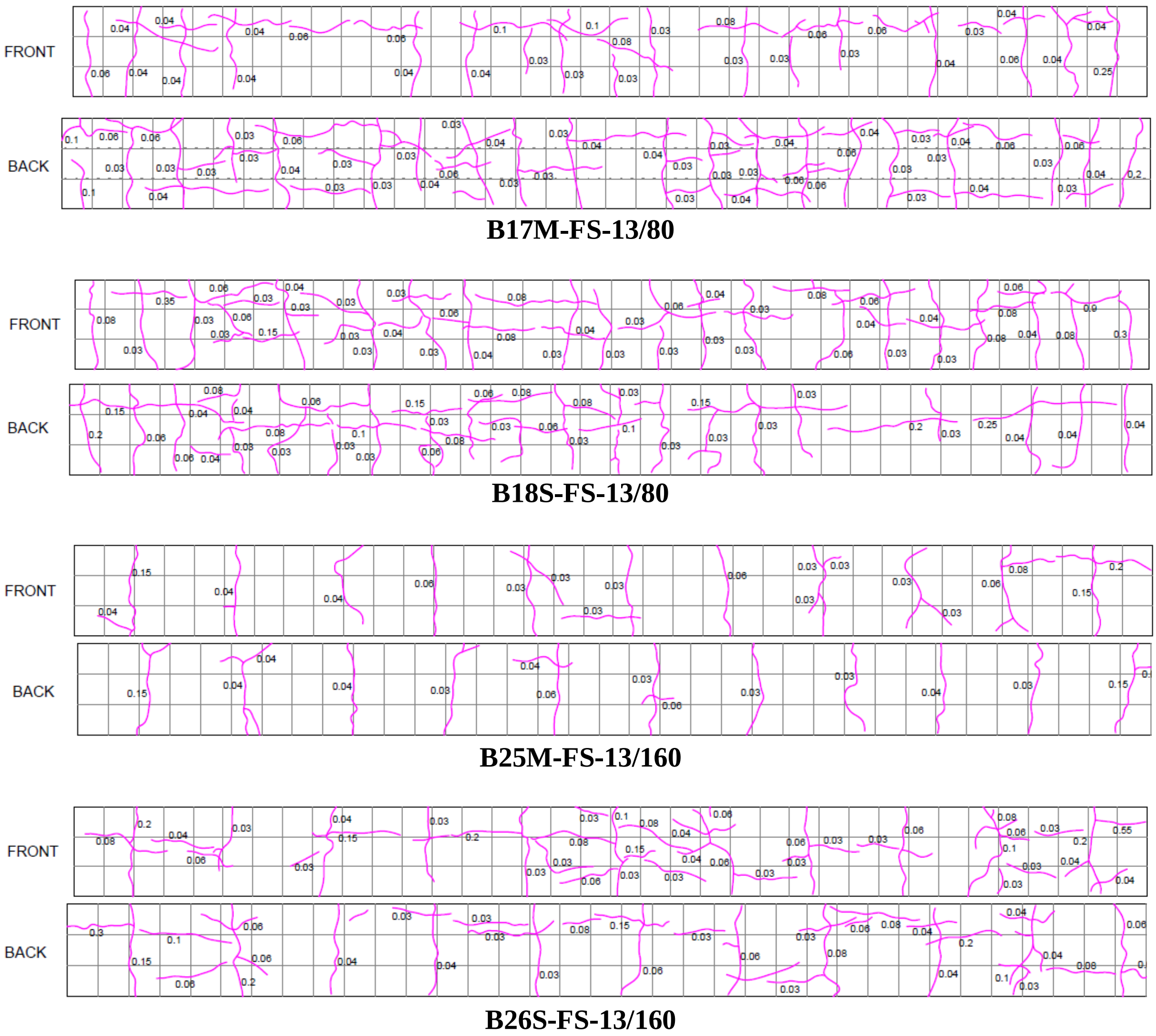

Figure 3.15 Corrosion cracks distribution of D13, 80 mm and 160 mm beams

3.2.3 Over Reinforced Section

(1) Mildly corroded beams with 120 mm stirrup spacing

Figure 3.16 shows the corrosion crack widths frequency of beams with D16 as flexural reinforcement, 120 mm stirrup spacing and mildly corroded in shear span, middle span or full span. B32M-SS-16/120 had 32 corrosion cracks with the maximum cracks in the narrower crack width range of 0.03-0.05 mm comprising 63% of the total corrosion cracks. As the corrosion level is mild and the corrosion span is only shear span, the corrosion cracks were not much compared with the severe corrosion beams and other cases. 7 corrosion cracks lied in the range of 0.06-0.09 mm while 5 cracks were wider than 0.1 mm. B33M-MS-16/120 had also same situation as B32M-SS-16/120 and 26 corrosion cracks were observed in this beam. B32M-MS-16/120 had also stirrup corrosion in the middle span only and mild level, so much cracking was not observed. 22 corrosion cracks which were 85% of the total corrosion cracks lied in the narrower crack width range of 0.03-0.05 mm. B34M-FS-16/120 had 117 total corrosion cracks which is much higher than the shear span or the middle span corroded beams. Maximum corrosion crack in this beam also lied in the narrower crack width range of 0.03-0.05 mm and 73 cracks, 63% of corrosion cracks were observed. In this beam relatively wider corrosion cracks were observed compared with the shear and middle span mildly corroded beams. 21 cracks lied in the range of 0.06-0.09 mm while 14 cracks lied in the range of 0.1-0.15 mm with 18% and 12%

respectively. 8% of the corrosion cracks were wider than 0.2 mm. Figure 3.17 shows the corrosion crack widths and distribution of D16, 120 mm mildly corroded beams in shear span, middle or full span.

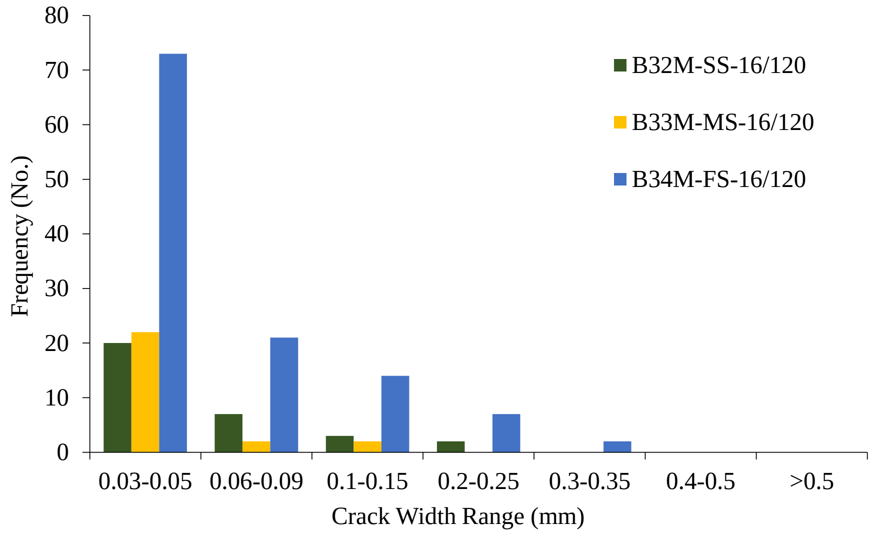

Figure 3.16 Corrosion cracks frequency of D16, 120 mm beams mildly corroded

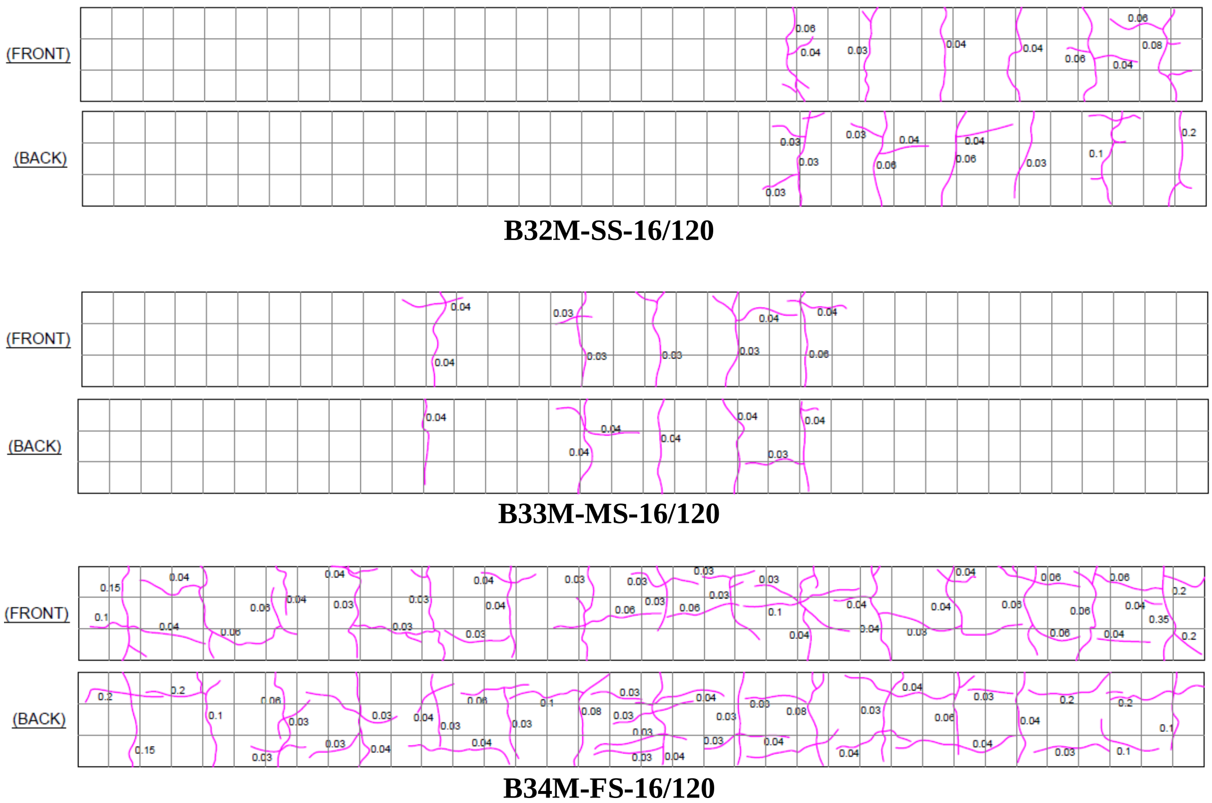

Figure 3.17 Corrosion cracks distribution of D16, 120 mm beams mildly corroded

(2) Severely corroded beams with 120 mm stirrup spacing

Figure 3.18 shows the corrosion crack widths frequency of beams with D16 as flexural reinforcement, 120 mm stirrup spacing and severely corroded in shear span, middle span or full span. B35S-SS-

16/120 had 112 corrosion cracks with maximum cracks in the crack width range of 0.03-0.05 mm and 40 corrosion cracks forming 36% of corrosion cracks were observed. This beam had exceptionally high corrosion cracks and wider corrosion cracks were observed in this beams. 37 cracks lied in the range of 0.06-0.09 mm while 23 in the range of 0.1-0.15 mm with 33% and 21% respectively. 12 cracks which are 10% of the corrosion cracks were wider than 0.2 mm. B36S-MS-16/120 had 69 corrosion cracks and 44 cracks lied in the range of 0.03-0.05 mm, 64% of corrosion cracks. 11 cracks were wider than 0.1 mm making 16% of corrosion cracks. B37S-FS-16/120 had 141 total corrosion cracks, and maximum cracks observed was in the crack width range of 0.03-0.05 mm with 69 cracks and 49% of corrosion cracks. In this beam, relatively wider cracks were observed and 20 cracks were in the range of 0.1-0.15 mm, 14% and 10 cracks were wider than 0.2 mm. Corrosion cracks wider than 0.3 mm were also observed in this beam. Figure 3.19 shows the corrosion crack widths and distribution of D16, 120 mm severely corroded beams in shear span, middle or full span.

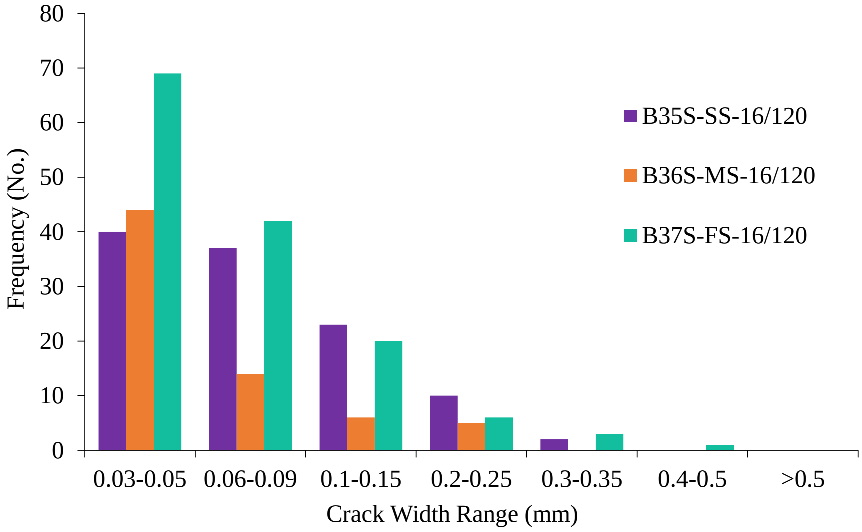

Figure 3.18 Corrosion cracks frequency of D16, 120 mm beams severely corroded

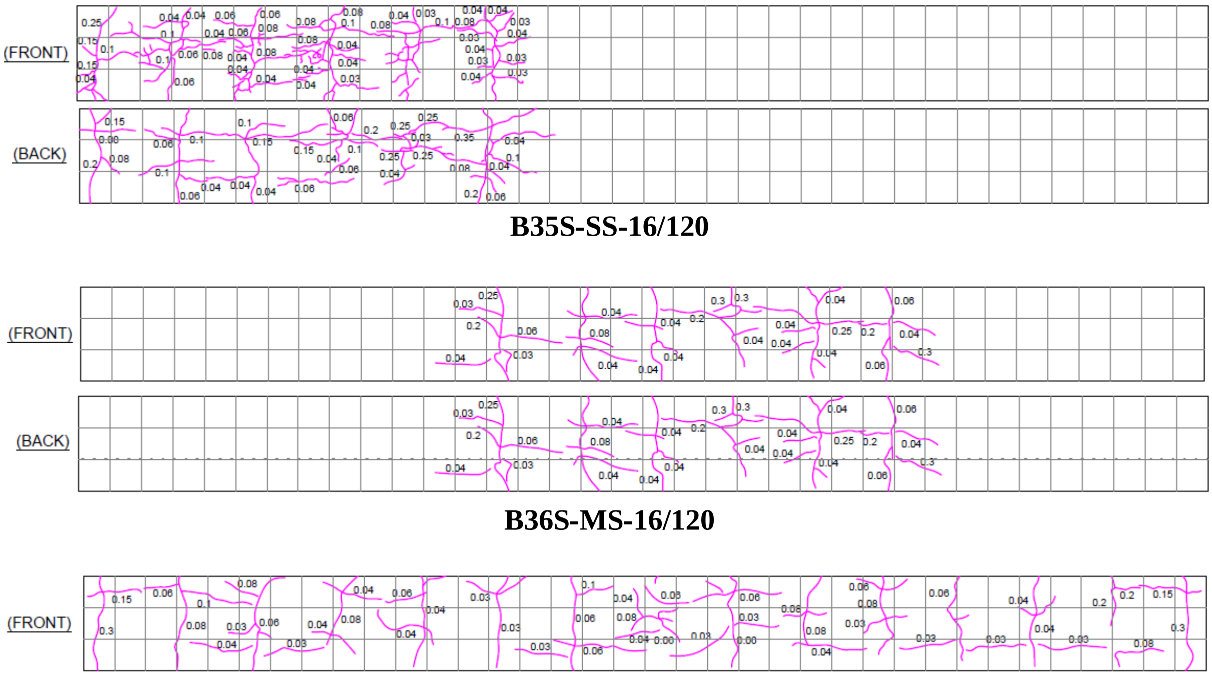

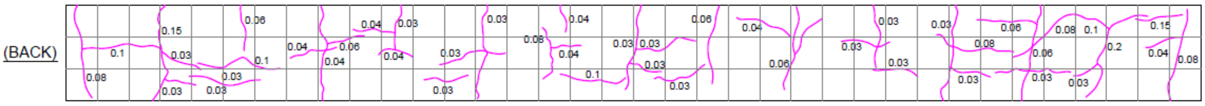

B37S-FS-16/120

Figure 3.19 Corrosion cracks distribution of D16, 120 mm beams severely corroded

(3) Mildly and severely corroded beams with 80 and 160 mm stirrup spacing

Figure 3.20 shows the corrosion crack widths frequency of beams with D16 as flexural reinforcement, with stirrup spacing 80 mm and 160 mm, mildly and severely corroded in full span. It can be seen again that as the corrosion level increases, the maximum number of corrosion cracks also increased. B30M-FS-16/80 had a total of 136 corrosion cracks and maximum corrosion cracks lie in the range of 0.03-0.05 mm with 98 cracks comprising 60% of the corrosion cracks. No crack wider than 0.2 mm crack width was observed and 10 cracks lied in the range of 0.1-0.15 mm with 7.5% of corrosion cracks. B31S-FS-16/80 had 146 total corrosion cracks, 75 cracks in the narrower crack width range 0.03-0.05 mm with 51.5% of corrosion cracks. Relatively wider cracks compared with 80 mm mildly corroded beam B30M-FS-16/80 was observed and 12 cracks were wider than 0.2-0.25 mm forming 8% of the corrosion cracks while 31 cracks in the crack width range of 0.1-0.15 mm with 21% of the corrosion cracks. Although maximum corrosion cracks lied in the narrower crack width range but with the percentage was quite less as compared to the identical mildly corroded beam. B38M-FS-16/160 had 63 corrosion cracks and it can be seen that B30M-FS-16/80 had 136 corrosion cracks where every parameter is exactly same except the stirrup spacing. Maximum corrosion cracks lied in the narrower corrosion crack width range of 0.03-0.05 mm and 45 corrosion cracks were observed forming 71.5% of the total corrosion cracks. 8 cracks lied in the range of 0.06-0.09 mm while 7 in the range of 0.1-0.15 mm, whereas 3 cracks were wider than 0.2 mm. B39S-FS-16/160 had 100 corrosion cracks and 57 cracks lied in the narrower crack width range of 0.03-0.05 mm, 59 % of the corrosion cracks. In this case not so wide corrosion cracks were observed despite the fact that this beam was severely corroded. One of the reason can be that the stirrup spacing is much higher than the other beams. Figure 3.21 shows the corrosion crack widths and distribution of D16, 80 mm and 160 mm stirrup spacing with mild and severe corrosion in the full span.

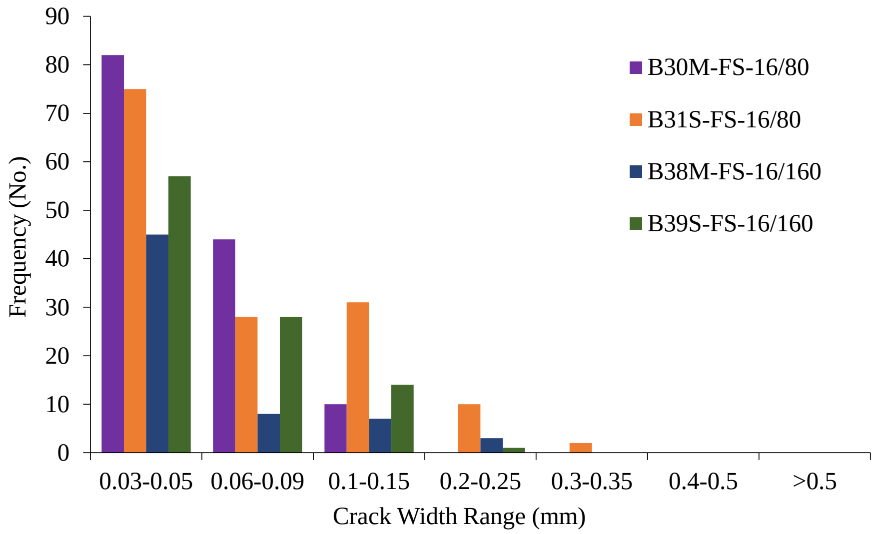

Figure 3.20 Corrosion cracks frequency of D16, 80 mm and 160 mm beams

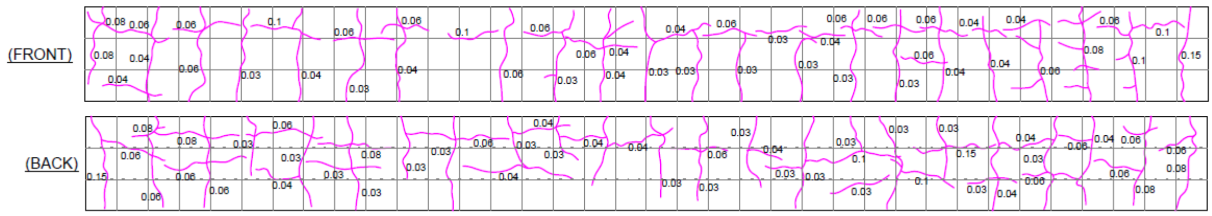

B30M-FS-16/80

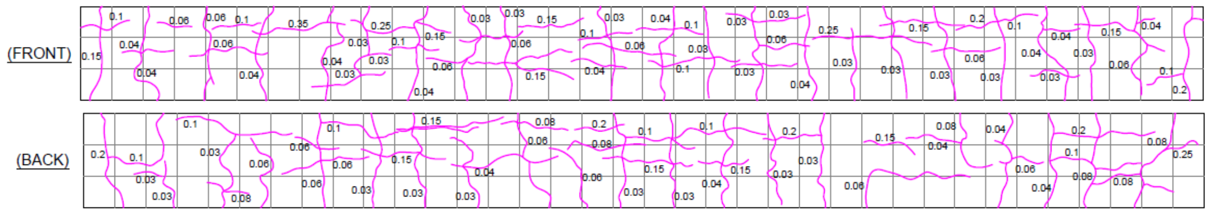

B31S-FS-16/80

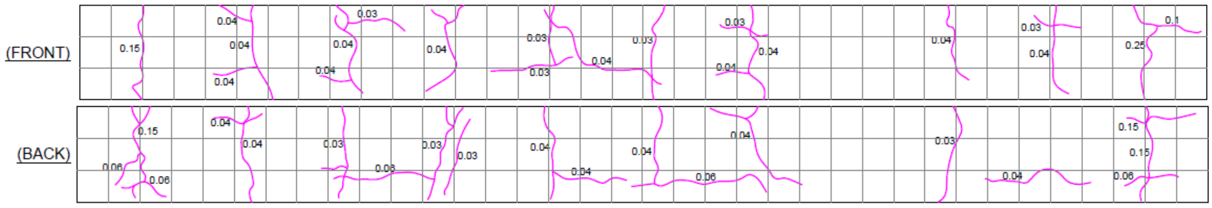

B38M-FS-16/160

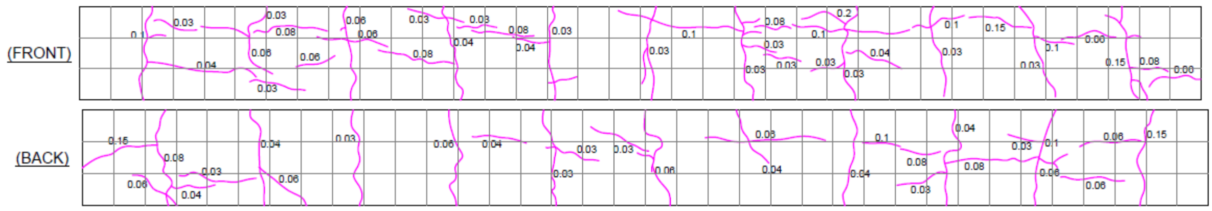

B39S-FS-16/160

Figure 3.21 Corrosion cracks distribution of D16, 80 mm and 160 mm beams

3.3 GENERAL DISCUSSION ON CORROSION CRACKS

The corrosion cracks in all the corroded beams had somewhat similar patterns. Wider corrosion cracks were observed near the edges of the beam. At the edges, the surround concrete is not enough to resist the tensile stresses induced due to corrosion resulting in the wider cracks. This phenomenon was observed more in 80 mm and 120 mm stirrup spacing beams and in both mildly and severely corroded beams. The corrosion cracks were present all around the four sides of the beam. The either sides of the beams had many corrosion cracks as the sides of the stirrup was focused to be corroded. At the location of each stirrup, the corrosion crack was observed on all four sides. The corrosion cracks on the sides of the beams can be divided in three types depending on the location.(a) Cracks along the depth of the beam(vertical cracks), (b) Cracks along the length of the beam (horizontal cracks), (c) the diagonal cracks which are at an angle to horizontal and vertical cracks. In case of mild corrosion, the cracks were mostly vertical and to some extent horizontal with only a few diagonal cracks connecting the vertical corrosion cracks. However, in case of severe corrosion, the vertical and horizontal cracks both were in abundance and with a number of connecting diagonal cracks. The hook of the stirrup was also corroded and the diagonal cracks were probably because of the corrosion of stirrup hook.

The number of corrosion cracks were much greater than the mild corrosion. Also, for shear span and middle span corrosion the number of corrosion cracks were almost same as the length of shear and middle span is same and there were 6 stirrups in either of the spans. The corrosion cracks were lesser for shear and middle span corrosion as compared with the full span corrosion. In both cases, mild and severe corrosion, the maximum corrosion cracks lied in the narrower crack width range of 0.03-0.05 mm. However, relatively wider corrosion cracks were observed for severely corroded beams. Mostly for mildly corroded beams, the cracks were not wider than 0.15 mm but for severely corroded beams, corrosion cracks wider than 0.2 mm was commonly observed. The formation of corrosion crack is not a function of flexural reinforcement ratio and the differences in the corrosion crack pattern must be due to the difference in the corrosion level. However, the flexural reinforcement ratio is critical in understanding the flexural capacity of the corroded beams and the corrosion cracks will influence in the bending test.

Figures 3.22, 3.23 and 3.24 show the percentage frequency of corrosion cracks in different crack width ranges for D10, D13 and D16 as flexural reinforcement respectively. It can be seen that about 60-65% of the corrosion cracks lie in the narrower crack width range of 0.03-0.05 mm in case of mild corrosion while for severe corrosion this percentage is reduced to 47-53%. This implies that wider corrosion cracks occurred for severely corroded beams. Moreover, the percentage frequency of corrosion cracks wider than 0.1 mm is much higher for severely corroded beams as compared with the mildly corroded. Corrosion cracks wider than 0.2 mm are commonly found for severely corroded beams whereas almost no crack wider than 0.2 mm was found in all mildly corroded beams.

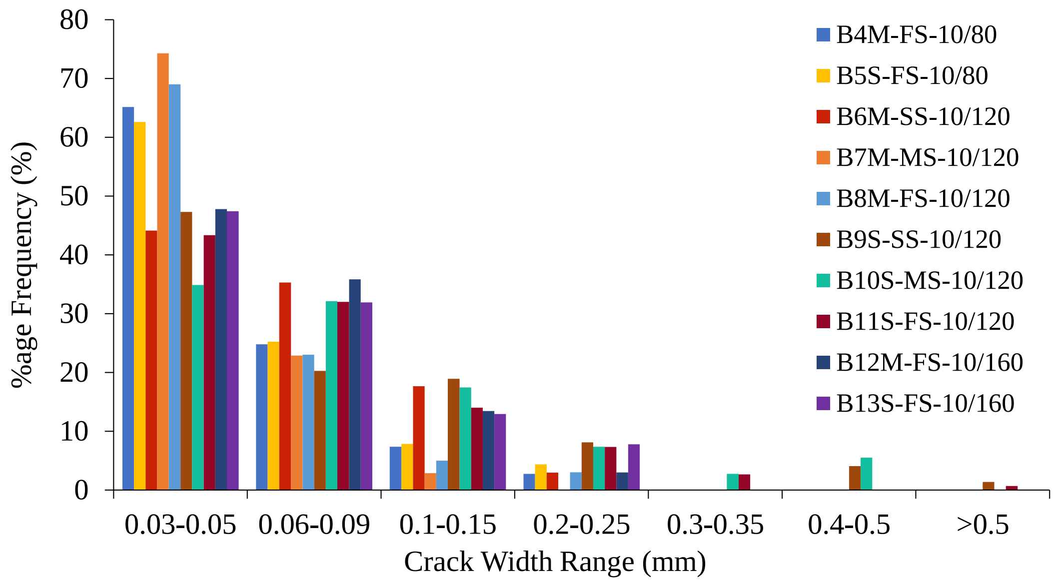

Figure 3.22 Percentage of corrosion cracks frequency of D10 beams

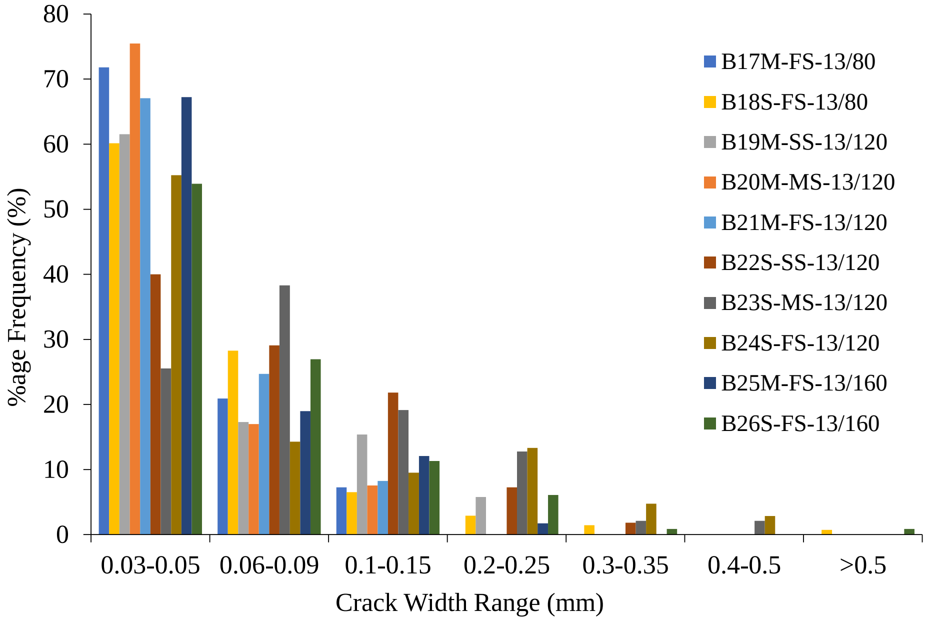

Figure 3.23 Percentage of corrosion cracks frequency of D13 beams

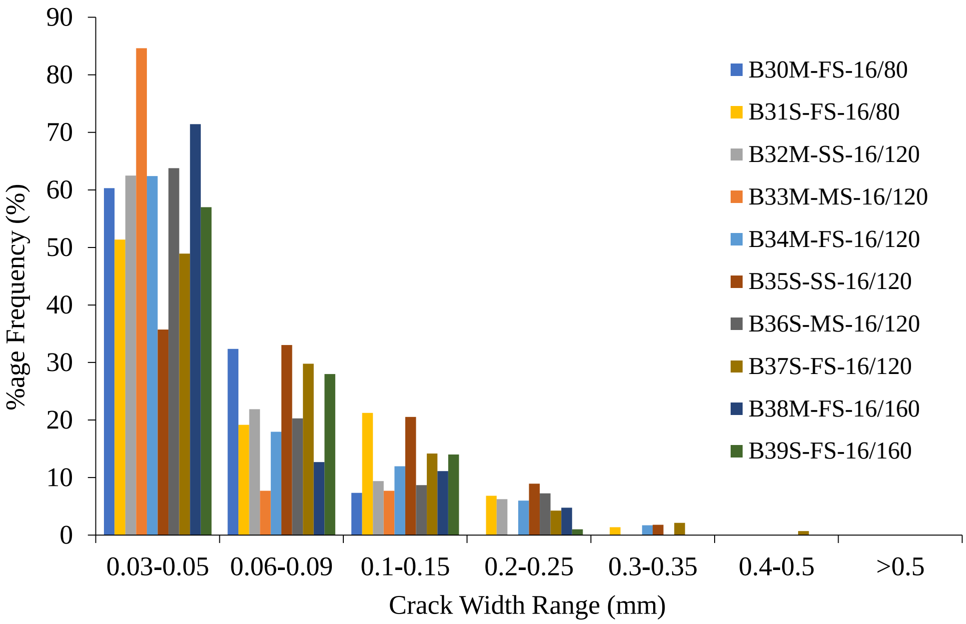

Figure 3.24 Percentage of corrosion cracks frequency of D16 beams

3.4 MEASURED STRENGTH AND DEFLECTION

Four-point bending test was selected to find the ultimate load carrying capacity and deflection of all the beams. The reason to select four point bending test was that the middle span will have zero shear force. In the middle span, the stirrup will not contribute to the strength of the beam but the corrosion of stirrup will induce corrosion cracks and hence deteriorating the concrete too. In case of three-point bending test was selected, there will be only one point (center) where the maximum bending moment will occur. However, in four-point bending test, the complete middle span will have maximum bending moment which was desired in this research. For these two reasons four-point bending test was selected; to have zero shear force and maximum bending moment in the middle span instead of a single point. Figure 3.25 shows the loading arrangement; shear force and bending moment diagrams of the beam.

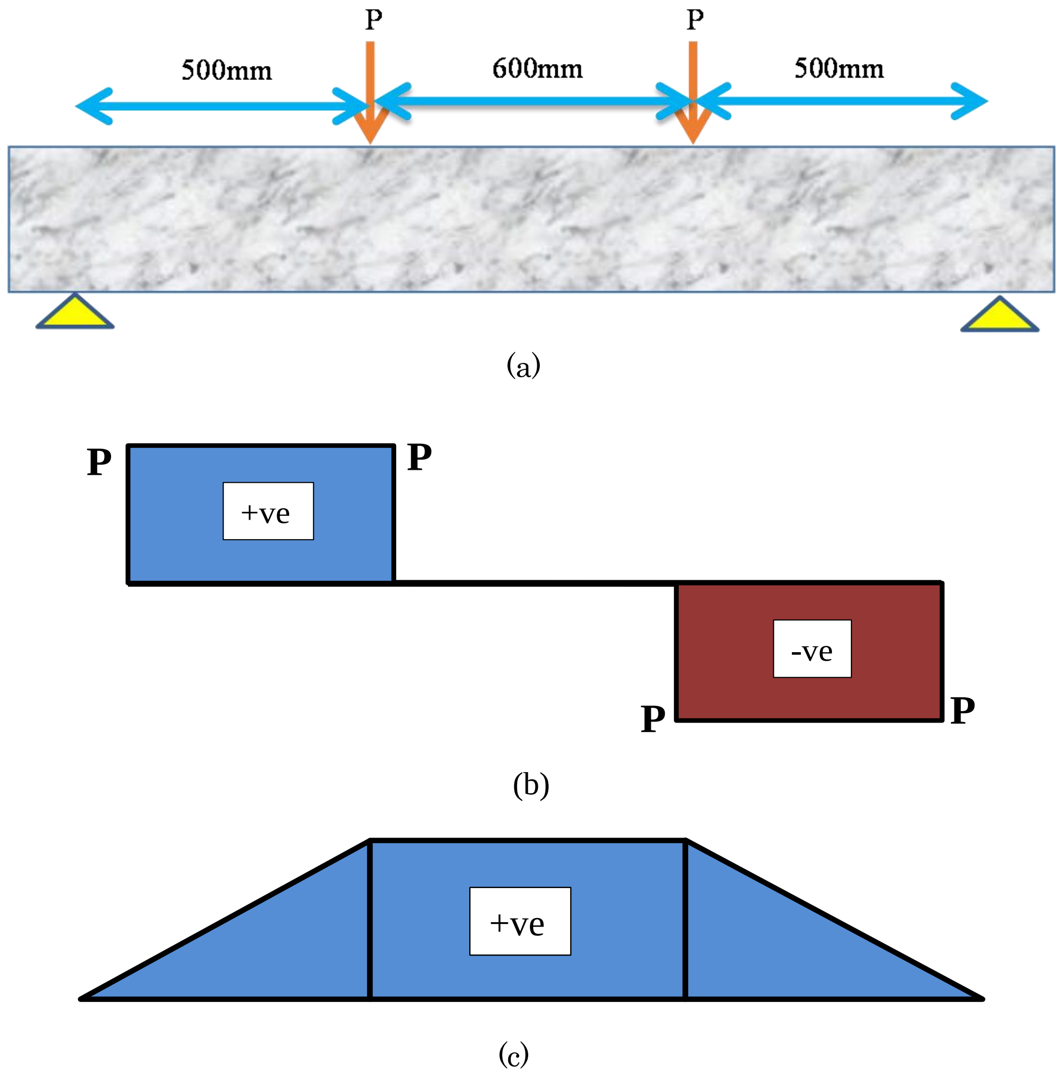

Figure 3.25 (a) Loading arrangement (b) Shear force diagram and (c) Bending moment diagram

As described earlier, there are three kinds of beams with different types of failure and flexural reinforcement ratio. The design failure load, failure mode and other aspects of all the control and corroded beams are discussed in the subsequent sections.

3.4.1 Under Reinforced Section

3.4.1.1 D10 Beams

(1) D10 control beams

All D10 beams are identical in terms of dimensions and longitudinal reinforcement and the only difference amongst these beams are the stirrup spacing. As mentioned earlier, the stirrup spacing used in this research is 80 mm, 120 mm and 160 mm. This means that the yield point and the flexural capacity of all D10 beams must be nearly the same. Nonetheless, the shear capacity of D10 beams are varied as the amount of shear reinforcement varies. Figure 3.26 shows the results of four-point bending test: load-midspan deflection curves of the control beams without stirrup corrosion. It can be seen clearly that all the three control beams yield almost at the same load and deflection. The yield points of B1C-10/80, B2C-10/120 and B3C-10/160 in the force-deflection curve were 23.85 kN, 23.85 kN and 24.35 kN with the deflections 8.48 mm, 9.13 mm and 9.43 mm respectively. The plastic region of all the three control beams varied as concrete is not a homogenous material and the increase in stirrups amount increases the confinement of the beam resulting in a little better behavior. The maximum peak load was observed in B1C-10/80, 32.4 kN at a deflection of 35.15 mm. The second peak load was obtained in the beam with 120 mm spacing beam B2C-10/120 measuring 30.2 kN at the deflection of 37.32 mm. The force-deflection curves of D10 beams follow a typical behavior of beams whose flexural reinforcement ratio is well below from balanced failure ratio. After the yield load all the control beams follow to the plastic region and with the increase in the load. There is an ample amount of increase after the yielding of beams showing good ductile behavior. After the ultimate loads the strains in the top concrete became nearly 0.003 and crushing of concrete in the middle top compression part was observed which is also reflected in the force-deflection curves. In B3C-10/160, a shear crack was also observed after the peak load. No change in the flexural stiffness was observed in all control beams.

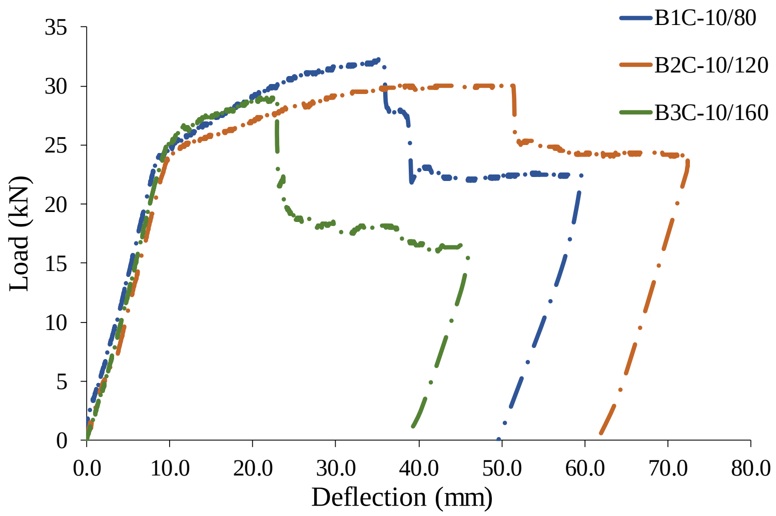

Figure 3.26 Load-Deflection curves of D10 control beams

(2) D10 corroded beams with 80 mm stirrup spacing

Figure 3.27 shows the results of four-point bending test: load-midspan deflection curves of stirrup corroded beams with 80 mm stirrup spacing. B4M-FS-10/80 and B5S-FS-10/80, both beams follow almost same force-deflection curve and both beams were yielded same as the representative control beam, B1C-10/80. After the yielding of the longitudinal reinforcement, both the beams showed good plastic behavior and an increase in the load capacity can be seen in Figure 3.27. However, the peak load was observed at deflections much lesser than the control beam, showing there might a decrease in the deflection ductility. Ultimate flexural strength loss in both beams were observed, and the ultimate capacity of B4M-FS-10/80 was reduced by 9.26% while B5S-FS-10/80 was decreased by 16.60%. The peak loads for both the beams were observed at a deflection of 24.57 mm and 23.62 mm respectively. The difference in the ultimate capacity loss was higher for severely corroded beam but did not fail in shear as the shear reinforcement ratio is higher. Both beams yielded, showed plastic behavior and after the peak load suffered crushing of concrete. Both the beams had earlier crushing of concrete much earlier than the control beams resulting in flexural compression failure. It can be said that the stirrup corrosion induced the corrosion cracks which probably played a vital role in changing the behavior of the corroded beams. With the stirrup corrosion, the confinement provided by the stirrup and the adherence between the stirrup and the concrete matrix is also deteriorated.

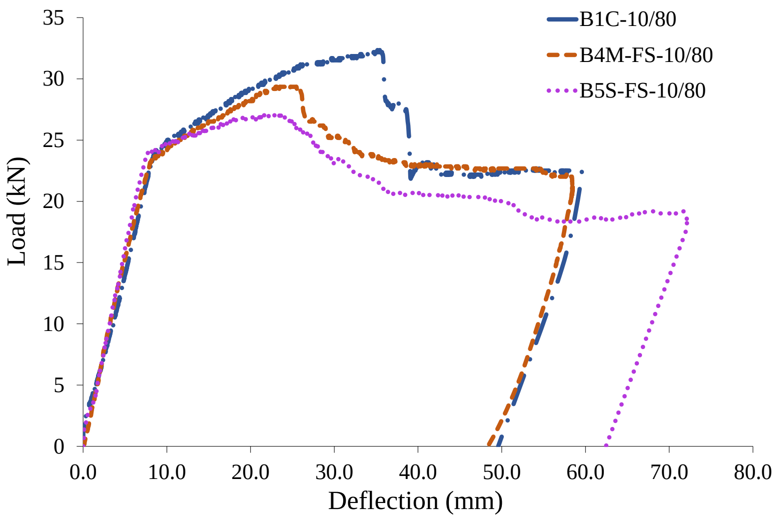

Figure 3.27 Load-Deflection curves of D10 beams with 80 mm stirrup spacing

(3) D10 corroded beams with 120 mm stirrup spacing

Figure 3.28 shows the results of four-point bending test: load-midspan deflection curves of stirrup corroded beams with 120 mm stirrup spacing. Using 120 stirrup spacing, the stirrup corrosion was allowed in shear span, middle span or in full span with mild and severe corrosion. In total there were six beams with 120 mm stirrup corroded beams. D10 beams have much lesser longitudinal reinforcement ratio and the failure mode is flexure with good shear strength. The calculated yield load of D10 beams is 26.86 kN whereas the total shear strength of the un-corroded beam is 67.74 kN. It can be seen that the difference between the yield load and the shear strength is much higher and the beam is expected to fail in flexure. All the mildly corroded beams failed in flexure with the reduction in the ultimate load. Even the failure is flexure, a decrease in the flexural capacity was observed due to stirrup corrosion. B6M-SS-10/120 showed almost same behavior as the control beam as the stirrup corrosion and corrosion cracks were only present in the one of the shear span. Only at the junction of shear and middle span the corrosion cracks and corroded stirrups contributed, and the deflection at maximum load was lowered. The yield points of the mildly corroded beams were almost same as the control beams, also the slopes of the plastic region were nearly same. B7M-MS-10/120 and B8M-FS-10/120 had stirrup corrosion and corrosion cracks in the middle span which contributed in earlier crushing of concrete resulting in flexural compression failure. This illustrates that the corrosion cracks and stirrup corrosion adversely affected the post peak behavior of the corroded beams. The flexural capacity of B7M-MS-10/120 was reduced by 14.97% while B8M-FS-10/120 was reduced by 9.93%.

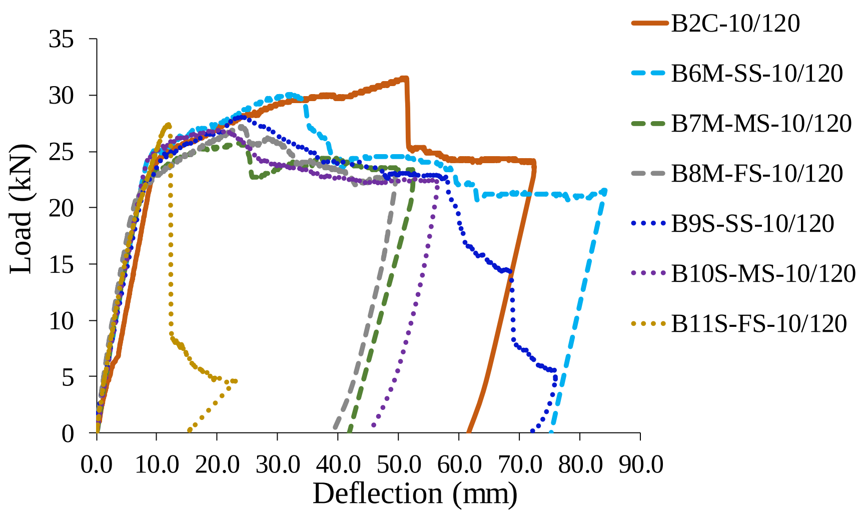

Figure 3.28 Load-Deflection curves of D10 beams with 120 mm stirrup spacing

The severely corroded beams had more strength loss than mild corrosion as the stirrups are corroded more and the corrosion cracks are also wider. Even B9S-SS-10/120 had flexural strength loss, meaning that the stirrup corrosion at the junction of shear and middle span was critical. The beams which failed in flexure had almost same yield point as the control beam showing there was no decrease in the yield point. The reduction was observed in the ultimate flexural strength and the deflection at which the peak load was observed. B9S-SS-10/120 suffered 7.2% strength loss whereas B10S-MS-10/120 reduced 10.53% of ultimate strength. B11S-FS-10/120 failed in shear nearly at the yield load, 27.35 at a deflection of 12.03 mm. Until the yield point, the beam behavior was a typical ductile beam behavior but soon after the failure became shear. Although, the strength loss compared to the control beam is only 9.44% but if it is compared with the nominal shear capacity of the beam which was 67.74 kN, this loss is quite considerable. Hence it can be seen that the stirrup corrosion is quite detrimental and can change the failure mode even for well below under reinforced beam. As the strength loss compared with the shear capacity is huge, it can be predicted that all the shear capacity of the section was not completely exhausted but the deterioration of the adherence between the concrete matrix and the stirrup was also occurred.

(4) D10 corroded beams with 160 mm stirrup spacing

Figure 3.29 shows the results of four-point bending test: load-midspan deflection curves of stirrup corroded beams with 160 mm stirrup spacing. Both the beams, mildly and severely corroded, yielded nearly at the same point as the respective control beam at the almost same deflections. The beams failed in flexure without any shear cracks. The post yield behavior of both beams show typical behavior of an under reinforced beam, showing the peak load in the plastic region and ductile behavior. However, a decrease in the ultimate load was observed and for both beams, mild and severe corrosion, the strength loss was around 14%. This also implies that the stirrup spacing also affects the structural performance of the stirrup corroded beams. In this case where the longitudinal reinforcement was well below the balance failure, the level of corrosion was not significantly affected. Nonetheless, with stirrup corrosion at extremely higher levels, might affect the mechanical behavior of these beams.

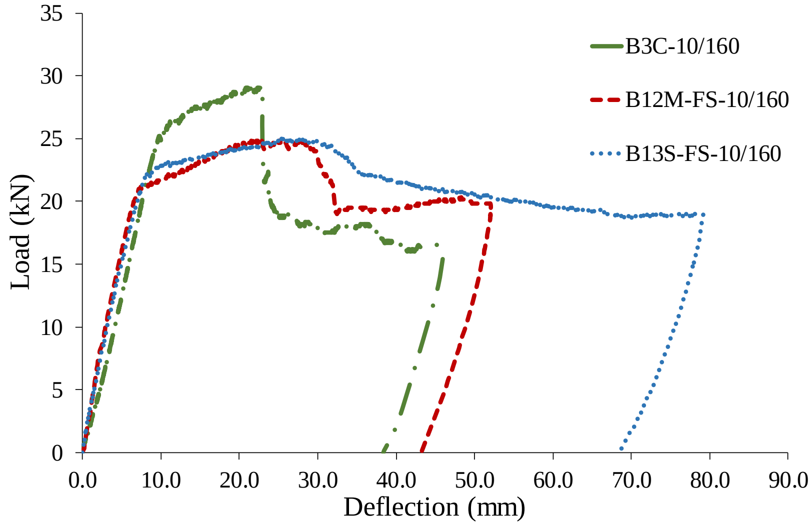

Figure 3.29 Load-Deflection curves of D10 beams with 160 mm stirrup spacing

3.4.1.2 D13 Beams

(1) D13 control beams

The design failure mode of D13 control beams is flexure as they are also under reinforced beams. Nonetheless, the flexural reinforcement ratio of D13 beams is higher than the D10 beams which depicts that the plastic region after the yield load will be shorter in D13 control beams compared with D10 beams. In other words, the ductility of D13 beams will be lesser than D10 beams and the flexural reinforcement ratio of D13 beams is much closer to the flexural reinforcement ratio at balanced failure. As the flexural reinforcement and other aspects of the D13 beams are identical, the yield point and the flexural capacity should be nearly same. A minor difference between the ultimate capacity of control beams might be observed as the concrete strength varies a little and stirrup spacing is also varied. All the three control beams B14C-13/80, B15C-13/120 and B16C-13/160 yielded nearly at the same yield point and almost same as the nominal or design yield load. The design yield load of D13 beams is 41.28 kN whereas the observed yield loads were 43.03 kN, 41.02 kN and 40.53 kN at the deflections of 11.59 mm, 11.60 mm and 11.80 mm. The beam with closely spaced stirrups has a little higher yield and ultimate load. However, all the three control beams yielded about the same deflections. Figure 3.30 shows the results of four-point bending test: load-midspan deflection curves of the D13 control beams without stirrup corrosion. From the figure, it is clear that the plastic region of D13 beams are much lesser than the D10 beams showing the ductility of D13 beams are lesser than the D10 beams. It is assumed that the 80 mm stirrup spacing provides more steel and better confinement to concrete throughout the beam, so the ultimate flexural strength of B14C-13/80 should be relatively higher. B14C-13/80 had the ultimate flexural strength of 47.53 kN at a deflection of 19.63 mm. From the force-deflection curve of B14C-13/80, it can be seen clearly that after the peak load at the 19.63 mm deflection, crushing of concrete took place and flexural compression failure occurred. The ultimate flexural load capacity of B15C-13/120 and B16C-13/160 were almost same, 45 kN with varied deflections at the peak loads. The flexural stiffness of D13 beams were also same as indicated in Figure 3.30.

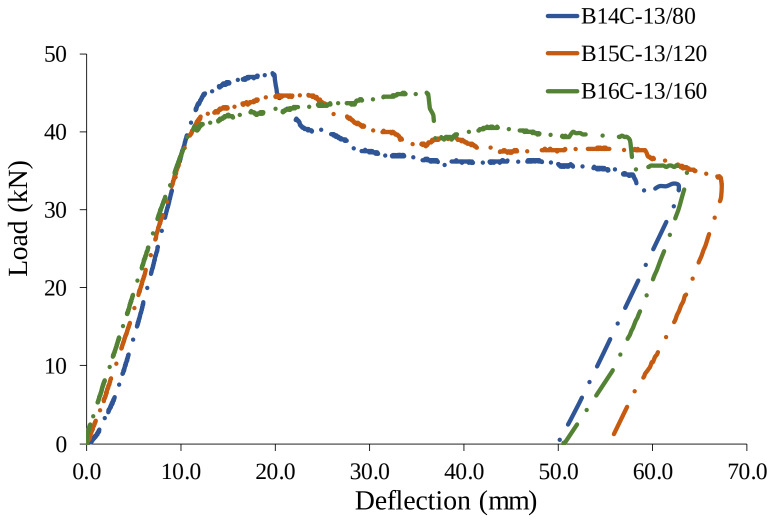

Figure 3.30 Load-Deflection curves of D13 control beams

(2) D13 corroded beams with 80 mm stirrup spacing

The shear capacity of D13 beams with 80 mm stirrup spacing is very high and the nominal strength is 90.06 kN, where shear strength of concrete is 23.08 kN and by stirrup is 66.98 kN without stirrup corrosion. The beams were corroded with mild and severe levels of corrosion in the full span. Figure 3.31 shows the results of four-point bending test: load-midspan deflection curves of stirrup corroded beams with 80 mm stirrup spacing. Both the beams, had decreased ultimate strength. The yield load of mildly corroded beam B17M-FS-13/80 was almost the same as the control beam, but a reduction of 11.57% in the ultimate flexural strength was observed. At the point of failure, the B17M-FS-13/80 had narrower cracks than the control beam which might be because of the existence of corrosion cracks and the loss of confinement due to stirrup corrosion. B18S-FS-13/80 failed in shear with minor flexural cracking. The ultimate peak load was 40.86 kN which is nearly same as the nominal yield load which means that the beam failed in shear near its yield load. The formation of minor flexural cracks also an indication that the beam is close to its yield point. The decrease in ultimate strength compared with the control beam was 14% at a deflection of 15.49 mm which is higher than the deflection of control beam at yield point. If the reduction in the shear strength of corroded beam is compared with the nominal shear strength of the control beam, the decrease in the shear strength loss is 54.63% which is huge. The mass loss reduction and this huge decrease in the nominal shear strength loss is an indication that the mechanism of load transfer from stirrup to concrete matrix and vice versa was also disturbed.

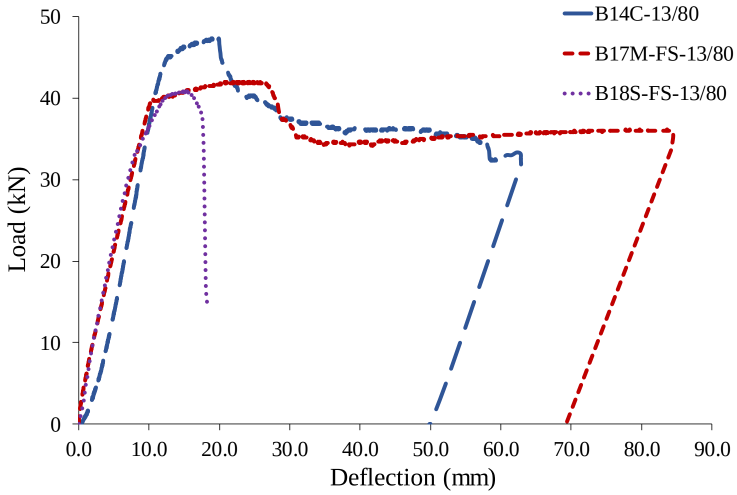

Figure 3.31 Load-Deflection curves of D13 beams with 80 mm stirrup spacing

(3) D13 corroded beams with 120 mm stirrup spacing

Figure 3.32 shows the results of four-point bending test: load-midspan deflection curves of stirrup corroded beams with 120 mm stirrup spacing. Using 120 stirrup spacing, the stirrup corrosion was allowed in shear span, middle span or in full span with mild and severe corrosion. The nominal shear capacity of beams with 120 mm stirrup spacing is 67.74 kN, where 23.08 kN is provided by concrete and 44.66 kN by stirrups without corrosion. Mildly corroded beams B19M-SS-13/120, B20M-MS-13/120 and B21M-FS-13/120 had flexural failure with a decrease in the ultimate load carrying capacity. It implies that the mild corrosion is not sufficient to produce shear failure in beams with 120 mm stirrup spacing and D13 as longitudinal reinforcement. The mildly corroded beams yield nearly at the same load as the respective control beam. B19M-SS-13/120 suffered a decrease in the flexural strength of 8.15% while B21M-FS-13/120 ultimate strength was reduced by 4.44%. The corrosion cracks in the top portion of B20M-MS-13/120 played an important role and widen up in the bending test. The crushing of concrete occurred at the location of corrosion cracks in the middle span, resulting in flexural compression failure and a decrease of 6.66% in the flexural strength was observed.

The severely corroded beams were significantly affected by the stirrup corrosion. B22S-SS-13/120 failed in shear with minute flexural cracking with a peak load of 30.19 kN at a deflection of 10.42 mm and a decrease of 32.96% in the ultimate strength was observed. B24S-FS-13/120 was affected the most and also failed in shear. The peak load was observed at 24.68 kN at a deflection of 11.93 mm with a decrease of 45% in the ultimate strength. Shear cracks appeared in both the shear spans and started to widen at the higher load values. The shear cracks followed the corrosion cracks and after near the peak load multiple shear cracks were noted in this beam. Flexural cracks were not observed in this beam. At all the critical locations, the formation of cracks occurred at or near the corrosion cracks. This multiple crack pattern and overall weakening of this beam can also be predicted from force-deflection curve, as the failure after the peak load is not pure shear which is a sudden drop of load with the formation of sudden wide shear crack like B22S-SS-13/120. B23S-MS-13/120 was also affected by stirrup corrosion and wide corrosion cracks were present in the top part of middle span. These wider corrosion cracks widened up considerably during the bending test resulting in flexural compression failure without yielding of longitudinal reinforcement. The peak load observed was 33.52 kN and a decrease of 25.56% in the flexural strength at a deflection of 9.97 mm. This shows that the stirrup corrosion is detrimental even at the places where the shear force is zero and affects the structural performance of RC beams.

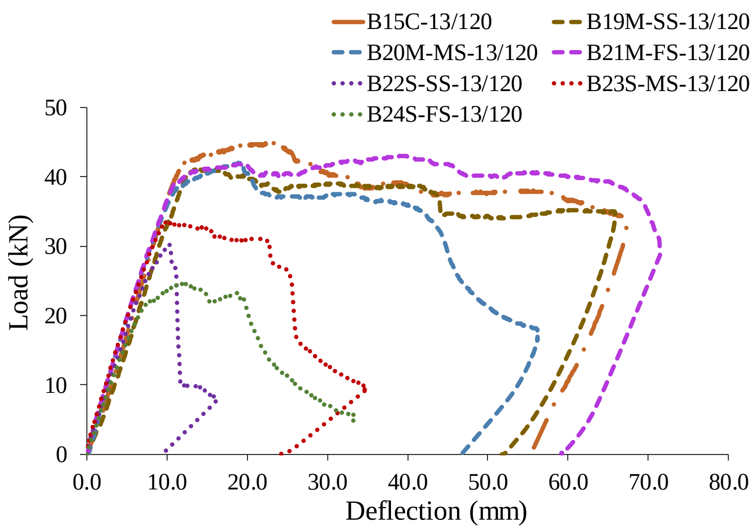

Figure 3.32 Load-Deflection curves of D13 beams with 120 mm stirrup spacing

(4) D13 corroded beams with 160 mm stirrup spacing

Figure 3.33 shows the results of four-point bending test: load-midspan deflection curves of stirrup corroded beams with 160 mm stirrup spacing. The nominal shear strength of beams with 160 mm stirrup spacing is 56.56 kN, where the shear strength provided by the concrete and stirrup is 23.08 kN and 33.48 kN respectively. B25M-FS-13/160 yielded at the same point as the control beam with a slight decrease in the ultimate flexural capacity. The failure mode after mild stirrup corrosion did not change and the beam failure in flexure. A reduction of 4.45% in the ultimate flexural load was noted at a deflection of 18.86 mm. The mild corrosion of 160 mm stirrup beam did not significantly change the structural performance of the corroded beam but when the stirrups were corroded severely, the failure mode was changed from flexure to shear and brittle failure. B26S-FS-13/160 failed at a load of 36.4 kN at a deflection of 11.60 mm with a decrease of 19.47% in the ultimate load. The longitudinal reinforcement did not yield which can also be seen the force-deflection curve. The failure mode was sudden and brittle with the formation of wide shear crack in one of the shear span.

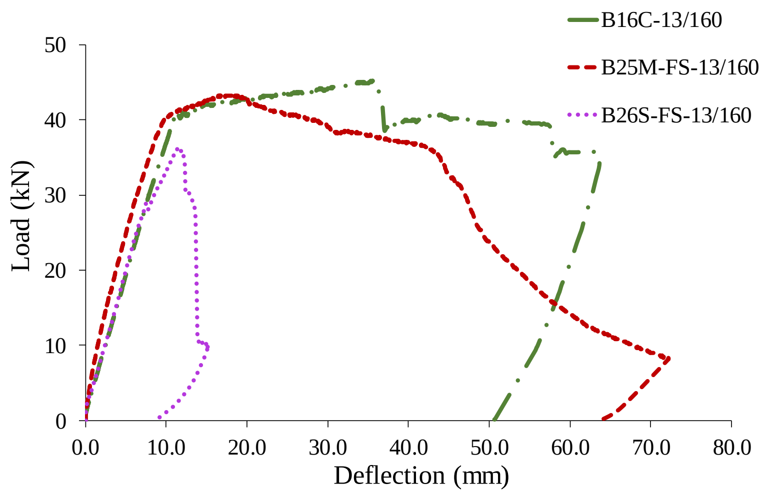

Figure 3.33 Load-Deflection curves of D13 beams with 160 mm stirrup spacing

3.4.2 Over Reinforced Section

3.4.2.1 D16 Beams

(1) D16 control beams

The longitudinal reinforcement ratio of D16 beams is higher than the longitudinal reinforcement ratio at balanced failure. It implies that the D16 beams are over reinforced beams and either the control beams will have flexural compression failure (crushing of concrete) near the yield load or soon after the yield load. These beams cannot develop complete plastic region as was seen in D10 and D13 beams. The shear strength of the control beams is the same as D10 and D13 beams because the stirrup spacing used is same 80 mm, 120 mm and 160 mm. The calculated nominal yield load is 60.20 kN of D16 beams without stirrup corrosion. The nominal shear capacity of D16 and 160 mm stirrup spacing beam is 56.56 kN and theoretically the design failure mode of B29C-16/160 is shear failure. Figure 3.34 shows the results of four-point bending test: load-midspan deflection curves of control beams with 80 mm, 120 mm and 160 mm stirrup spacing without corrosion. B27C-16/80 yielded at a load of 65.87 kN at a deflection of 13.25 mm. The peak load was much higher from the yield load and was 66.54 kN at a deflection of 16.23 mm. As depicted from the force-deflection curve, the flexural compression failure of the beam occurred due to crushing of concrete. B28C-16/120 also had flexural compression failure after yielding at 63.54 kN at a deflection of 15.04 mm. The peak load obtained was 68 kN at a deflection of 20.94 mm. The nominal shear capacity was 67.74 kN which is shows the beam must have shear cracks also. However, the shear crack was minute, occurred in both the shear span but did not affect the failure mode. B29C-16/160 yielded at 62.37 kN and at a deflection of 15.82 mm. The peak load observed was 65.87 kN and the flexural compression failure of beam occurred due to crushing of concrete. There was an increase in the shear strength of B28C-16/120 and B29C-16/160. ACI 318-11 do not take the shear strength contribution from the longitudinal reinforcement which JSCE suggests and cater in the shear strength calculations of concrete. Also, El-Chabib (2011) suggested that the addition of stirrups provide confinement to concrete, resulting in increasing the compressive strength f'_c of concrete and thus enhancing the contribution of basic shear mechanisms to V_c [27]. Because of these reasons, the shear capacity of the un-corroded beams might got improved. It can be seen from the force-deflection curves that the plastic regions of the control beams are much smaller than the D10 and D13 beams because of higher flexural reinforcement ratio than D10, D13 and balanced failure ratio.

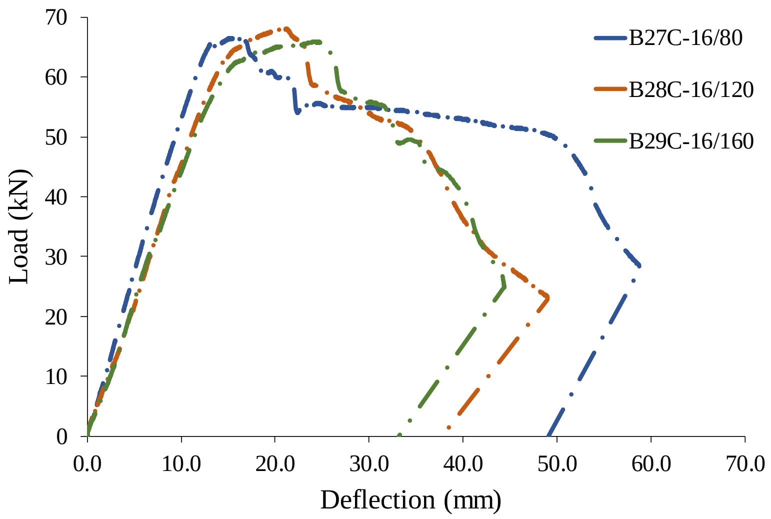

Figure 3.34 Load-Deflection curves of D16 control beams

(2) D16 corroded beams with 80 mm stirrup spacing

Figure 3.35 shows the results of four-point bending test: load-midspan deflection curves of stirrup corroded beams with 80 mm stirrup spacing. The mildly corroded beam B30M-FS-16/80 follows almost the same force-deflection curve as the respective control beam B27C-16/80. The ultimate load observed was 63.37 kN at a deflection of 16.02 mm and a reduction of 4.76% in the flexural strength was obtained. The yield point was also near the yield load of the control beam. The severely corroded beam B31S-FS-16/80 failed in the shear without showing yielding of the longitudinal reinforcement. A reduction of 24.32% in the ultimate strength was observed and the peak load noted was 50.36 kN at a deflection of 50.36 mm. It can be seen that a considerable loss of strength occurred in the severely corroded beam even when the stirrup was closely spaced. Approximately 45% of the strength is lost if we compare the shear strength loss with the nominal shear strength of the beam.

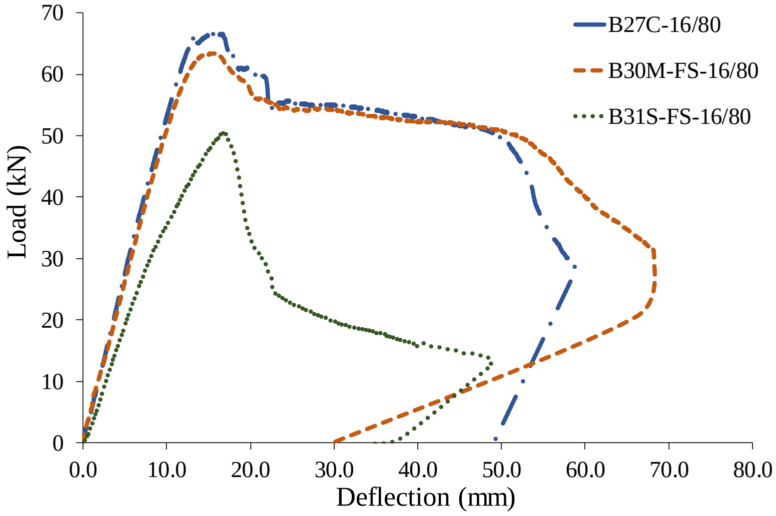

Figure 3.35 Load-Deflection curves of D16 beams with 80 mm stirrup spacing

(3) D16 corroded beams with 120 mm stirrup spacing

The stirrup corrosion of D16 beams with 120 mm stirrup spacing was corroded in the shear span, middle span or full span with mild and severe corrosion levels and the result of load-midspan deflection curves are shown in Figure 3.36. All the corroded beams had the ultimate load carrying capacity less than the control beam. Those beams which did not fail in shear yielded at the load almost same as the control beam. The beams which had stirrup corrosion in shear span, both mildly and severely corroded, failed in shear. The strength loss obtained was 7.1% and 10.54% for B32M-SS-16/120 and B35S-SS-16/120 at a deflection of 20.19 mm and 13.96 mm respectively. Although the beams did not yielded as reflected in the force-deflection curves also, there were few minute flexural cracks in the bending test. The beams with stirrup corrosion in the middle span was not significantly affected by the stirrup corrosion. Both mildly and severely corroded beams, B33M-MS-16/120 and B36S-MS-16/120 followed almost same pattern as the control beam in the force-deflection curve. There was a decrease in the ultimate load, 2.5% and 3.92% respectively which is not so significant. This shows that the deterioration of stirrups and the corrosion cracks influence was not so considerable to change the structural performance of the corroded beams. In case of full span corrosion, the mildly corroded beam B34M-FS-16/120 same failure mode as the control beam and followed almost the same as control beam in the force-deflection curve with a decrease of 10.79% in the ultimate load carrying capacity. The decrease in the ultimate strength of the severely corroded beam B37S-FS-16/120 was more and 14.46% was observed.

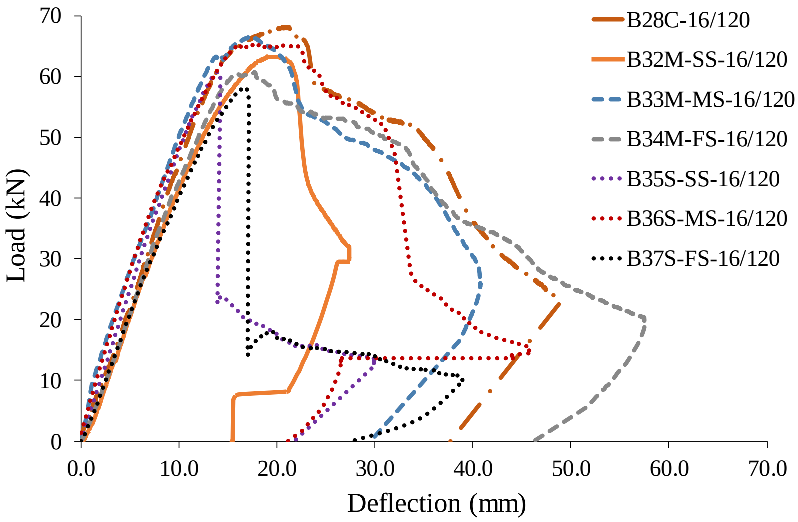

Figure 3.36 Load-Deflection curves of D16 beams with 120 mm stirrup spacing

(4) D16 corroded beams with 160 mm stirrup spacing

Figure 3.37 shows the results of four-point bending test: load-midspan deflection curves of stirrup corroded beams with 160 mm stirrup spacing. The nominal shear capacity of 160 mm stirrup spacing beams without corrosion is 56.56 kN, and the strength provided by the concrete and stirrup is 23.08 kN and 33.48 kN respectively. The theoretically calculated yield load for D16 beams is 60.20 kN which is higher than the shear capacity. This means that the design failure mode of D16 and 160 stirrup spacing beams is shear failure. It was expected that the mildly and severely corroded beams will fail in shear after stirrup corrosion. However, the mildly corroded beam, B38M-FS-16/160 failed in flexural compression failure (crushing of concrete). The corrosion cracks in the middle span in the compression zone tends to widen up in the bending test. Once the cracks were formed, they resulted in the crushing of concrete which got extended in the complete compression zone. The beam did not yield but few minute flexural cracks were present. The ultimate peak load was noted as 59.37 kN which is close to the yield load at a deflection of 14.67 mm. Nonetheless, the beam did not fail in flexure tension and crushing of concrete took place resulting in flexural compression failure. The severely corroded beam failed in shear as expected at a peak load of 52.37 kN at a deflection of 13.48 mm. A reduction of 9.87% and 20.49% in the ultimate load capacity was observed in B38M-FS-16/160 and B39S-FS-16/160 respectively.

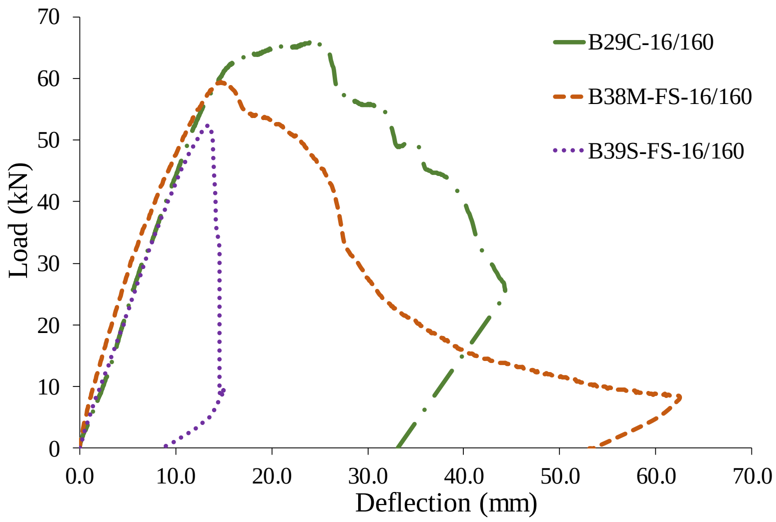

Figure 3.37 Load-Deflection curves of D16 beams with 160 mm stirrup spacing

3.5 CRACKS FORMATION IN THE BENDING TEST

Generally, the formation of flexural or shear cracks for an cracked and undamaged RC beam in the bending test depends on the beam design criterion, which includes the amounts of flexural and shear reinforcement ratio, the dimensions of the beam and the loading arrangement etc. When the RC beam is damaged, then the crack formation also become a function of degree of deterioration, crack formation due to the deterioration, damage to concrete and steel, and the adherence between the concrete matrix and the steel rebars.

In this study, once the stirrups of beams are corroded, formation of corrosion cracks occurred on all the sides of the beam. The corrosion cracks had different crack widths, orientation and location depending on the extent of corrosion and stirrup spacing. It was observed that the formation of flexural and shear cracks in the bending test followed the paths of the corrosion cracks. The corrosion cracks act as pre-defined failure paths and tend to widen up in the bending tests. The inclined corrosion cracks in the shear span, the lower and top part of the beam in the middle span were the critical locations where the corrosion cracks influenced the formation of cracks in bending test. Detailed explanation is provided in the subsequent sections according to the longitudinal reinforcement used.

3.5.1 D10 Beams

The amounts of flexural reinforcement ratio of these beams are well below the criteria of under reinforced beams. The yield and the ultimate load is much lesser than the shear capacity of the section. The nominal yield load for D10 beams is 26.86 kN whereas the least nominal shear capacity was for 160 mm stirrup spacing which is more than twice the capacity of the yield load. This depicts that the D10 beams should have bending or flexural cracks near the yield load for undamaged beams exhibiting a good ductile behavior. The shear capacity of D10 beams is too high and it was expected that the stirrup corrosion might not change the failure mode and the beams will still have ductile failure after stirrup corrosion. All beams were failed in flexure except B11S-FS-10/120 which was failed in shear. All the other beams had flexural cracks at the maximum moment location which was in the middle span. Figure 3.38 shows the formation of flexural cracks in B1C-10/80 during the bending test.

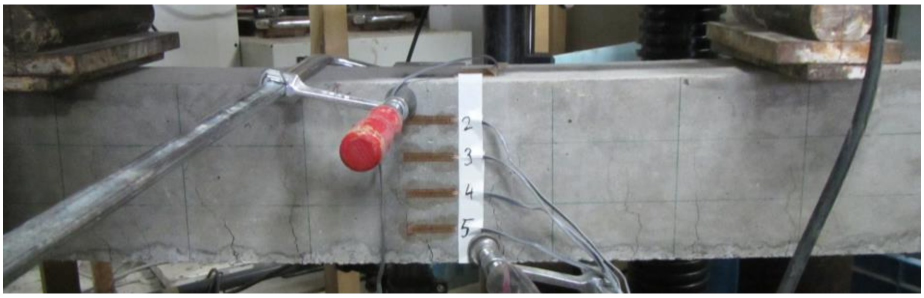

Figure 3.38 Formation of cracks during bending test of B1C-10/80

The only beam which failed in shear was B11S-FS-10/120 but the load at which shear failure occur was close to the yield load. This implies that the formation of flexural cracks also formed along with the shear cracks. However, shear cracks became critical and the beam failed in shear. As the beam had stirrup corrosion in full span, the shear crack occurred in both the shear spans and can be inferred that the damage due to corrosion was on both the shear spans. Both the shear cracks widen up with the application of load but one crack became critical and shear failure occurred in one of the shear span. Figure 3.39 shows the formation of critical shear crack in the bending test of B11S-FS-10/120

Figure 3.39 Formation of shear crack during bending test of B11S-FS-10/120

3.5.2 D13 Beams

D13 beams also had good flexural design and the design failure mode is flexure. The longitudinal reinforcement ratio is less than the balanced failure condition but the ratio is higher than the D10 beams. It can be said that D13 beams had good economical design as the longitudinal reinforcement ratio is just a little less than the balanced failure. This illustrates that the D13 beams will have good ductile behavior, and higher flexural strength than D10 beams. The calculated yield load of D13 beams were 41.28 kN which is very less than the nominal shear capacity of the un-corroded beams. It means that the beam will fail in flexure with no major or critical shear cracks. Figure 3.40 shows the cracks formation of B14C-13/80 in the bending test and can be seen the flexural cracks formation at the time of failure.

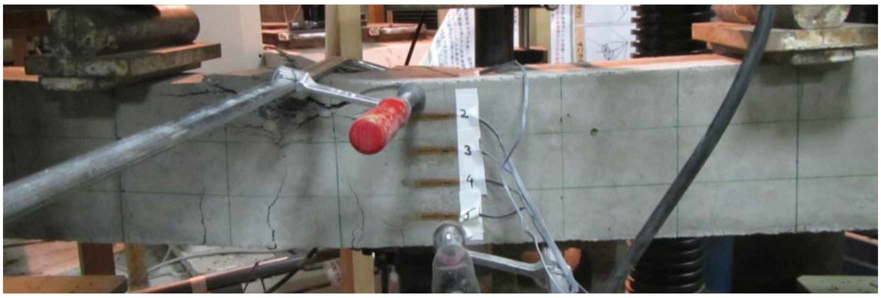

Figure 3.40 Formation of cracks during bending test of B14C-13/80

All the severely corroded D13 beams, where the stirrups were corroded in the shear or full span failed in shear. This implies that the shear failure occurred for the beams when ample shear strength of RC beam was used at higher longitudinal reinforcement ratio. When the longitudinal reinforcement ratio is high, the shear strength contribution from the section becomes critical as higher load is applied. When the stirrups are corroded, it induces damage to the stirrup and concrete resulting in the lowering of the shear capacity, and hence shear failure occurs. Figure 3.41 shows the shear crack formation in the severely corroded beam B17S-FS-13/80. It can be seen that the cracks during the bending test followed the corrosion cracks and even the concrete cover is spalled down. The corrosion crack is present at much higher position where the shear crack generally occurs but the presence of corrosion cracks changed the formation of cracks during the bending test. Besides this, there were shear cracks in both the shear spans which tend to widen up during the application of higher loads. The load at which the shear failure occurred was close to the yield load, so flexural cracks were also observed in this beam.

Figure 3.41 Formation of cracks during bending test of B17S-FS-13/80

B24S-FS-13/120 also failed in shear at much lesser load and almost no flexural crack was observed in this beam. Figure 3.42 shows the cracks formation in B24S-FS-13/120 during the bending test. It is evident from the figure that the shear cracks occurred in both the shear span illustrating that both shear span stirrups undergone severe deterioration. Multiple shear cracks were observed and the corrosion cracks tend to widen up in the bending test. The corrosion cracks also facilitate the formation of shear cracks. The presence of corrosion cracks is a proof that this is the weak zone so the crack propagation was generally noted around the corrosion cracks. The shear cracks in this beam is propagating near the concrete cover which is generally not seen in the un-corroded beams. A clear sharp shear crack mostly occur, propagating from support at an angle to the point load for an un-corroded beam unlike the shear crack observed in B24S-FS-13/120. Moreover, the presence of multiple shear cracks is an indication that the concrete is also deteriorated when the stirrups were corroded.

(a) (b)

Figure 3.42 Formation of shear cracks during bending test of B24S-FS-13/120

B23S-MS-13/120 failed in the flexural compression (crushing of concrete) without yielding of longitudinal reinforcement and almost no flexural cracks were observed in the middle span. The corrosion cracks in the middle span widen up in the bending test specially the ones present in the compression zone (in the Whitney stress block diagram), where the strength of the beam comes majorly from compressive strength of concrete f'_c. Figure 3.43 shows the crack formation in the compression region of B23S-MS-13/120 during the bending test. The cracks propagating in the compression zone in the middle span and hence resulting in the crushing of concrete in this region. This is also one indication that the stirrup corrosion induced damage to the compressive strength of concrete and the corrosion cracks acts as the pre-defined failure paths.

Figure 3.43 Formation of cracks during bending test of B23S-MS-13/120

3.5.3 D16 Beams

The longitudinal reinforcement ratio of D16 beams are higher than the ratio at balanced failure which means that the failure mode will be flexural compression with a little or no ductility. The longitudinal reinforcement ratio of D16 beams is 0.0267 whereas the reinforcement ratio at balanced failure is 0.0241. The difference in the reinforcement ratio is not much high, so there is a possibility that the longitudinal reinforcement might yield and the beams without corrosion have flexural cracks. Soon after yielding, the beam will fail in the flexural compression, reducing the ductility compared to D10 and D13 beams. As explained in the previous section, the yield load of D16 is closer to the nominal shear strength of 160 mm and 120 mm stirrup spacing beams. This depicts the presence of shear cracks in B28C-16/120 and B29C16/160. In the bending test, the control beams had flexural cracks near the yield point and after the higher application of loads the failure occurred was flexural compression (crushing of concrete). Minute shear crack and a flexural shear crack was observed in one of the shear span of B28C-16/120 whereas minute shear crack appeared in both spans of B29C-16/160. Figure 3.44 shows the cracks formation and crushing of concrete in B27C-16/80 which failed in flexural compression during the bending test.

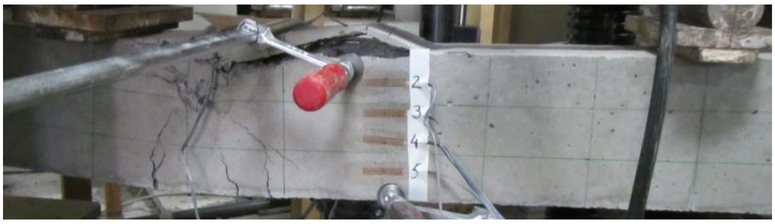

Figure 3.44 Formation of cracks during bending test of B27C-16/80

All the severely corroded beams, and stirrup mildly corroded in shear span failed in shear. The middle span corrosion were not supposed to fail in shear and the crack formation in the bending test showed that the corrosion cracks acted as pre-defined failure paths where the cracks in bending propagated. Almost all the beams which failed in shear failure had flexural cracks because the peak load observed was approximately close to the yield load. Like the crack formations detected in D13 corroded beams, D16 beams also faced spalling of the concrete cover, resulting in reducing the cross-sectional area of concrete. The shear crack propagated along the corrosion cracks near the concrete cover and moved towards the application of the point load. This is an indication that the concrete is damaged and the shear strength of the concrete is reduced and influenced by the corrosion cracks. Figure 3.45 shows the formation of cracks in B37S-FS-16/120 during the bending test. The shear cracks occurred in both shear spans with the spalling of the concrete cover on both sides and resulted in the shear failure.

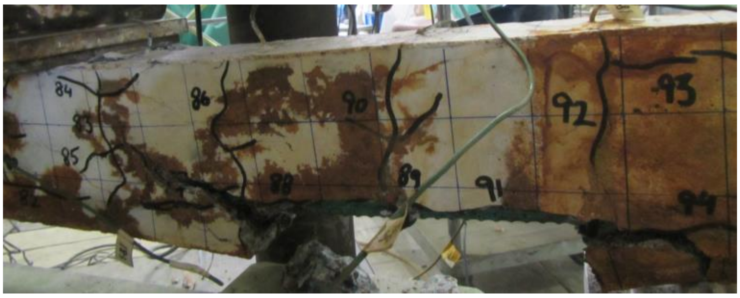

Figure 3.45 Formation of cracks during bending test of B37S-FS-16/120

B38M-FS-16/160 failed due to the flexural compression failure (crushing of concrete) near the yield load. The beam did not show any plastic behavior in the force-deflection curve nor shear failure. This illustrates that the yield strain in longitudinal reinforcement still did not reach and the longitudinal reinforcement did not yield properly. The presence of flexural cracks in the middle span shows that the beam is somewhere near the yielding of longitudinal reinforcement. Figure 3.46 shows the cracks formation of B38M-FS-16/160 during the bending test. Intensive cracking of the compression concrete can be seen in the bending test and the top compression concrete spalling out. The flexural cracks along with minute shear cracks also occurred during the test.

Figure 3.46 Formation of cracks during bending test of B38M-FS-16/160

3.6 DUCTILITY

Ductility describes the ability of a structure or its components to provide resistance in the inelastic domain. It includes the ability to sustain large deformations and a capacity to absorb energy by hysteretic behavior, the characteristics that are vital for seismic loads. Ductility of RC beams is generally determined by the ductility ratio or ductility factor (μ), which is defined as the ratio of maximum (i) deflection ($\triangle$), (ii) curvature ($\emptyset$) or (iii) energy (E) at failure to the corresponding property at the yield point [28], as shown below:

Deflection ductility	$\mu_{\triangle} = \triangle_u/\triangle_y$	(1)
Curvature ductility	$\mu_{\emptyset} = \emptyset_u/\emptyset_y$	(2)
Energy ductility	$\mu_E = E_{tot}/E_y$	(3)

where $\triangle_u$ = mid-span deflection at failure; $\triangle_y$ = mid-span deflection at yielding of tension reinforcement; $\emptyset_u$ = curvature at mid-span section at failure; $\emptyset_y$ = curvature at mid-span section at yield of tension reinforcement; E_{tot} = area under the load deflection curve at failure (total energy); and E_y = area under the load-deflection curve at yield of tension steel. For this study, the ductility is determined by Eq. (1), deflection ductility. Figures 3.47, 3.48 and 3.49 illustrates the deflection ductility factor of the corroded beams and the control beams of D10, D13 and D16 respectively. The deflection ductility factor is believed to depend on the failure mode and, in this study, the beams failed in flexural tension, shear and flexural compression after corrosion of stirrups only. However, the deflection ductility factor varied for all the corroded beams, as the location and degree of deterioration was not the same. The deflection ductility factor can only be calculated which failed in flexure as the shear failure is brittle and cannot show any ductility.

The deflection ductility factor of D10 beams is the highest compared to D13 and D16 control beams as the longitudinal reinforcement ratio was well below the balanced failure and this is also illustrated in Figure 3.47. The deflection ductility of D10 beams with 80 mm and 120 mm stirrup spacing was significantly reduced due to stirrup corrosion. For 80 mm spacing, the reduction in deflection ductility was irrespective of the corrosion level but for 120 mm spacing, the deflection ductility was lesser for severely corroded beams. The stirrup corrosion not only damaged the stirrups but also affected the overall structural performance of the RC beams. Even for the middle span stirrup corrosion, the deflection ductility was reduced considerably. In case of 160 mm stirrup spacing beams, the deflection ductility increased. Some researchers found that sometimes the stirrup corrosion improves the deflection ductility but it depends on the flexural design, stirrup spacing and extent of deterioration to the beam. They observed that for an identical load, both the strain of corroded tension bars and the deformation of cracked compression concrete of corroded beams become greater than that of the non-corroded and non-cracked control beam [7]. As a result, the deflection ductility was improved for 160 mm spacing beams and this improvement was irrespective of the degree of corrosion

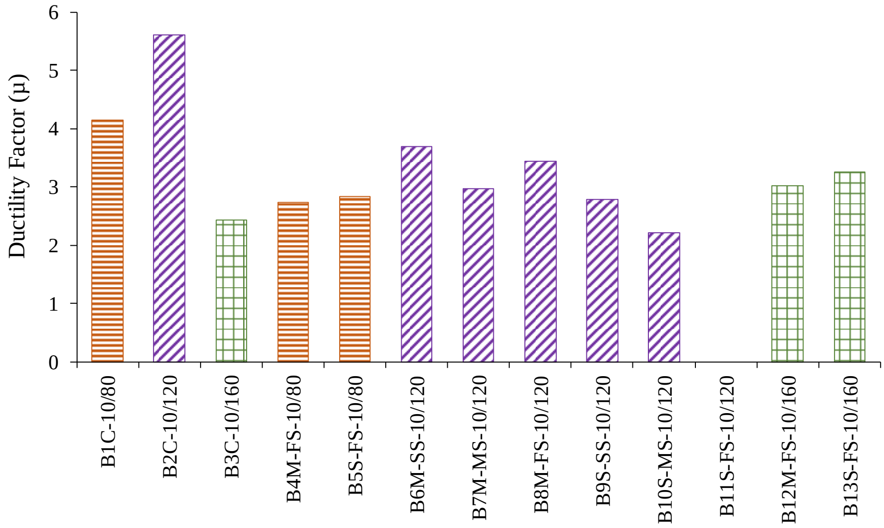

Figure 3.47 Deflection ductility factor of D10 beams

The deflection ductility of D13 beams are almost have of D10 beams as the longitudinal reinforcement ratio was more and close to the balanced failure ratio. The severely corroded D13 beams failed in shear and therefore no deflection ductility can be calculated as illustrated in Figure 3.48. The deflection ductility of B17M-FS-80 and B21M-FS-13/120 was improved for D13 beams while the others reduced significantly.

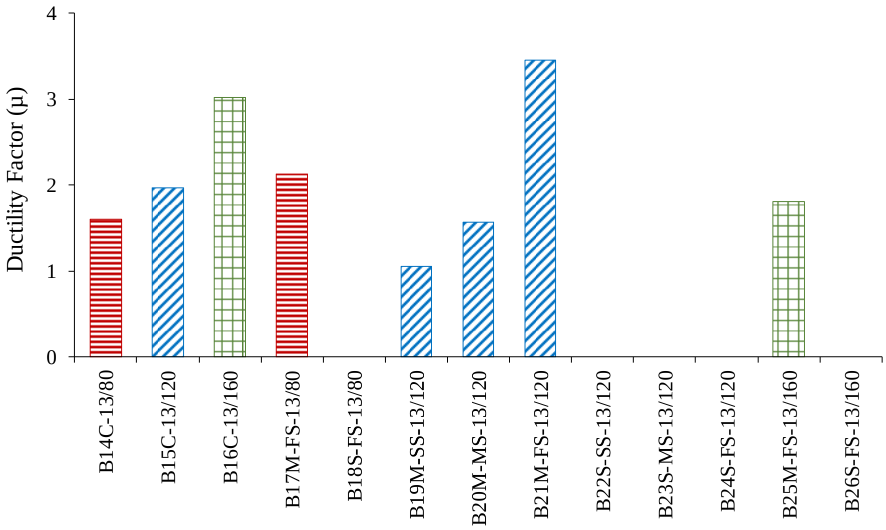

Figure 3.48 Deflection ductility factor of D13 beams

The deflection ductility of D16 control beams is the least compared to D10 and D13 beams as the longitudinal reinforcement ratio was higher than the balanced failure ratio. The deflection ductility of B27C-16/80, B28C-16/120 and B29C-16/160 was noted as 1.22, 1.39 and 1.59 respectively. All the severely corroded D16 beams and B32M-SS-16/120 failed in shear which is sudden and brittle so no deflection ductility can be noted for these beams. For D16 beams, the deflection ductility of all the corroded beams were less than the control beams and no improvement in the deflection ductility was observed.

The ultimate load of control beams with 80 mm stirrup spacing were relatively higher than 120 mm spacing beams and the 120 mm beams were higher than 160 mm spacing beams. As the relative ultimate load increases with decreasing stirrup spacing for the same longitudinal reinforcement ratio, the deflection ductility reduces as the stirrup spacing is reduced. The reason for this behavior is, when the capacities are high for the same longitudinal reinforcement ratio, the deterioration to the beam will be more resulting in lesser deflections and hence reducing the deflection ductility. The improvement and impairment in the deflection ductility is difficult to explain at this stage because it is not apparently depending on the stirrup spacing or load carrying capacity loss which indicates the degradation in the corroded beam. It was observed that for D10 beams the deflection ductility was improved for 160 mm stirrup spacing beams, for D13 beams deflection ductility was improved for 120 mm spacing and, for D16 beams, no improvement in the deflection ductility was noted.

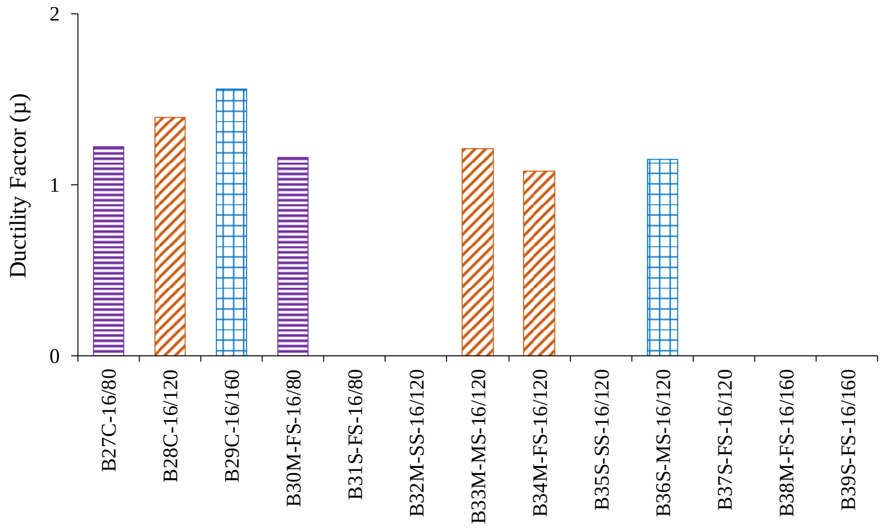

Figure 3.49 Deflection ductility factor of D16 beams

3.7 LOAD CARRYING MECHANISM OF RC BEAMS DUE TO STIRRUP CORROSION

As the stirrup corrodes in the RC beam, cracks are induced in the surrounding concrete resulting in deterioration of the concrete and the stirrup. The amount of concrete damage depends on stirrup spacing, cover distance, and degree of corrosion [29]. The corrosion cracks due to stirrup corrosion also provides the pre-defined failure paths in the bending test particularly at the critical locations, e.g. corrosion cracks in the shear span, under the point loads, in the maximum bending moment span specially the corrosion cracks in the extreme tension and compression sides, etc. The corrosion cracks formed due to stirrup corrosion are vertical cracks along the length of the stirrup with some horizontal or connecting cracks which pass through the vertical cracks. These horizontal cracks and the vertical cracks tend to widen during the bending test. At higher values of applied load, the horizontal and vertical cracks which are present in the middle span at the top of the beam in the compression zone, also tend to widen, separating the concrete cover in the compression zone resulting in spalling of the concrete cover. This reduces the cross-sectional area of the beam as the top concrete cover is spalled out, reducing the width of the compression zone. This reduction in the width of the compression zone has a potential to lower the flexural capacity of the corroded beam, as observed in this study. Because of these reasons, the failure mode of corroded beam may also change depending on the crack widths and their distribution after stirrup corrosion. Therefore, a reduction factor should be applied while calculating the residual strength of concrete, once the stirrup is corroded and corrosion cracks are initiated.

When the shear force is applied to RC beam, the applied shear force is resisted by the concrete together with the stirrups. In the strut and tie model, the stirrups should transfer the load to the concrete and vice versa to effectively transfer the shear loads to the support [29]. The applied shear force cannot be taken by concrete or stirrup alone but can resist the applied loads together. The stirrup allows transference of the diagonal tension forces between the concrete matrix and steel reinforcement by adherence which is also known as the bond between the stirrup and the concrete matrix. This adherence or bond must be strong enough to allow the transfer of diagonal tension force between the concrete matrix and the stirrup. Juarez et al. observed that, at lower levels of stirrup corrosion, this adherence is not affected [20]. However, as the stirrup transversal sections start to diminish at higher levels of corrosion, deterioration of this adherence was affected significantly, generating a main failure plain and sudden cracks. This behavior is produced by the corrosion in the stirrups which caused an accumulation of corrosion products resulting in tensile stress on the concrete cover. This condition provokes a loss of bonding between the steel and the concrete. Under these conditions, the transfer of stress between the stirrup and the concrete is affected and the diagonal cracks progress faster in the stirrup corroded beam causing brittle failure. Research has confirmed that loss of steel-concrete adherence is much more critical when corrosion levels have produced a mass loss > 1%, whereas at levels <1% adherence strength increases [30].

It is a well-established fact now that cracked concrete under compression exhibits lower strength than un-cracked concrete [31]. This compression softening effect depends on the degree of transverse cracking and straining. Tjhin and Kuchma found that the capacity of struts is significantly affected by any disturbance in the strut such as initial cracks parallel or inclined to the strut axis and tensile transverse stress or strain induced by a crossing tie or another effect [32]. The experimental results by previous researchers showed that cracks developed due to corrosion of stirrups significantly affected the capacity of the diagonal struts and subsequently the effective concrete compressive strength is reduced as a consequence of corrosion cracks [13, 33]. Shanhua et al. showed that stirrup corrosion, even reduced the aggregate interlock capacity of concrete, also the ductility and shear capacity in flexural members [34].

The addition of stirrups is known to provide confinement to concrete, and therefore, enhances the contribution of basic shear mechanisms to V_c [27]. Current shear design provisions of ACI 318-11 are yet to account such enhancement and they simply calculate concrete contribution to V_n assuming that no confinement is provided by the stirrups. Although in the design calculations, this confinement is not taken into account for strength enhancement but for an un-corroded and un-cracked beam, this confinement and enhancement in the shear strength will be present. Also, the stirrups help confining the longitudinal reinforcement in place, thus preventing shear cracks from widening, and allowing an increase in dowel action [27]. When the stirrup is corroded, this confinement, though not counted in the shear design calculation, is deteriorated and can be a reason for the loss in the shear capacity loss at higher levels of corrosion. Moreover, the corroded steel rebars show brittle fracture with no indication of necking at failure [19]. In short, the stirrup corrosion is not only associated to the diameter loss of stirrup but also have associated deterioration which are explained in this section.

3.8 PREDICTION OF SHEAR CAPACITY OF CORRODED BEAMS

3.8.1 Shear Capacity of RC Beam

The shear capacity of reinforced concrete beams is generally predicted using the traditional approach of $V_c + V_s$, where V_c is the concrete contribution to the shear capacity of the beam and V_s is stirrup contribution to that of the beam. The summation of V_c and V_s represents the shear capacity of the section. The design codes provide separate equations for evaluating V_c and V_s of reinforced concrete slender beams. The ACI 318M-11 [25], recommends a simplified equation for calculating the undamaged and un-cracked concrete shear strength V_c as follows:

$$V_c = 0.17\,\lambda\,\sqrt{f'_c}\,b_w\,d \tag{4}$$

where λ is a factor accounting for the concrete density ($\lambda = 1$ for normal weight concrete); b and d are the beam width and depth, respectively; and $f'c$ is the concrete compressive strength. The ACI 318 also recommends the following equation for calculating V_s for members with vertical stirrups

$$V_s = A_v f_{yv} d/s \tag{5}$$

where A_v is area of shear reinforcement within spacing s; and f_{yv} is the yield strength of the stirrups.

The test results indicated that damages directly result from corrosion, including the cross-sectional area loss of the reinforcing steel bars of stirrup and the corrosion cracks. The average mass loss percentage represents the corrosion of the stirrup and the corrosion crack width reflects the damage of concrete cover. The results from previous studies also indicated that the reduction in shear capacity due to stirrup corrosion was proportional to both cross-sectional loss and corrosion crack width, and consequently may be linked to the residual shear capacity of corroded beams [21]. For this research, Eqs. (4) and (5) are modified to be used for predicting the shear strength of RC beams with corroded stirrup. The other deteriorations, e.g. confinement pressure loss due to stirrup corrosion, adherence (bonding) deterioration between the concrete and stirrup, loss in the load transfer mechanism due to stirrup corrosion etc. cannot be quantitatively determined in this study because these were out of scope in this study. Separate extensive research and finite element analysis should be carried out to understand the complete behavior of stirrup corrosion.

In this study, the corrosion damage is incorporated into the shear design equations in two ways. First, a reduction in the V_s, shear component provided by stirrup, is determined by estimating the remaining effective cross-sectional area of stirrup after corrosion. Second, a reduction in the V_c, shear component of damaged and cracked concrete, is determined by estimating the effective cross-section width of the beam accounting for the formation of significant corrosion cracks and attributing to the shear strength of concrete, V_c.

3.8.2 Effective Area of Corroded Stirrup

In case of stirrup corrosion, the shear strength loss occurs due to the reduction in the effective area of stirrup, resulting in the stress concentration at the legs of stirrups, loss of confinement which was provided by the un-corroded stirrups, loss of adherence (bonding) between the concrete and the stirrup.. In this study, only the determination of the average sectional loss of stirrup is estimated for evaluating the residual shear capacity of RC beams with corroded stirrups as major strength reduction is because of cross sectional area loss. The remaining effective area of corroded stirrup is calculated using two approaches; (i) according to the amount of current applied for specific number of days and (ii) according to the corrosion crack width formation.

Rodriguez & Andrade [36] derived an equation for conversion of corrosion rate, or applied current Icorr, to diameter decrease which is shown in Eq. (6).

$$\Phi(t) = \Phi(\mathrm{i}) - 0.023\, I_{\mathrm{corr}}\, t \tag{6}$$

where $\Phi(t)$ is the rebar diameter (mm) at a time t; $\Phi(\mathrm{i})$ is the initial rebar diameter (mm); I_{corr} is the corrosion intensity ($\mu A/cm^2$); and t is the time elapsed since propagation period began (year). In this study the duration of exposure and the intensity did not change for mild and severe corrosion. Thus, using Eq. (6) the remaining diameter of the corroded stirrup comes to be 5.23 mm and 4.45 mm for mild and severe corrosion respectively, assuming homogenous corrosion.

The mass loss of stirrups in real structures is difficult to be evaluated and there is no reliable nondestructive method available at present for determining this mass loss [10]. The corrosion crack width, which can be measured in real structures, can be used to estimate the mass loss of the corroded steel bars. From a practical perspective, the corrosion cracks are readily and easily available for inspection in the real structures, and can be an asset parameter to assess the corrosion damage if can give reliable and acceptable results. Vidal et al. developed a semi-empirical model that correlates the mass loss in the reinforcement with corrosion crack width [37]. However, this model was originally developed for the longitudinal reinforcement but researchers extend this model for stirrup corrosion also. This model consists of two steps; the first step is to determine the section loss at which cracking in the concrete will be initiated, and the second step is to determine the actual mass loss based on a measured crack width. Eq. (7) gives the section loss at which cracking in the concrete is initiated whereas Eq. (8) gives the mass loss based on the measured corrosion crack width.

$$\Delta A_{s,cr} = A_s \left[1 - \left(1 - 0.001\alpha \frac{7.53 + 9.32c/d_b}{d_b}\right)^2\right] \tag{7}$$

$$\Delta A_s = \frac{w}{0.0575} + \Delta A_{s,cr} \tag{8}$$

where A_s is the un-corroded steel cross sectional area (mm^2); $\Delta A_{s,cr}$ is the local steel cross-sectional area loss necessary for crack initiation (mm^2); ΔA_s is the steel cross sectional area loss due to corrosion (mm^2); d_b is the corroding bar diameter (mm); c is the concrete cover (mm); α is a factor accounts for pit concentration ($\alpha = 2$ for homogenous corrosion; $4 < \alpha < 8$ for localized corrosion); and w is the corrosion crack width (mm). Thus, by knowing the actual corrosion crack width, the cross-sectional area loss of the stirrups can be predicted as presented in Eq. (8). The remaining effective cross sectional area of stirrup, $A_{v,eff}$, can be determined using Eq. (9)

$$A_{v,eff} = A_s - \Delta A_s \tag{9}$$

3.8.3 Effective Beam Width for Concrete Shear Strength Calculation

Previous researchers, when the studies of stirrup corrosion recently started, believed that the shear strength of concrete is not diminished by the stirrup corrosion. However, with the advancement of study in this field, recent researchers suggest that the concrete cross section of the beam is affected by corrosion of stirrups resulting in decrease of the shear strength of concrete. The corrosion of the shear reinforcement causes cracking, delamination, and spalling of the concrete cover. This makes the beam cross section less effective in resisting imposed loads. El-Sayed [38] in his strut and tie model for stirrup corroded beams, suggested a simply and conservative approach to consider the effects of stirrup corrosion on the concrete section at the ultimate stage to reduce the width of the beam section by completely ignoring the concrete cover. Eq. (10) provides the proposed effective width formulation.

$$b_{eff} = b - 2c \tag{10}$$

where b_{eff} is the effective width and c is the side concrete cover.

Higgins et al. used an effective section width model based on the concrete cover thickness, stirrup diameter, and stirrup spacing [39]. The amount of concrete damage depends primarily on the stirrup spacing, concrete cover, and degree of corrosion of underlying reinforcement. For largely spacing of the reinforcement and smaller concrete cover, the cracks may tend to extend directly outward rather than reach out between the rebars [40]. They suggested that when the stirrups were spaced closer together, more interaction between corrosion cracks occurred and this interaction can cause an increase in the severity of the spalling. The reason is for widely spaced stirrups there was non-overlapping spall damage, but as the stirrup spacing becomes closer, spall wedges will begin to interact and the entire cover area may spall. Based on observed pall patterns for experimental beams and field observed damages, the angle of discrete spalls was taken as approximately 20°, originating at the intersection pf the concrete core and the stirrup cross-section. Using this angle for corrosion induced spalling at stirrup locations and smearing the remaining area over the stirrup spacing, s, the effective concrete beam width available to resist shear force may be estimated as Eq. (11) or (12).

$$b_{eff} = b_w - 2\,(c + d_b) + s/5.5 \qquad \text{if } s \leq 5.5\,(c + d_b) \tag{11}$$

$$b_{eff} = b_w – (5.5/s) \times (c + d_b)^2 \qquad \text{if } s > 5.5 (c + d_b) \tag{12}$$

where b is the original undamaged beam width; b_{eff} is the effective beam width; c is the concrete cover; d_b is the corroding bar diameter of stirrup; and s is the stirrup spacing. Higgins et al. (2003) indicated that the use of Eq. (11) and (12) are for cases when the concrete cover is no longer effective, when significant corrosion cracks are formed on the concrete surfaces [39]. Based on their experimental findings, cracking was observed at relatively low amounts of stirrup section loss (2% on average). As additional corrosion occurred, the damage progressed and the corrosion cracks started to become wider, indicating delamination.

3.8.4 Threshold Corrosion Crack Width at Which Concrete Degradation Initiates

Higgins et al. proposed that effective beam width should be considered in accordance with Eqs. (11) and (12) when the corroded stirrup exhibited an average sectional area loss of 10% or greater or based on field observation of concrete distress [39]. El-Sayed et al. also suggested the same and showed a good agreement with their experimental findings stating that the degradation in shear strength of the corroded beams started at sectional area loss of 9%, and below that percent no degradation in shear strength was observed [21]. It should be pointed out that the degradation only in shear strength below 9% was not observed and they did not investigate the influence of stirrup corrosion on the flexural strength, which was carried in this study.

As discussed earlier, the cross-sectional area loss is not available in real time situations without destructive testing. In this case, Eq. (11) is very convenient to be used to calculate the corrosion crack width, $w_{10\%}$, corresponding to the 10% threshold level of cross-sectional area loss of stirrup. ΔA_s is substituted by $A_s/10$ in Eq. (11) and after rearranging the equation, Eq. (13) is formed.

$$w_{10\%} = 0.0575 \, [(A_s/10) - \Delta A_{s,cr}] \tag{13}$$

The actual corrosion crack width, which can be easily measured in real structures, should be compared with the calculated value of $w_{10\%}$. If the value of the measured corrosion crack width is equal to or greater than $w_{10\%}$, the effective beam width should be considered as per Eq. (11) or (12); otherwise, the undamaged original width of the beam should be considered.

Using the parameters of the beams designed in this study, the minimum corrosion crack width comes out to be 0.03 mm. It means if the corrosion crack width is equal to or greater than 0.03 mm, the effective beam width defined in Eqs. (11) and (12) should be used to estimate the residual shear strength of concrete.

3.8.5 Calculating Residual Shear Capacity of the Corroded Beam

The residual shear capacity of reinforced concrete beams with corroded stirrup can be easily predicted using the same approach of V_c and V_s stated in Eq. (4) and (5) respectively, with a small modification. In Eq. (4) the width of the beam, b_w, is replaced with b_{eff} which can be obtained from Eq. (11) or (12) whereas in Eq. (8) A_v is replaced by $A_{v,eff}$ which can be obtained by using different approaches stated in section 3.7.2. Hence the modified form of Eq. (4) and (5) are

$$V_{c,res} = 0.17 \, \lambda \, \sqrt{f'_c} \, b_{eff} \, d \tag{14}$$

$$V_{s,res} = A_{v,eff} \, f_{yv} \, d/s \tag{15}$$

where $V_{c,res}$ is the calculated residual shear capacity of the corroded beam; while $V_{s,res}$ is the calculated residual shear capacity of corroded stirrup. The summation of $V_{c,res}$ and $V_{s,res}$ represents the calculated residual shear capacity of the stirrup corroded beam. It is important to note that some researchers suggest that the compressive strength of concrete, f'_c is also deceased due to stirrup corrosion. In that case Eq. (14) will be further modified to account for the residual compressive strength of concrete, $f'_{c,res}$ after stirrup corrosion. In this study, this factor is not considered to be in the defined scope of study.

Table 3.1. Residual capacities of concrete and stirrup after corrosion using Eq. (6)

Beam No.	For Concrete			For Steel by Eq. (6)		Residual Shear Capacity		Observed Max. Load (kN)	$V_{u,exp}/V_n^1$
	b_{eff} (mm)	V_c^1 (kN)	V_c^2 (kN)	d (mm)	V_s^1 (kN)	V_n^1 (kN)	V_n^2 (kN)		
B11S-FS-10/120	65.82	15.19	23	4.45	24.6	39.79	47.6	27.35	0.69
B18S-FS-13/80	58.55	13.51	23	4.45	36.8	50.31	59.8	40.86	0.81
B22S-SS-13/120	65.82	15.19	23	4.45	24.6	39.79	47.6	30.19	0.76
B24S-FS-13/120	65.82	15.19	23	4.45	24.6	39.79	47.6	24.68	0.62
B26S-FS-13/160	73.09	16.87	23	4.45	18.4	35.27	41.4	36.4	1.03
B31S-FS-16/80	58.55	13.51	23	4.45	36.8	50.31	59.8	50.36	1.00
B32M-SS-16/120	65.82	15.19	23	5.23	33.9	49.09	56.9	62.03	1.26
B35S-SS-16/120	65.82	15.19	23	4.45	24.6	39.79	47.6	60.87	1.53
B37S-FS-16/120	65.82	15.19	23	4.45	24.6	39.79	47.6	58.2	1.46
B39S-FS-16/160	73.09	16.87	23	4.45	18.4	35.27	41.4	52.37	1.40

V_c^1 is the residual shear strength of concrete obtained from Eq. (11) after stirrup corrosion
V_c^2 is the shear capacity of concrete without stirrup corrosion
V_s^1 is the calculated shear capacity of corroded stirrup using the remaining diameter of stirrup obtained from Eq. (6)
V_n^1 is the total calculated residual shear strength of corroded beam ($V_c^1+V_s^1$)
V_n^2 is the total calculated residual shear strength of corroded beam ($V_c^2+V_s^1$)
Observed Max. Load is the maximum load carried by the corroded beam during the bending test

Using Eq. (4) the calculated shear capacity of concrete without stirrup corrosion is 23 kN for all the beams as the dimensions and compressive strength of concrete, f'_c did not change. Table 3.1 lists the residual shear capacity of concrete; and that of stirrup using Eq. (6) for calculating $A_{v,eff}$ and compared with the observed maximum load. Only the beams failed in shear are used for this comparison as the shear strength loss is evaluated for concrete and stirrup.

It can be observed from Table 3.1 that the predicted shear capacity varied for all the beams. The prediction of the residual shear capacity of beams is made based on the diameter loss of the stirrup by knowing the current density. The mean of $V_{u,exp}/V_n^1$ ratio of all the presented is 1.10 with the coefficient of variation 30% which is a high percentage. It can be seen that for D10 and D13 beams the predicted values are higher than the experimental values whereas for D16 beams, the predicted values are less than the experimental values which shows better estimation. Two beams from these data shows the same predicted value as the experimental value. Figure 3.50 shows the comparison of experimental and predicted shear capacities of corroded tested beams.

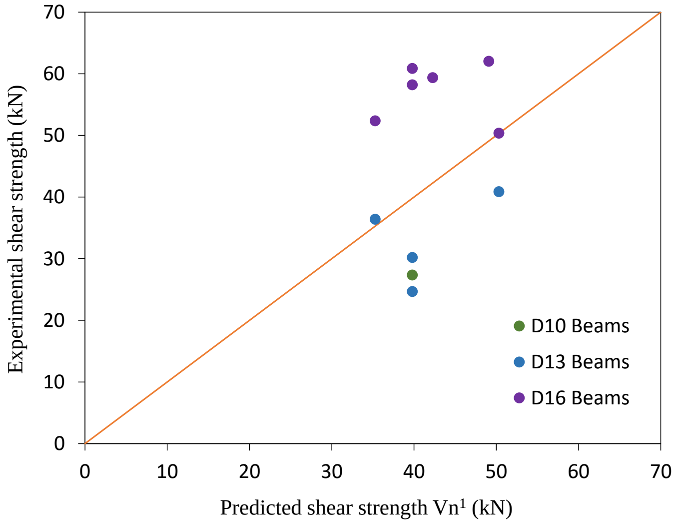

Figure 3.50 Comparison of experimental and predicted shear capacities of corroded beams obtained for Table 3.1

Table 3.2 lists the residual shear capacity of concrete which is the same as Table 3.1 and stirrup using Eq. (9) which is based on the corrosion cracks formation. It can be observed from the table that the shear capacity prediction is still not very accurate using the corrosion crack width data. However, the ratio of $V_{u,exp}/V_n^3$ becomes more close to 1.0, showing the prediction of shear capacities using corrosion crack widths give relatively better results. The mean value of the $V_{u,exp}/V_n^3$ is 0.86 with the coefficient of variation of 29%. Though not much difference in the coefficient of variation but the predicted values are much closer the experimental values especially for D16 beams. The predicted residual shear capacities of D10 and D13 beams also depict that additional deteriorations due to stirrup corrosion might also occurred other than the reduced cross-sectional area of the stirrup.

Eq. (9) is developed considering the longitudinal reinforcement which are generally larger in diameter than stirrup and the concrete cover to the longitudinal reinforcement is the same as the reinforcement is placed longitudinally. In case of stirrup, the governing factor is not only the diameter of stirrup and the side concrete cover; but also the interaction of adjacent stirrups which includes spacing of stirrups and the shape of stirrup. Therefore, a new model should be prepared and studied which takes into account the stirrup corrosion, corrosion crack widths and the location. Software modeling with FEM is a good tool to understand the behavior of stirrup corroded beam but till now, considerable work has not been done in this field and the earliest extensive study was carried by Higgins and Farrow [13]; to the best of the author knowledge. The corrosion crack width can be a good parameter to study but the model should be made considering the cracks not in one stirrup but in a certain length as the shear crack will propagate throughout the shear span once it is formed.

Table 3.2. Residual shear capacities of concrete and stirrup after corrosion using Eq. (9)

Beam No.	For Concrete		For Steel by Eq. (9)			Residual Shear Capacity		Observed Max. Load V_u (kN)	$V_{u,exp}/V_n^3$
	V_c^1 (kN)	V_c^2 (kN)	Crack (w) mm	d (mm)	V_s^2 (kN)	V_n^3 (kN)	V_n^4 (kN)		
B11S-FS-10/120	15.19	23	0.40	4.92	30.01	45.20	53.01	27.35	0.61
B18S-FS-13/80	13.51	23	0.48	4.73	41.72	55.23	64.72	40.86	0.74
B22S-SS-13/120	15.19	23	0.33	5.07	31.94	47.13	54.94	30.19	0.64
B24S-FS-13/120	15.19	23	0.28	5.18	33.31	48.5	56.31	24.68	0.51
B26S-FS-13/160	16.87	23	0.09	5.57	28.90	45.77	51.9	36.4	0.80
B31S-FS-16/80	13.51	23	0.09	5.57	57.80	71.31	80.80	50.36	0.71
B32M-SS-16/120	15.19	23	0.04	5.67	39.91	55.10	62.91	62.03	1.13
B35S-SS-16/120	15.19	23	0.30	5.14	32.76	47.95	55.76	60.87	1.27
B37S-FS-16/120	15.19	23	0.08	5.59	38.81	54.00	61.81	58.2	1.08
B39S-FS-16/160	16.87	23	0.04	5.67	29.93	46.80	52.93	52.37	1.12

V_c^1 is the residual shear strength of concrete obtained from Eq. (11) after stirrup corrosion
V_c^2 is the shear capacity of concrete without stirrup corrosion
V_s^2 is the calculated shear capacity of corroded stirrup using the remaining diameter of stirrup obtained from Eq. (9)
V_n^3 is the total calculated residual shear strength of corroded beam ($V_c^1+V_s^2$)
V_n^4 is the total calculated residual shear strength of corroded beam ($V_c^2+V_s^2$)
Observed Max. Load is the maximum load carried by the corroded beam during the bending test

Figure 3.51 shows the comparison of experimental and predicted shear capacities of corroded tested beams using Eq. (9).

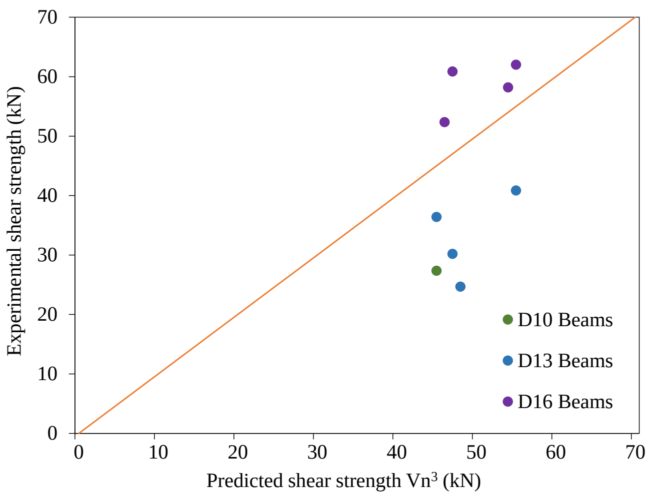

Figure 3.51 Comparison of experimental and predicted shear capacities of corroded beams obtained for Table 3.2

Table 3.3 lists the residual shear capacity of concrete and stirrup using the mass loss conversion to diameter loss using simple relation of density, mass and volume. It can be observed from the table that the predicted residual shear capacities of D10 and D13 beams are higher than the experimental values, even if when the original diameter loss is retrieved. The limitation of this approach is that it gives the homogenous diameter loss and do not consider localized or pitting corrosion loss. However, the corrosion was allowed using accelerated methods which generally produces homogenous corrosion, pitting corrosion and non-homogeneous corrosion was also observed in many stirrups. However, Higgins et al. [29] suggested in their analytical modeling analysis that average cross-sectional loss of stirrup gives better results as compared to the minimum cross-sectional loss as the later underestimates the residual shear capacity. D16 beams shows lower predicted residual shear capacity than the experimental strength and provided better estimation the other methods defined in Tables 3.1 and 3.2.

Table 3.3. Residual shear strengths of concrete and stirrup after corrosion using mass loss

Beam No.	Concrete	Stirrup using mass loss		Residual Shear Capacity	Observed Max. Load V_u (kN)	$V_{u,exp}/V_n^5$
	V_c^1 (kN)	d (mm)	V_s^5 (kN)	V_n^5 (kN)		
B11S-FS-10/120	15.19	4.40	24.01	39.2	27.35	0.70
B22S-SS-13/120	15.19	4.58	26.02	41.21	30.19	0.73
B24S-FS-13/120	15.19	4.35	23.47	38.66	24.68	0.64
B35S-SS-16/120	15.19	5.33	35.24	50.43	60.87	1.21
B37S-FS-16/120	15.19	5.21	33.67	48.86	58.2	1.19

V_c^1 is the residual shear strength of concrete obtained from Eq. (11) after stirrup corrosion
V_s^3 is the calculated shear capacity of corroded stirrup using the remaining diameter of stirrup obtained from Eq. (9)
V_n^5 is the total calculated residual shear strength of corroded beam (V_c^1+V_s^3)
Observed Max. Load is the maximum load carried by the corroded beam during the bending test

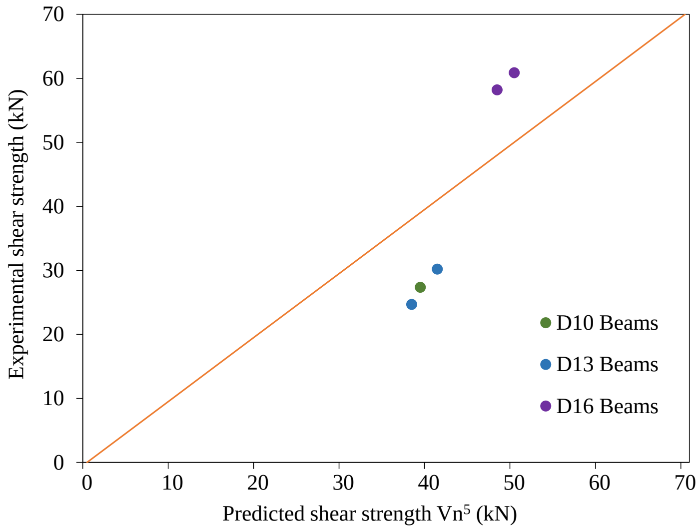

Figure 3.52 Comparison of experimental and predicted shear capacities of corroded beams obtained for Table 3.3

Figure 3.52 shows the comparison of experimental and predicted shear capacity of corroded tested beams using the actual mass loss. The average of $V_{u,exp}/V_n^5$ ratio is 0.89 while the coefficient of variation is 28%. Figure 3.52 illustrates that the calculated nominal shear capacity of D13 beams is higher than the experimental values whereas for D16, the nominal shear capacity underestimates the shear capacity after stirrup corrosion. From this observation, it can be concluded that for D13 beams, the loss in ultimate load was also contributed by the loss in adherence between the concrete and the stirrup and localized corrosion. For D16 beams, the shear capacity of the cracked concrete is assumed to be higher than D13 beams as the diameter loss of stirrup is considerably less than D13 beams. This also implies that the strength loss of concrete does not linearly depend on the stirrup corrosion. Further studies are required to investigate the load transfer mechanism and to evaluate the remaining shear strengths of concrete and stirrup after stirrup corrosion.

CHAPTER 4

CONCLUSIONS

AND

RECOMMENDATIONS

Chapter 4

CONCLUSIONS AND RECOMMENDATIONS

4.1 CONCLUSIONS

After detailed research and experiments conducted on the effects of stirrup localized corrosion on structural performance of reinforced concrete beams, following conclusions are drawn:

1. The total number of corrosion cracks were observed more in severe corrosion. The ends of the beam, irrespective of the corrosion level had wider corrosion cracks.

2. Narrower corrosion cracks were observed for mild corrosion. For all cases more than 50% corrosion cracks lie in the crack width range of 0.03-0.05 mm. For severe corrosion, relatively wider cracks were observed. Corrosion cracks wider than 0.3 mm were also observed in the case of severe corrosion.

3. The number of corrosion cracks increased as the shear reinforcement ratio increased. It means that more corrosion cracks were observed for closely spaced stirrups. However, the corrosion crack widths were not significantly affected by the stirrup spacing. Vertical cracks were formed due to stirrup corrosion and horizontal cracks were also observed which pass through the vertical cracks. For higher shear reinforcement ratio, more horizontal cracks were observed which connect the vertical crack at a few locations. For severely corroded beam, the frequency of horizontal or connecting cracks were also more frequent than the mildly corroded beam.

4. The failure mode of severely corroded beams was changed from flexural tension failure to shear failure. The failure mode of mildly corroded beams did not change in most of the cases. However, as the flexural reinforcement ratio increased, mild corrosion also changed the failure mode and shear failure was observed.

5. The ultimate capacities of all the corroded beams were less than those of the control beams. Even the failure mode was flexural tension after stirrup corrosion, decrease in the flexural capacity was observed. The corrosion cracks formed due to stirrup corrosion in the maximum bending moment zone which is the middle span acted as the pre-defined failure paths during the bending test. The corrosion cracks tended to widen during the bending test. Moreover, the corrosion cracks in the concrete reduced the concrete compressive strength, effective beam width, confinement pressure provided by stirrup and also cause other associated damages. This depicts that the stirrup corrosion has tendency to decrease the ultimate load carrying capacity of the corroded beams even if the failure mode is not shear failure.

6. Although the stirrup generally does not contribute to the flexural strength in the middle span, the stirrup corrosion in the middle span has tendency to reduce the flexural capacity of the beams. The corrosion cracks presented in the middle span contributed in the failure of the corroded beams but the failure also depended on the location of corrosion cracks and the flexural design. The corrosion cracks produced due to stirrup corrosion are vertical and horizontal cracks which facilitates larger parts of concrete cover to spall down and hence reducing the load carrying capacity. Due to this spalling of concrete cover especially from the top compression portion, the failure mode of the corroded beam changed to flexural compression failure. Severely corroded beams had more reduction in the flexural capacity than the mildly corroded beams.

7. The shear capacity loss was greater for higher shear reinforcement ratio (which is the case of closely spaced stirrups). The shear capacity loss was not only contributed by the stirrup but also by the strength loss in the concrete. For higher shear reinforcement ratio, more damage will be the caused to the effective cross-sectional area of stirrup and strength of concrete, as also depicted by the corrosion cracks distribution.

8. The load carrying capacity loss for higher flexural reinforcement ratio was observed more and the shear failure was more common failure mode for D16 beams, despite the fact that it also depended on the degree of corrosion. Using the higher flexural reinforcement increases the flexural capacity while the shear capacity was kept the same as the other beams. The probability to get shear failure becomes higher and therefore, flexural reinforcement ratio is also a significant factor for the consideration of the load carrying capacity loss.

9. The deflection ductility of the beams was considerably reduced for most of the cases. However, an improvement in the deflection ductility was also observed in some cases but no particular relationship was found between deflection ductility and stirrup spacing. The deflection ductility was improved for D10 with 160 mm stirrup spacing and D13 beams with 120 mm spacing.

10. The available models to predict the residual shear capacity of stirrup locally corroded beam are not very reliable as these models have been mainly developed considering one or two straight corroded rebars with higher diameters which are mostly used as longitudinal reinforcement. In case of stirrup corrosion, there is an interaction of the tensile stress due to the corrosion of the adjacent stirrups which results in more cracking which are vertical and horizontal cracks. When the stirrup is closely spaced and the shear reinforcement ratio is high, more horizontal corrosion cracks are observed which pass through the vertical cracks. These corrosion cracks are the indication of confinement loss provided by stirrup which also results in the loss of compressive strength of concrete, and are absent in case of longitudinal reinforcement corrosion. It can be said that the mechanism of stirrup corrosion is a bit different from the available models which were mainly developed for the straight and higher diameter rebar mostly used as longitudinal reinforcement.

4.2 RECOMMENDATIONS

The results of this study have opened a new area of research. The stirrup corrosion leads to ultimate capacity loss, even if the stirrups are corroded in the middle span. The stirrup corrosion is not only adversely affecting the mechanical properties of steel rebar but also deteriorating the strength of concrete. After concluding this study, the following recommendations are given for future studies:

1. Research should be carried out to investigate more precisely the load carrying mechanism and develop models to incorporate losses to concrete, stirrup and to the overall beam, after stirrup corrosion, especially when the failure is not shear. Finite Element Analysis (FEM) can be a handy tool for this investigation. The constitutive laws of concrete, stirrup, strength losses in concrete due to corrosion cracks, decrease in the compressive strength of the concrete; and the bond between concrete and corroded stirrups should be carefully examined.

2. In this research all important parameters were not altered. To fully understand the behavior of stirrups corrosion, different aspects of design parameters which are mostly used in real structures should be studied. For example, shear deformations are critical in deep beams and most of the contributions to resist shear force will be provided by stirrups. Different depth of beams should be studied to see the effect of stirrup corrosion and also, the shear span to depth ratio (a/d) should also be varied. Nevertheless, the stirrup corrosion of short beams also have to be thoroughly investigated in order to fully understand and develop the behavior of stirrup corroded beams.

3. Altering the flexural reinforcement ratio is also very important. For a ductile failure, the longitudinal reinforcement should be less than steel for balance failure. A series of experiments should be conducted by altering the reinforcement ratio from minimum to maximum area of steel. Likewise, the diameter of stirrup is also important and it can be varied.

4. As shown in this research also, the stirrup spacing has a strong connection with the degree of deterioration. The specimens with 160 mm stirrup spacing were not degraded significantly even for the severely corroded beams. It is important to investigate the effect of spacing of stirrups in more detail while varying the design and dimensions of beam and to figure out, at what spacing the deterioration is constant or insignificant, like in this case 160 mm stirrup spacing is not considerable affected.

5. This study is conducted using river coarse aggregates. Previous research show that the interlocking of aggregates is one of the critical factor for consideration of the shear strength of concrete. When the stirrups are corroded, the interlocking of aggregates is also deteriorated and shear failure may occur. More investigations, whether experimental or analytical, should be carried out to fully understand the deterioration of interlocking of aggregates due to stirrup corrosion.

6. In real structures generally the corrosion takes place while the structures are in the service life. These structures might have some cracks also which can facilitate corrosion process and makes easier for aggressive agents to penetrate in concrete. A study should be conducted in which the stirrup is allowed to corrode while having sustained loads in order to simulate with the real situation more accurately.

References

[1]. Castel A, Francois R, Arliguie G., (2000) "Mechanical behaviour of corroded reinforced concrete beams – Part 1: Experimental study of corroded beams." *Materials and Structures*.

[2]. Maaddawy, T., Soudki, K., Topper T., (2005). "Long-term performance of corrosion-damaged reinforced concrete beams." *ACI Structural Journal*.

[3]. Yoon Sanchun, Wang Kejin, Jason Weiss W, Shah Surendra P. (2000). "Interaction between loading, corrosion and serviceability of reinforced concrete." *ACI Materials Journal*.

[4]. Malumbela Goitseone, Moyo Pilate, Alexander Mar, (2009). "Behavior of RC beams corroded under sustained service loads." *Construction and Building Materials*.

[5]. Azad Abul K, Ahmad Shamsad, Azher Syed A., (2007). "Residual strength of corrosion damaged reinforced concrete beams." *ACI Material Journal*.

[6]. Mangat Pritpal S, Elgar Mahmoud S., (1999). "Flexural strength of concrete beams with corroding reinforcement." *ACI Structural Journal*.

[7]. Du Y., Clark L.A, and Chan A.H.C., (2007). "Impact of reinforcement corrosion on ductile behavior of reinforced concrete beams." *ACI Structural Journal*, 104 (3), 285-293.

[8]. Vidal T, Castel A, Francois R., (2007). "Corrosion process and structural performance of a 17 year old reinforced concrete beam stored in chloride environment." *Cement Concrete Research.*

[9]. Zhang Ruijin, Castel A, Francois R., (2010). "Concrete cover cracking with reinforcement corrosion of RC beam during chloride-induced corrosion process." *Cement Concrete Research*.

[10]. Xia, J.; Jin, W.; and Li, L., (2011). "Shear Performance of Reinforced Concrete Beams with Corroded Stirrups in Chloride Environment." *Journal of Corrosion Science*, 53 (5), 1794-1805.

[11]. O'Flaherty, Fin, Mangat, Pal, Lambert, Paul and Brown, E. H., (2010). "Influence of shear reinforcement corrosion on the performance of under-reinforced concrete beams." *Sheffield Hallam University Archive*.

[12]. Nobuaki O, Shin-ichi M, Nathaniel BD, Hirotaka S., (2000). "Influences of bending crack and water–cement ratio on chloride-induced corrosion of main reinforcing bars and stirrups." *ACI Materials Journal*.

[13]. Higgins C, Farrow III W., C., (2006). "Tests of reinforced concrete beams with corrosion damaged stirrups." *ACI Structural Journal*.

[14]. Yingang D, Clark LA, Chan A., (2007). "Impact of reinforcement corrosion on ductile behavior of reinforced concrete beams." *ACI Structural Journal*.

[15]. Abul KA, Ahmad S, Azher SA., (2007). "Residual strength of corrosion-damaged reinforced concrete beams." *ACI Materials Journal*.

[16]. Torres-Acosta AA, Navarra-Gutierrez S, Teran-Guillen J., (2007). "Residual flexure capacity of corroded reinforced concrete beams." *Engineering Structures*.

[17]. Dario Coronelli, Kamyab Zandi Hanjari, Karin Lundgren, (2013). "Severely corroded RC with cover cracking." *ASCE Journal of Structural Engineering*, 221-232.

[18]. Zandi Hanjari, K., Kettil, P., Lundgren, K., 'Analysis of the mechanical behaviour of corroded reinforced concrete structures.' ACI Structural Journal, 108(5), 2011, 532-541.

[19]. Vu Hiep Dang, Raoul Francois, (2013). “Influence of long-term corrosion in chloride environment on mechanical behavior of RC beam.” *Engineering Structures 48*.

[20]. C.A.Juarez, B. Guevara, G. Fajardo, P. Castro-Borges, (2011). “Ultimate and nominal shear strength in reinforced concrete beams deteriorated by corrosion.” *Engineering Structures,* 33.

[21]. Sayed, A.,K.,E., Hussain, R.,R., and Shuraim, A.,B., (2016). “Influence of stirrup corrosion on shear strength of reinforced concrete slender beams.” *ACI Structural Journal,* Vol. 113 (6), 1223-1232.

[22]. Mehta, P., Monterio, J., “Concrete, structure properties, and materials”. *2nd edition Englewood Cliff: Prentice-Hall*, 160-164.

[23]. R. T. Foley., 1975 “Complex ions and corrosion.” *Journal of the Electrochemical Society*, 122 (11), 1493-1549.

[24]. JSCE, ‘Structural performance of concrete structures with materials deterioration.’ Concrete Engineering Series, 85, JSCE, 2009.

[25]. Building Code Requirements for Structural Concrete ACI 318M- 2011 and Commentary (2011), *Farmington Hills (MI), American Concrete Institute*.

[26]. Nilson AH, Winter G., “Design of concrete structures.” *14th edition, McGraw-Hill*.

[27]. El-Chabib, H., (2011). “Effect of Stirrups on the contribution of concrete compressive strength and tensile steel to the shear strength of RC beams using artificial neural networks.” *Structures Congress, ASCE*.

[28]. Taranath, B.S., (2010). “Reinforced concrete design of tall buildings.” *Taylor and Francis Group*.

[29]. Higgins, C., Farrow, W.,C., and Turan, O., T., (2012). “Analysis of reinforced concrete beams with corrosion damaged stirrups for shear capacity.” *Structure and Infrastructure Engineering* 8 (11), 1080-1092.

[30]. Auyeeung Y, Balaguru P, Chung L., (2000). “Bond behavior of corroded reinforcement bars.” *ACI Material Journal*, 97 (2), 214–220.

[31]. Vecchio, F., and Collins, M., P., (1986). “The modified compression field theory for reinforced concrete elements subjected to shear.” *ACI Journal, Proceedings,* 83 (2), 219-231.

[32]. Tjhin, T., and Kuchma, D., (2002). “Computer-based tools for design by strut-and-tie-model method: Advances and Challenges.” *ACI Structural Journal,* 99 (5), 586-594.

[33]. Suffern, C., El-Sayed, A., K., and Soudki, K., (2010). “Shear strength of disturbed regionswith corroded stirrups in reinforced concrete beams.” *Canadian Journal of Civil Engineering*, 37 (8), 1045-1056.

[34]. Xu, S., Zhang, Z., Li, R., and Qiu, R., L., (2017). “Experimental study on the shear behaviour of RC beams with corroded stirrups.” *Journal of Advanced Concrete Technology*, Vol. 15, 178-189.

[35]. El-Sayed, A., K., Hussain, R., R., and Shuraim, A., B., (2015). “Effect of stirrup corrosion on the shear strength of reinforced concrete short beams.” *Journal of Civil Engineering and Management*, 22 (6), 491-499.

[36]. Rodriguez, J. and Andrade, C., (1990). “Load-bearing capacity loss in corroding structures.” *Proceedings of ACI Convention.*

[37]. Vidal, T.; Castel, A.; and François, R., (2004). "Analyzing Crack Width to Predict Corrosion in Reinforced Concrete." *Cement and Concrete Research*, 34 (1), 165-174.

[38]. El-Sayed, A., K., (2014). "Strut and tie modelling for RC short beams with corroded stirrups." *Latin American Journal of Solids and Structures*, Vol. 11, 2255-2270.

[39]. Higgins, C., Farrow, W.C., Potisuk, T., Miller, T.H., Yim, S.C., Holocomb, G.R., Cramer, S.D., Covino, B.S., and Bullard, S.J., (2003). "Shear capacity assessment of corrosion damaged reinforced concrete beams." *Oregon Department of Transportation*, 62-64.

[40]. Dagher, H., J., and Kulendran, S., (1992). "Finite element modelling of corrosion damage in concrete structures." *ACI Structural Journal*, 89 (6), 699-708.